FOREST NUTRIENT CYCLING AND REMOTE SENSING OF LAND COVER IN MIOMBO WOODLANDS: INSIGHTS FOR BIOGEOCHEMISTRY AND ENVIRONMENTAL MONITORING OF AFRICAN TROPICAL DRY FOREST LANDSCAPES

BY MARC THOMAS MAYES

SCB., GEOLOGY-CHEMISTRY, BROWN UNIVERSITY, 2009

M.S., ENVIRONMENT AND RESOURCES, UNIVERSITY OF WISCONSIN-MADISON, 2011

SC.M., BROWN UNIVERSITY, 2014

A DISSERTATION SUBMITTED IN PARTIAL FULFILLMENT OF THE

REQUIREMENTS FOR THE DEGREE OF DOCTOR OF PHILOSOPHY

IN THE DEPARTMENT OF EARTH, ENVIRONMENTAL AND PLANETARY SCIENCES AT BROWN UNIVERSITY

PROVIDENCE, RHODE ISLAND, UNITED STATES OF AMERICA

MAY 2017

This dissertation by Marc Thomas Mayes is accepted in its present form

by the Department of Earth, Environmental and Planetary Sciences

as satisfying the dissertation requirements for the degree of Doctor of Philosophy.

Date______________ ____

Dr. John F. Mustard, Advisor

Date______________ ____

Dr. Jerry M. Melillo, Advisor

Recommended to the Graduate Council

Date______________ ____

Dr. Christopher Neill, Reader

Date______________ ____

Dr. Jung-Eun Lee, Reader

Date______________ ____

Dr. Ralph Milliken, Reader

Date______________ ____

Dr. Lyndon Estes, Reader

Approved by the Graduate Council

Date______________ ____

Dean of the Graduate School

MARC THOMAS MAYES

Ecosystems Scientist
PhD Candidate (Expected 2016)
Brown University
Department of Earth, Environmental & Planetary Sciences (DEEPS)
324 Brook Street, Box 1846, Providence, Rhode Island USA 02912

Phone: 813-326-5849
Email: mthomasmayes@gmail.com

PERSONAL DETAILS:
Date of Birth: 25 January 1987, Chicago, Illinois, USA

SUMMARY:
Geoscientist interested in a career combining applied research and advising programs on clean water and water conservation, adaptation of land use systems (forestry, agriculture) to climate change, local scientific capacity-building and development in semi-arid and arid regions. Experienced leader and co-developer of international projects in East Africa and Turkey with scientists and non-scientists across universities, NGOs and local groups to assess land use effects on ecosystem carbon, nutrient and water cycles underpinning availability of natural resources. Trained and practiced in facilitation, managing project teams with diverse cultural and educational backgrounds, and representing peers in governance settings. Core competencies: Ecosystem science and geology, remote sensing, plant physiology, soil science, limnology, hydrology, natural resources, land use planning, project management, communication skills.

EDUCATION

PhD, Earth, Environmental and Planetary Sciences. GPA: Not Calculated. May 2016 (exp.)
Brown University DEEPS – Marine Biological Lab (MBL) Joint PhD Program
in Environmental Sciences. Providence, RI and Woods Hole, MA.
Advisors: Dr. John Mustard (Brown DEEPS), Dr. Jerry Melillo (The Ecosystems Center, MBL).
Thesis: Forest nutrient cycling and remote sensing of land cover in Miombo Woodlands.

Sc.M., Earth and Environmental Sciences. GPA: Not Calculated. May 2014.
Brown University DEEPS – Marine Biological Lab Joint PhD Program in Environmental Sciences.
Advisors: Dr. John Mustard (Brown DEEPS), Dr. Jerry Melillo (The Ecosystems Center, MBL).

M.S., Environment and Resources. GPA: 4.0 August 2011
University of Wisconsin-Madison.
Nelson Institute for Environmental Studies, Center for Sustainability and the Global Environment (SAGE), Madison, WI.
Advisors: Dr. Mutlu Ozdogan, Dr. Erika Marin-Spiotta, Dr. Robert Beattie.
Thesis*:* Land use and Parent Material Effects on Soil Carbon and Nitrogen
in the Konya Basin, Turkey.

Certificate, NSF-IGERT CHANGE (Course on Humans and the Global Environment) Program, SAGE, University of Wisconsin-Madison.
Program coordinators: Dr. Jonathan Patz, Dr. Robert Beattie.
Capstone Project: Health Effects of Oil in the Amazon (HOLA).
Note: The CHANGE-IGERT program was a 2-year program designed to give

scholars skills to collaborate effectively with colleagues across the academe, private industry, government and other organizations. Skills included active listening, facilitation, public speaking and conflict resolution.

ScB., Geology-Chemistry, Cum Laude. **GPA: Not Calculated.** May 2009
Brown University DEEPS (formerly Department of Geological Sciences).
Providence, Rhode Island.
Advisor: Dr. James Russell.
Thesis: High-Resolution Reconstructions of Temperature and Productivity Show Unprecedented Warming in Lake Tanganyika, East Africa, 500-2000 CE.

PUBLICATIONS

PEER-REVIEWED SCIENTIFIC ARTICLES

Mayes, M.T., Mustard, J.F., Melillo, J.M., 2015. Forest cover change in Miombo Woodlands: modeling land cover of African dry tropical forests with linear spectral mixture analysis. *Remote Sensing of Environment* 165, 203-2015, doi: 10.1016/j.rse.2015.05.006

Mayes, M., Marin-Spiotta E., Szymanski, L et al., 2014. Soil type mediates effects of land use on soil carbon and nitrogen in the Konya Basin, Turkey. *Geoderma* (232-234): p. 517-527, DOI: 10.1016/j.geoderma.2014.06.002

Tierney, J., **Mayes, M**., et al., 2010. Late twentieth century warming in Lake Tanganyika unprecedented since AD 500. *Nature Geoscience* 3: 422-425, DOI: 10.1038/NGEO865.

PEER-REVIEWED CONFERENCE PRESENTATIONS

-Mayes, M., Melillo, J., Neill, C., Nyadzi, G., 2015. Carbon, nitrogen cycling and land cover changes during regrowth in African dry tropical forests: integrating perspectives from field and satellite data across a chronosequence in the Miombo Woodlands of western Tanzania. Oral presentation, AGU Fall Meeting, San Francisco, CA. B21L-08.

-Mayes, M., Mustard, J, Melillo, J 2014. Responses of forest cover loss and regrowth to local and national drivers of agricultural development in the Miombo Woodlands of western Tanzania. Oral presentation, Global Land Project Open Science Meeting, Berlin, Germany.

- **Mayes, M**., Mustard, J.F., Melillo, J.M., 2014. Identifying forest loss and regrowth trends in a Tanzanian Miombo Woodland landscape from 1990-2013 with multi-temporal spectral mixture analysis and spectra indices in MODIS and Landsat data. Poster., EARSeL (European Association of Remote Sensing Laboratories)-NASA LCLUC Joint Workshop on Land Use and Land Cover, Berlin, Germany.

- **Mayes, M.,** Mustard, J.F., Melillo, J.M., 2013. Responses of forest cover and agricultural land changes to local and national drivers of land development in the Miombo Woodlands of western Tanzania. Poster, AGU Fall Meeting, San Francisco, CA. B51F-0363.

-Mayes, M., Marin-Spiotta E., Ozdogan M., Erdogan M.A., 2011. A landscape-scale study of land use and parent material effects on soil organic carbon and total nitrogen in the Konya Basin, Turkey. Oral presentation, AGU Fall Meeting, San Francisco, CA. B43G-04.

- Mayes, M.T., Ozdoğan, M, Marin-Spiotta, E.M., 2011. Multi-temporal land cover classification of the Konya Basin, Turkey, based on a Landsat TM-derived NDVI/NDMI time series. Poster., American Society of Photogrammetry and Remote Sensing, Annual Meeting: 2000.

- **Mayes, M.T.,** Ozdoğan, M, Marin-Spiotta, E.M., 2010. Multi-temporal land cover classification of the Konya Basin, south-central Turkey: satellite remote sensing in support of landscape-scale soil biogeochemistry research. Poster, AGU Fall Meeting**:** GC51F-0798.

- **Mayes, M.T.,** Tierney, J.E., Huang, Y.H., Russell, J.M., 2008. High-Resolution Reconstructions of Temperature and Precipitation During the Last Millennium from Lake Tanganyika, Africa. Oral Presentation, EOS Transactions AGU, Fall Meeting Supplement 89: PP12E-01.

RESEARCH AND WORK EXPERIENCE:

International research and project management in Geosciences, Environmental and Natural Resource Assessment

- Remote sensing of landscape changes in sub-Saharan Africa, Turkey and the USA to study land use impacts on ecosystem carbon, water and nutrient cycles, and to support work of NGOs and government agencies in balancing human natural resource needs with ecosystem health.
  - Earned degrees in Geosciences (2) and environmental management (1) with interdisciplinary coursework spanning image processing, GIS, statistics hydrology, quantitative public policy and land use planning.
  - Applied image analyses in terrestrial and aquatic ecosystem research over 7 years of experience, using multi- and hyperspectral satellite and airborne sensors (e.g. Landsat, WorldView, AVIRIS), LiDAR products, and communication training on the sensitivity of map data on natural resources. Recently trained on the use of unmanned aerial vehicles (UAVs) for environmental monitoring.
  - Completed over 10 new land cover mapping and landscape change analyses for research, land use planning and needs of NGOs and governments. These included a forest change assessment using spectral mixture analysis for Miombo Woodland ecosystems in sub-Saharan Africa (part of PhD thesis), and combining landscape greenness and wetness metrics to map agricultural lands in central Turkey (part of M.S. thesis).
  - Key accomplishments:
    - Published peer-reviewed article on forest change and remote sensing methods for semi-arid woodlands in sub-Saharan Africa (Miombo Woodlands) in *Remote Sensing of Environment* (2015).
    - Produced forest, agricultural land maps and maps of water well-drilling projects for the United Nations-sanctioned Millennium Village Project-Mbola in Tabora, Tanzania (2013-2015).
    - Burned-area maps in Rwenzori Mountains, Uganda for the Uganda Wildlife Authority (2013).
    - Agriculture and rangeland maps in central Asian steppes (Konya Basin, Turkey) (2010-2011).
    - Presented report on city tree cover produced for the City of Madison, WI (2009-10).

- Managed 7 major field campaigns of 4 weeks or more in Tanzania and Turkey between 2010-2015 for projects validating remote sensing analyses, and quantifying forest and agricultural land use effects on carbon, nutrient and water cycles. Planned and supervised site selection and data collection on forests, soil, water and land cover. Trips involved significant management, logistics, responsibility for $2,000-$10,000 budgets, adapting activities to ensure safety and achieve science objectives in unexpected situations with limited infrastructure and connectivity.
  - Trained in collection, analysis and interpretation of field data on forest and canopy structure, soils, surface and groundwater with 10 years' experience, including field courses in forestry, hydrogeology and, soil science.
  - Experienced in proposal writing, securing international research permits, import/export logistics (e.g. USDA permits), liaising with NGOs and government agencies, negotiating site

access with local authorities and land owners, recruiting and managing field teams of up to 12 people aged 25-75 with diverse backgrounds.

- Collected data from over 30 forest and agricultural sites in Tanzania enabled analyses of how ecosystem function and resource availability recovers with forest regrowth; data from Turkey enabled quantification of long-term land use impacts on agricultural and rangeland areas.
- Key accomplishments:
    - Quantified forest structure, carbon stock and nutrient cycling recovery across 18 sites spanning a 40-year age gradient in dry tropical forests of Tanzania (Miombo Woodlands), contributing to 3 chapters in my PhD thesis and upcoming publications (2015-16).
    - Shared data and maps on forest resources with the Tanzania Forest Service and UN-sanctioned Millennium Villages Project-Mbola, Tabora, Tanzania (2015-16) have informed forest monitoring.
    - Earned invited participation in an international science and planning workshop on reforestation for ecosystem restoration, and oral presentation on the benefits of forest regrowth for natural resources and ecosystem function in African dry tropical woodlands at the 2015 American Geophysical Union Meeting (October-December 2015).
    - Published peer-reviewed article on agricultural and rangeland use impacts for soil carbon and nitrogen in the Konya Basin, Turkey, published in the journal *Geoderma* (2014).

➢ Designed and led implementation of well-water quality assessment project in Tabora, Tanzania, which combined goals of baseline resource assessment with scientific training and outreach for local scientists and NGO staff to make recommendations for safe water use in rural villages.

- Project awarded $5,000 from competitive Brown University program to compare prevalence of nitrate pollution and coliform bacteria in deep and surficial aquifer wells, supplementing PhD projects.
- Planned work collaboratively with input from 3 organizations (UN-sanctioned Millennium Villages Project, the Tanzanian Agricultural Research Institute at Tumbi, and Tabora Development Trust Foundation, a local NGO in Tabora) to measure wells for which baseline data was lacking.
- Trained 5 staff members from 3 organizations in use of GPS units to collect well coordinates, clean water sampling techniques and field tests, and data organization and reporting using Microsoft Excel.
- Key Accomplishments (all 2014-15):
    - Following training, local scientists and staff successfully completed water sampling, data organization and analysis using project tools and protocols.
    - Unexpected finding of nitrate and bacteria contamination in deep wells led UN-MVP community health programs to recommend boiling water from deep wells, and explore causes of contamination in deep wells.
    - Produced report detailing project methods, successes and challenge of staff trainings, and water quality findings, which will be published as a book chapter in the upcoming 2015 MVP-Mbola Final Assessment report.

➢ Co-authored interdisciplinary assessment of human and ecosystem health impacts of oil development in the Ecuadorian and Peruvian Amazon for the Pan-American Health Organization (PAHO).

- Organized project with a team of 4 graduate students at University of Wisconsin-Madison spanning Sociology, Public Health and Geoscience backgrounds, and a representative from

PAHO, who identified the need for integrative study of oil development in lowland tropical rainforest regions.

- Developed non-technical written and graphical descriptions of terrestrial oil exploration and development processes through researching scientific/technical literature for the project team. The team co-wrote assessment report by learning and combining comparable summaries of literature from public and environmental health, sociology and other disciplines.
- Key accomplishments:
    - Completed final "HOLA" Report (Health impacts of OiL in the Amazon) summarized development opportunities, human health and environmental challenges of oil with a life-cycle and systems analysis approach; presented by teleconference to PAHO (2011).
    - Compilation of a new GIS including environmental data, publicly disclosed oil leases and other infrastructure for PAHO to identify future study areas in the Amazon (2010-2011).

➢ Established a volunteer water quality-monitoring chapter at Brown University DEEPS to participate in the University of Rhode Island Water Quality Watch extension program.

- Motivated to contribute to practical environmental projects in my hometown and learn about organization of citizen-science initiatives.
- Coordinated with URI program directors to follow a 24-week water-sampling schedule from May - October, supervised volunteers in taking basic limnology data (e.g. temperature, dissolved oxygen), schedule, led weekly sampling trips to a local lake, and reported data back to the URI directors.
- Key accomplishments:
    - Completed three consecutive seasons of water quality monitoring at a popular pond in Roger Williams Park, the largest city park in Providence, Rhode Island (2013-2015).
    - Recruited and trained10-15 volunteers per year, including students and staff across science and non-science departments at Brown University.

➢ Facilitated a collaboration among undergraduate remote sensing students and a Latin American-focused conservation non-profit (EcoLogic) to produce satellite-derived land and water quality change maps targeted toward EcoLogic's data needs

- Driven to connect teaching and mentorship of students with applied research and practical projects
- Successfully proposed an extended curriculum for student semester final projects by facilitating dialogue between Brown University professor and the EcoLogic Director, whom I met at a professional conference
- Developed two seminars and a short-course on digitizing geospatial data to teach undergraduate students and EcoLogic staff skills to link field and satellite data
- Key Accomplishments:
    - Six undergraduate students completed semester projects addressing forest cover change, land cover and water quality characterization in EcoLogic project sites in Honduras, Guatemala and Belize
    - Working as mentor and peer with students, led completion of a professional memo and presentation to EcoLogic's annual board meeting to share project results with the organization

Communication, facilitation and university government service

- Represented 50 graduate students from the Brown Department of Earth, Environmental and Planetary Sciences (DEEPS) and the 2500 graduate student body in university governance, including the University Resources Council (URC), which advises the President's Office in managing Brown's $960M budget.
    - Elected a departmental graduate student council representative for 3 annual terms and successfully applied to the Graduate Student Council Executive to serve as 1 of 2 representatives on the URC for a 2-year term (2014-2016).
    - Advocated for DEEPS graduate student concerns about academic support, employment policy, salaries, and health benefits with University administration.
    - Trained on budget structure and analysis of a large endowment-funded organization (URC), including budget modeling to balance major sources of revenue and expenditure, and participated in writing policy recommendations and voting on annual budget priorities such as faculty and staff compensation, facilities maintenance, and investments in University programs.
    - Key accomplishments:
        - Advocated successfully for graduate student salary raises and inclusion of dental among health benefits packages starting in 2015-2016 in University Resource Council deliberations (2014-15).
        - Negotiated successfully with the Graduate School to raise limits on graduate student employment hours within the university, but outside their major funding source, from as little as 20 hours per semester in some cases to 20 hours per week (2012-13).

- Employed as a writing coach and peer-mentor (emphasis on scientific and technical writing) for a combined 5 years between 2007-2013, and pursued training in facilitation skills and teaching development through undergraduate and graduate education.
    - Began studying the theory and practice of teaching writing and persuasive communication skills in the Brown Writing Fellows Program in 2006-2007, a course segueing into a work-study position as a peer-mentor for writing.
    - Pursued numerous opportunities to develop communication, teaching and facilitation skills: employed as a Writing Fellow peer-mentor (2007-2009), completed communication and facilitation training at UW-Madison, the Sheridan Center Teaching Certificate I at Brown, and worked as a Brown Writing Center Associate specialized on coaching revision of science and policy documents (2011-2013) before extended time away in Tanzania.
    - Key accomplishments:
        - Earned 3 certificates in training programs on communication, facilitation and teaching skills (2009-2012).
        - Completed 2 independent projects on science writing and communication skills: a group independent study project (GISP) organized at Brown University to explore communication challenges among professionals of different science disciplines (2007-2009), and a Writing Fellows project that reviewed what features of writing make scientific and technical texts clear and concise (2006).

PROFESSIONAL AFFILIATIONS:
PARTNERS: People and Reforestation in the Tropics: A Network for Education Research and Synthesis

(2014-present)
Member, American Geophysical Union (2008-present).

AWARDS AND HONORS:

- Nature Conservancy NatureNet Science Fellowship. 2016-2018.
- Presidential Management Fellowship – Science, Technology, Engineering and Math (STEM). 2016-2017
- Dissertation Fellowship, Brown University Graduate School. Full Tuition and Stipend Awarded Fall 2015 for Spring 2016.
- Graduate Research, Training and Travel Award, Brown Institute for Environment and Society (IBES), 2014. $5,000. Project title: Land cover change and land-use impacts on water quality of surficial aquifer and borehole wells in a developing Miombo Woodland landscape.
- Fellowship, US National Science Foundation (US-NSF) Partnership for International Research and Education (PIRE) Program, #0968211. "Land Use, Ecosystem Services and the Fate of Marginal Lands in a Globalized World." Full tuition and stipend for Spring 2013-Summer 2015. PI: Christopher Neill, Marine Biological Laboratory.
- Research Fellowship, Brown University Department of Geological Sciences, Full Tuition and Stipend Awarded Fall 2011- Spring 2012. .
- US-NSF IGERT Fellowship, (Interdisciplinary Graduate Education, Research and Training) #0549407, "Vulnerability and Sustainability in Coupled Human-Natural Systems." Awarded full tuition and stipend Sep. 2009 - Aug. 2011. PI: Dr. Jonathan Patz, University of Wisconsin-Madison. Affiliated Faculty Advisor: Dr. Mutlu Ozdogan.
- Senior Award, Department of Geological Sciences (now Earth, Environmental and Planetary Sciences), Brown University. May 2009. Awarded to member of the graduating class exemplifying Department values, ethic, service and citizenship.
- George I. Alden Trust UTRA Undergraduate Research Grant, Brown University Dean of the College. $3000. Jun-Aug 2008.

ADDITIONAL INFORMATION:

Citizenship:

- United States Citizen

Skills and Professional Development:

- Computing skills: Image processing (ENVI-IDL, Agisoft, R) with experience using Landsat, Modis, Quickbird, Worldview, AVIRIS, AVHRR data; GIS (ARCGIS), Statistics (R, Matlab), Microsoft Office.
- Field skills: Orienteering and GPS data management, forestry skills including tree inventory and measurement methods, use of photosensor equipment to measure leaf area (e.g. LICOR LAI-2200), soil profiling and sampling, field spectroscopy (e.g. use of ASD field spectrometer), hydrogeology methods including clean well water sampling and pump testing, limnology measurements including use of multi-probes (e.g. YSI probes) and gravity cores.
- Laboratory skills: Geochemical methods, use of dry combustion elemental analyzers, liquid-phase spectrophotomer, atomic emission spectrometer, basic reflectance spectroscopy of plants, soil and geological materials (e.g. ASD field spectrometer).
- Trainings and field courses:
    - Summer Field Course in Hydrology: Use of UAVs for Environmental Monitoring. University of Basilicata / Princeton University, Matera, Italy. Jul. 2015.
    - Training: Scientific Programming in IDL. Exelis ITT, Boulder CO. Nov. 2013

- Sheridan Center Teaching Certificate I: Sheridan Center, Brown University, Sep. 2011 – June 2012
- Training: Journey of Facilitation and Communication, UW-Madison, Madison, WI. June 2011.
- Hydrogeology Field Camp, University of Minnesota Twin Cities, Minneapolis, MN. Jul. 2008.
- Nyanza Project REU, Kigoma, Tanzania 2007.

Foreign Languages:

- Spanish. Low-Intermediate speaking, writing.

Swahili. Novice speaking, writing.

PREFACE

Introduction

Tropical dry forests cover large areas across the Americas, Asia, Australia and Africa and play important roles for global biogeochemical cycles and provision of natural resources in many countries (Murphy and Lugo 1986, Campbell 1996, Lambin *et al* 2003). They differ from humid tropical forests by having mean annual precipitation of less than 2000 mm, two to six-month dry seasons with little rainfall (<25 mm), lower mature forest biomass (<250 Mg ha^{-1}) and higher prevalence of deciduous trees (Murphy and Lugo 1986, Eamus and Prior 2001, Aber and Mellilo 1991). Seasonal and inter-annual water availability and fire dynamics exert strong influence on biogeochemical cycling, forest productivity and landscape phenology (Eamus & Prior, 2001). Forest structure and land cover are patchy mixtures of closed and open-canopy stands with variable tree (<30-100%) and grass cover, driven by variations in edaphic factors and past disturbance history (Eamus, 1999). Worldwide, they have long histories of land use and a low proportion of their global area under conservation management, compared to humid tropical forests and other biomes (Murphy and Lugo 1986, Bodart *et al* 2013). Studies across continents have found tropical dry forests re-growing after disturbance have the capacity to accrue biomass of mature systems within decades (Brown and Lugo 1990, Waring *et al* 2015, Williams *et al*

2008, McNicol *et al* 2015), indicating their viability as targets for restoration, and raising questions about how plant-soil biogeochemical processes work to support observed recoveries from disturbance.

Across global tropical dry forests, high net rates of forest loss (>2100 km^2 yr) indicate a need for improved conservation management (Hansen *et al* 2013). This need is acute in sub-Saharan Africa, which has the world's largest and most highly populated tropical dry forests (Murphy and Lugo 1986, Bodart *et al* 2013, Campbell 1996), and where land use and climate variability interactively exert extreme pressures on forest resources. Within the African dry tropics (3 million km^2, an area the size of Australia), the largest tropical dry forests are located in the Miombo Woodlands (Olson and Dinerstein 2002). The Miombo covers 2.5 million km^2 across ten countries, notably the Democratic Republic of Congo, Zambia, Zimbabwe, Malawi, Tanzania and Mozambique (Campbell 1996). Their landscapes are mosaics of mature forest, shifting cultivation and regrowing forests. As of 2015, over 150 million people in largely rural, poor communities depended directly on Miombo forests for resources such as wood-based fuels, timber, and ecosystem services supporting availability of food and clean water (United Nations, Department of Economic and Social Affairs 2015, Campbell 1996, Bodart *et al* 2013, Rudel *et al* 2013). By 2050, 190 million more people are projected to live in the Miombo – a change equivalent to adding the entire current population of Europe to this region (United Nations, Department of Economic and Social Affairs 2015). While activities of small land-holding households dominate land-use pressures and drivers of forest change, urban energy demands and demand for large-land acquisitions also contribute (Lambin and Meyfroidt 2011, Lyon and Dewitt 2012, Searchinger *et al* 2015, Hosonuma *et al* 2012, DeFries *et al* 2010). In increasingly common years of erratic rainfall, crop failure can result in increased incentive to harvest trees to sell as firewood, charcoal and timber as part of household incomes (Frost 1996, Lyon and Dewitt 2012, Chidumayo and Gumbo 2013). Feedbacks among population growth, demand for food and forest resources and climate variability amplify threats to Miombo forests.

Forest conservation needs in the Miombo create opportunities for ecosystem science to address key questions about biogeochemistry and land cover variability that inform land management and monitoring in African tropical dry forests. For nutrient cycling, it is unclear how the availability of nitrogen (N), phosphorus (P) and other elements important for tree growth change during regrowth following disturbance and widespread agricultural land use. Established nutrient cycling paradigms predict that phosphorus (P) ultimately limits productivity in tropical forests on highly weathered soils(Chadwick *et al* 1999, Davidson *et al* 2007). It is unclear if Miombo forest nutrient cycling behaves like other more-studied humid and dry Neotropical forests, or mixed tree-grass savanna systems(Davidson *et al* 2007, Bustamante *et al* 2004). Identifying patterns in nutrient cycling across regrowth and mature forest sites can expose mechanisms limiting or powering forest growth that might inform land-use strategies to encourage productivity or counteract negative impacts of variable rainfall.

The motivation to study land cover relationships to forest structure is that current widely-available optical satellite remote sensing products, using data such as Landsat and MODIS, fail to characterize Miombo forest cover change, or structural variables accurately at the spatial scales of forest cover variability and smallholder-managed land use (0.5-5 ha) (Tyukavina *et al* 2015, Palm *et al* 2010). Existing remote sensing methods do not account well for the complexity of Miombo forest structure and landscape phenology, which leads to patterns of land cover materials (green vegetation, non-photosynthetic vegetation and others) that confound many forest structure-satellite data relationships based on green vegetation measures. The orientation of much forest biomass mapping has been targeted for identifying high-biomass regions (100 Mg ha^{-1}or more) for REDD+ associated carbon credits (Baccini *et al* 2012). In contrast, much of the Miombo Woodland forest areas have biomass below 50 Mg ha^{-1}. The threshold of 50 Mg ha^{-1} biomass (roughly 25 Mg ha^{-1} carbon stocks) is important because it represents an average forest structure boundary between 30-40 year regrowth forests and mature forests found across the Miombo Woodland ecoregion (Williams *et al* 2008, Kalaba *et al* 2013, Chidumayo 2013, McNicol *et al* 2015). Attention to land cover-forest structure relationships in low-biomass regions is important for developing satellite monitoring methods to aid conservation management and restoration programs such as WRI's Afr100 initiative (WRI 2016), which focus on reforestation, afforestation and agroforestry in many low-biomass areas. Detailed comparisons between field data on land cover, forest structure, and satellite data has not been carried out for Miombo ecosystems. Development of better field-satellite forest data relationships, within and across different Miombo forest types, is a necessary step for improving the use remotely sensed data to monitor forest conditions and change at landscape scales in the Miombo and other tropical dry forests.

Research goals and questions

The overall goals of work in this thesis have been to assess forest nutrient cycling patterns during regrowth, and quantify land cover-tree structure relationships to improve optical remote sensing of forest conditions in the Miombo Woodlands. This thesis addresses three main research questions:

1. Across mature and regrowth Miombo forests, what are the patterns in availability of nitrogen, a key nutrient for forest growth, and evidence that it may constrain forest growth?

2. What land cover features, including tree canopy and ground cover materials, show the strongest relationships to tree basal area and biomass between field and satellite data across regrowth and mature Miombo forest sites comprising a low-to-high biomass gradient?

3. Between two distinct Miombo geographic regions, what relationships are consistent between satellite-derived land cover metrics and field data on tree structure that can improve estimation of tree biomass at landscapes scales over existing estimates, particularly for regions with low tree biomass (<50 Mg ha^{-1})?

Following this introduction, Chapters 1-3 are manuscripts reporting findings from three projects that addressed the questions above. Chapters 1 and 2 focus on a case study Miombo landscape in central Tanzania. Chapter 3 combines data and analyses for the western Tanzanian landscape and a contrasting Miombo landscape in southern Mozambique, including Gorongosa National Park. A synthesis concludes the thesis, which reviews key findings about biogeochemistry and forest land cover patterns in Miombo forests, unresolved questions, applications for conservation management, and priorities for future research.

A central motivation of this thesis has also been to address questions relevant for a concurrently active socioeconomic development project, The Millennium Villages Project (MVP). The MVP aimed to help rural communities achieve agricultural development, forest management, and other environmental, education and health-oriented Millennium Development (2000-2015) and Sustainable Development goals (2015+). Research projects were developed considering the ecosystem science information needs of scientists and staff in an MVP project area in western Tanzania, such as timescales of soil nutrient restoration during forest regrowth on fallow lands and map data on forest cover.

References

Aber J A and Mellilo J M 1991 *Terrestrial ecosystems*

Baccini a., Goetz S J, Walker W S, Laporte N T, Sun M, Sulla-Menashe D, Hackler J, Beck P S a., Dubayah R, Friedl M a., Samanta S and Houghton R a. 2012 Estimated carbon dioxide emissions from tropical deforestation improved by carbon-density maps *Nat. Clim. Chang.* **2** 182–5 Online: http://dx.doi.org/10.1038/nclimate1354

Bodart C, Brink A B, Donnay F, Lupi A, Mayaux P and Achard F 2013 Continental estimates of forest cover and forest cover changes in the dry ecosystems of Africa between 1990 and 2000 ed M McGeoch *J. Biogeogr.* **40** 1036–47 Online: http://doi.wiley.com/10.1111/jbi.12084

Brown S and Lugo A E 1990 Effects of forest clearing and succession on the carbon and nitrogen content of soils in Puerto Rico and US Virgin Islands *Plant Soil* **124** 53–64

Bustamante M M C, Martinelli L a., Silva D a., Camargo P B, Klink C a., Domingues T F and Santos R V. 2004 15 N Natural Abundance in Woody Plants and Soils of Central Brazilian Savannas (Cerrado) *Ecol. Appl.* **14** 200–13 Online: http://www.esajournals.org/doi/abs/10.1890/01-6013

Campbell B M 1996 *The Miombo in Transition : Woodlands and Welfare in Africa* vol 72 Online:

http://books.google.com/books?hl=en&lr=&id=rpildJJVdU4C&oi=fnd&pg=PR9&dq=The+Miombo+in+Transition+:+Woodlands+and+Welfare+in+Africa&ots=FMsmiYa2th&sig=_hEtp4U1rk54Sn8tgXWfkMD-v-8

Chadwick O a, Derry L a, Vitousek P M, Huebert B J and Hedin L O 1999 Changing sources of nutrients during four million years of ecosystem development *Nature* **397** 491–7

Chidumayo E N and Gumbo D J 2013 The environmental impacts of charcoal production in tropical ecosystems of the world: A synthesis *Energy Sustain. Dev.* **17** 86–94 Online: http://dx.doi.org/10.1016/j.esd.2012.07.004

Davidson E a, de Carvalho C J R, Figueira A M, Ishida F Y, Ometto J P H B, Nardoto G B, Sabá R T, Hayashi S N, Leal E C, Vieira I C G and Martinelli L a 2007 Recuperation of nitrogen cycling in Amazonian forests following agricultural abandonment. *Nature* **447** 995–8

DeFries R S, Rudel T, Uriarte M and Hansen M 2010 Deforestation driven by urban population growth and agricultural trade in the twenty-first century *Nat. Geosci.* **3** 178–81 Online: http://www.nature.com/doifinder/10.1038/ngeo756

Eamus D 1999 Ecophysiological traits of deciduous and evergreen woody species in the seasonally dry tropics *Trends Ecol. Evol.* **14** 11–6

Eamus D and Prior L 2001 *Ecophysiology of trees of seasonally dry tropics: Comparisons among phenologies* vol 32 Online: http://cat.inist.fr/?aModele=afficheN&cpsidt=14091981

Frost P 1996 *The Ecology of Miombo Woodlands* ed B M Campbell (Bogor, Indonesia: Center for International Forestry Research) Online: http://books.google.com/books?hl=nl&lr=&id=rpildJJVdU4C&pgis=1

Hansen M C, Potapov P V, Moore R, Hancher M, Turubanova S a, Tyukavina a, Thau D, Stehman S V, Goetz S J, Loveland T R, Kommareddy a, Egorov a, Chini L, Justice C O and Townshend J R G 2013 High-resolution global maps of 21st-century forest cover change. *Science* **342** 850–3 Online: http://www.ncbi.nlm.nih.gov/pubmed/24233722

Hosonuma N, Herold M, De Sy V, De Fries R S, Brockhaus M, Verchot L, Angelsen A and Romijn E 2012 An assessment of deforestation and forest degradation drivers in developing countries *Environ. Res. Lett.* **7** 044009 Online: http://stacks.iop.org/1748-9326/7/i=4/a=044009?key=crossref.1a00aa77eac35c904bf7e007011d4763

Lambin E F E and Meyfroidt P 2011 Global land use change, economic globalization, and the looming land scarcity *Proc. Natl. Acad. Sci. U. S. A.* **108** 3465–72

Lambin E F, Geist H J and Lepers E 2003 DYNAMICS OF LAND-USE AND LAND-COVER CHANGE IN TROPICAL REGIONS *Annu. Rev. Environ. Resour* **28** 205–41

Lyon B and Dewitt D G 2012 A recent and abrupt decline in the East African long rains *Geophys. Res. Lett.* **39** 1–5

Mayes M T, Mustard J F and Melillo J M 2015 Forest cover change in Miombo Woodlands: modeling land cover of African dry tropical forests with linear spectral mixture analysis *Remote Sens. Environ.* **165** 203–15

McNicol I M, Ryan C M and Williams M 2015 How resilient are African woodlands to disturbance from shifting cultivation? *Ecol. Appl.* 150407011925001 Online: http://www.esajournals.org/doi/abs/10.1890/14-2165.1

Murphy P G and Lugo A E 1986 Ecology of Tropical Dry Forest ECOLOGY OF TROPICAL DRY FOREST1 *Source Annu. Rev. Ecol. Syst.* **17** 67–88 Online:

http://www.jstor.org/stable/2096989

Olson D M and Dinerstein E 2002 The Global 200: Priority Ecoregions for Global Conservation *Ann. Missouri Bot. Gard.* **89** 199 Online: http://www.jstor.org/stable/3298564?origin=crossref

Palm C a., Smukler S M, Sullivan C C, Mutuo P K, Nyadzi G I and Walsh M G 2010 Identifying potential synergies and trade-offs for meeting food security and climate change objectives in sub-Saharan Africa *Proc. Natl. Acad. Sci.* **107** 19661–6 Online: http://www.pnas.org/content/107/46/19661\nhttp://www.ncbi.nlm.nih.gov/pubmed/20453198\nhttp://www.pnas.org/content/107/46/19661.full.pdf\nhttp://www.pnas.org/content/107/46/19661.short

Rudel T K, Rudel T, DeFries R, Rudel T, Uriarte M, Hansen M, Brink A, Hugh D, Chidumayo E, Mayaux P, Fisher B, Sayer J, Harcourt C, Collins N, Debroux L, Hart T, Kaimowitz D, Karsenty A, Topa G, Corden W, Neary J, Wunder S, Chidumayo E, Gumbo D, Malaisse F, Binzangi K, Rudel T, Asner G, Defries R, Laurance W, Grainger A, Hansen M, Stehman S, Potapov P, Harris N, Kauppi P, Ausubel J, Fang J, Mather A, Sedjo R, Waggoner P, Saatchi S, Ernst C, Philippe M, Astrid V, Catherine B, Musampa C, Pierre D, Peterson R and Janzen D 2013 The national determinants of deforestation in sub-Saharan Africa. *Philos. Trans. R. Soc. Lond. B. Biol. Sci.* **368** 20120405 Online: http://www.ncbi.nlm.nih.gov/pubmed/23878341

Searchinger T D, Estes L, Thornton P K, Beringer T, Notenbaert A, Rubenstein D, Heimlich R, Licker R and Herrero M 2015 High carbon and biodiversity costs from converting Africa's wet savannahs to cropland *Nat. Clim. Chang.* **5** 481–6 Online: http://www.nature.com/doifinder/10.1038/nclimate2584\npapers3://publication/d oi/10.1038/nclimate2584

Tyukavina A, Baccini A, Hansen M C, Potapov P V, Stehman S V, Houghton R A, Krylov A M, Turubanova S and Goetz S J 2015 Aboveground carbon loss in natural and managed tropical forests from 2000 to 2012 *Environ. Res. Lett. Environ. Res. Lett* **10** 74002–74002 Online: http://iopscience.iop.org/1748-9326/10/7/074002

United Nations, Department of Economic and Social Affairs P D 2015 *World population prospects: key findings and advance tables.* vol 1 Online: http://esa.un.org/unpd/wpp/Publications/Files/Key_Findings_WPP_2015.pdf

Waring B G, Becknell J M and Powers J S 2015 Nitrogen, phosphorus, and cation use efficiency in stands of regenerating tropical dry forest *Oecologia* 887–97 Online: http://dx.doi.org/10.1007/s00442-015-3283-9

Williams M, Ryan C M, Rees R M, Sambane E, Fernando J and Grace J 2008 Carbon sequestration and biodiversity of re-growing miombo woodlands in Mozambique *For. Ecol. Manage.* **254** 145–55

WRI 2016 AFR100: Africa Restoring 100 Million Hectares of Deforested and Degraded Land by 2030 Online: http://www.wri.org/our-work/project/AFR100/about-afr100

Table P1 Population of Miombo ecoregion nations in comparison to other major global population centers. The table below from the 2015 UN World Population prospects shows 2015 and project populations for 2050. Population growth remains a major factor affecting land use pressures and development in sub-Saharan Africa.

Miombo-ecoregion nations	2015 ($x10^6$)	2050 ($x10^6$)	Factor of increase
Tanzania	53.4	137.1	2.6
Mozambique	27.9	65.5	2.3
Angola	25.0	65.5	2.6
Malawi	17.2	43.2	2.5
Zambia	16.2	43.0	2.7
Zimbabwe	15.6	29.6	1.9
SUM	155.5	383.9	2.5
United States	321.7	388.9	1.2
Brazil	207.8	238.3	1.1
China	1,376.0	1,348.1	0.98
India	1 311.1	1,705.3	1.3
W. Europe	190.8	195.5	1.0

United Nations, Department of Economic and Social Affairs, Population Division (2015). World Population Prospects: The 2015 Revision

Figure P1 Location of the Miombo Woodlands (green) (2.5 million km^2) amidst seasonally dry tropical ecosystems globally (grey).

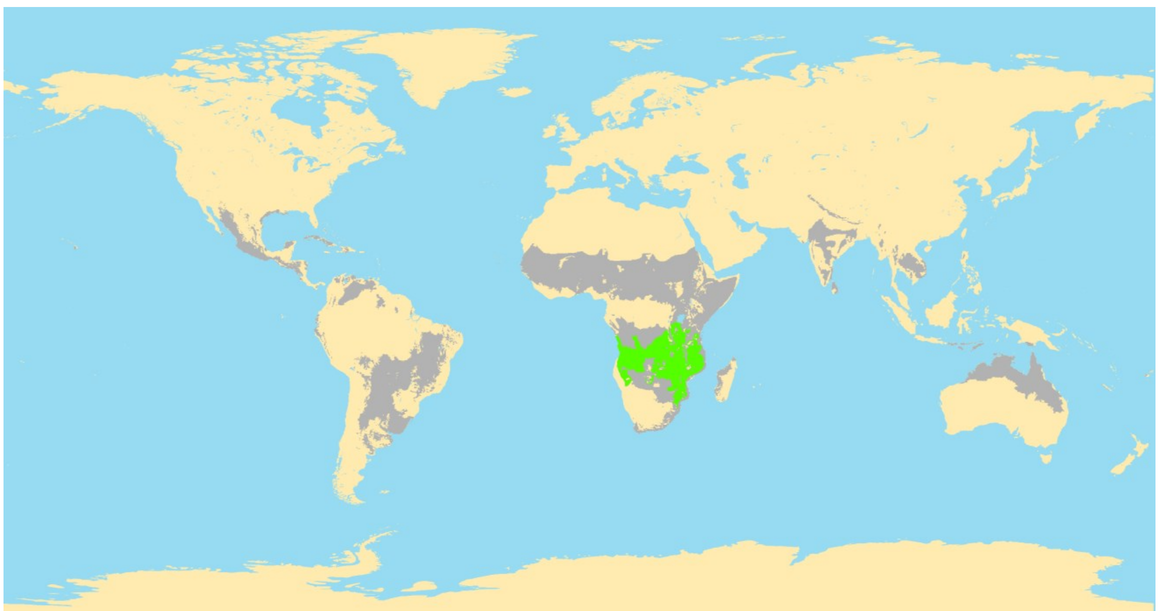

Data sources:

Dry tropical ecosystems GIS data: UMD global forest monitoring - http://www.glad.umd.edu/projects/gfm/drytropics/data.html

Miombo layer: Nature Conservancy ecoregions map - http://maps.tnc.org/gis_data.html

Figure P2 Drivers of forest loss and degradation across the global tropics. Though representing diverse landscapes, peoples and nations, African land use pressures differ broadly from other regions. Primary differences include the degree to which subsistence agriculture drives forest loss, and decentralized, small-scale forest resource use drives forest degradation (e.g. charcoal and wood fuel production).

Figure from Hosonua et al. 2012, Environmental Research Letters.

(A) Drivers of forest loss
(C) Drivers of forest degradation

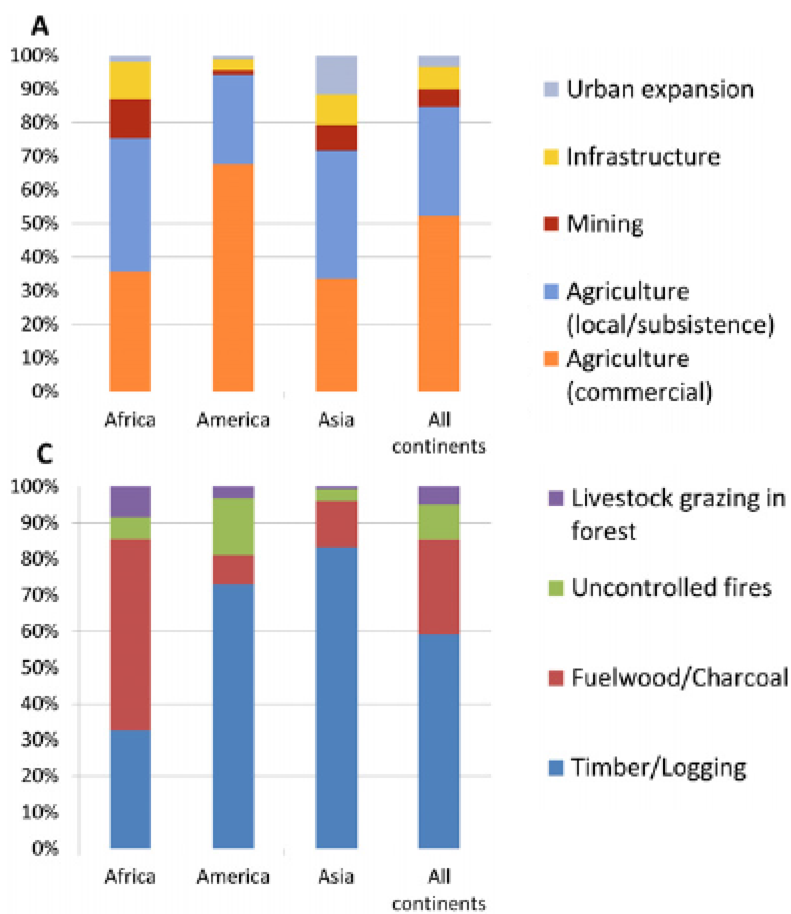

Figure P3 Photos of a Miombo landscape: Mbola, Uyui District, Tabora Region, Tanzania in wet and dry seasons, 2012. Tabora typifies developing Miombo landscapes as a patchy mosaic of shifting cultivation and woodlands under various status of maturity, regrowth age and recovery from disturbance. Agricultural practices at this time largely still depended on hand-hoes and limited use of livestock. Development pressures are building for larger-scale agricultural development, but given uncertainties in socioeconomic and political conditions, the future of these landscapes is still largely in question.

Wet season – January 2012. View at Mbola, Uyui District, Tabora, Tanzania.

Images shows a typical village agricultural scene (located in Region of Interest 4 in Chapter 2) with mixed maize-tobacco rotations.

ACKNOWLEDGEMENTS

My thanks extend to many people and institutions for inspiring my educational and professional journey before, during and after my PhD work. I first thank my advisors, Dr. John Mustard and Dr. Jerry Melillo for their guidance and support developing my PhD research. I thank Dr. Chris Neill, who led the NSF-PIRE project that drew me to apply to the Brown-MBL PhD program, for his enthusiastic guidance. I also thank Dr. Cheryl Palm and Dr. Gerson Nyadzi for important advising for framing conservation-relevant research. Thanks to my committee members Dr. Jung-Eun Lee, Dr. Ralph Milliken, and outside readers for their time reviewing this work.

On fronts of professional development, I thank Dr. Jan Tullis for her fundamental early and continuing guidance in Geosciences, teaching and science communication, especially in writing. I thank Dr. James Russell for his mentorship and friendship. Dr. Russell introduced me to the worlds of Geological Sciences, paleoclimatology, biogeochemistry, and overseas research in Africa, the importance of cultivating relationships with people for achieving large-scale scientific research, and the power of international research to improve livelihoods among communities where work occurs. Along with Dr. Russell, I thank Dr. Andrew Cohen (University of Arizona) and research mentor Dr. Jonathan Todd (The British Museum) for contributing to my first experience with independent research and ecosystem science in Africa, the Nyanza Project, which loomed large in inspiring me to think big about what and whom I wanted to work for as a scientist.

My M.S. work at University of Wisconsin-Madison was fundamental to developing the PhD work presented here, and I thank my M.S. committee members for their ongoing counsel: Dr. Mutlu Ozdogan, Dr. Robert Beattie and Dr. Erika Marin-Spiotta. Among these mentors, I deeply appreciate all Dr. Erika Marin-Spiotta's mentorship, attendance of my conference presentations and embrace of me as a colleague and friend since 2009. Special mention goes to Dr. Robert Beattie and Dr. Jonathan Patz at UW-Madison for the Certificate on Humans and the Global Environment (CHANGE) program, which was my foundation for strategic thinking on how to engage in inter- and multi-disciplinary work related to ecosystems science and natural resource conservation.

Close to my professional network of mentors and advisors, I thank all my colleagues in the Brown Department of Geological Sciences/Department of Earth, Environmental and Planetary Sciences, and larger Institute at Brown for the Study of Environment and Society (IBES) network for their humor, camaraderie and friendship, with special mention to my office-mate Stephanie Spera and close colleagues Xi Yang, Will Daniels, Will Longo and Sarah Ivory for pushing my thinking on topics relevant to my research. Thanks to Dr. David Murray, Dr. Joe Orchado and Dr. Yongsong Huang for helping me develop my laboratory and instrumental analysis skills along the way. At the Marine Biological Laboratory Ecosystems Center, I thank Rich McHorney, Dr. Marshall Otter, Dr. Kate Tully (University of Maryland) William Werner and the Plum Island LTER team for their assistance with lab and field equipment. I also thank Jessica Drysdale, KathiJo Jankowski for time spent discussing ecosystems science relating to land and sea.

In Tanzania, I have made many friends and developed networks which continue to teach and inspire my work. Asante sana to Dick Mlimuka at Tabora Development Foundation Trust for his far-reaching perspectives on environment and development issues in Tanzania, and for looking out for my well-being. Asante sana to my field crew: Kassim Massibuka, Ismail Raishidi, Temba Gilbert, Saidiki Omari and especially Moses Maganga for manning the front lines with me and reminding me, "Sema ni unataka." Kazi kubwa ni nzuri sana. Thanks to all village executive officers and elders who taught me about the Tabora landscape and many other things over multiple visits: Lazaro, Lady Sara, and others. Asante sana tena.

International field research involves logistics. I express warm appreciation two people who were fundamental for helping me stay on time and budget with my research: Bonnie Horta at IBES and Alison Maksym at The Ecosystems Center, MBL.

On personal fronts, spending upwards of 20 weeks per year traveling between Tanzania and the US, and splitting time between Brown in Providence, RI and The Marine Biological Lab in Woods Hole required patience and commitment on behalf of many friends. For your unwavering support, I thank friends Rhoni Rakos, Rich Rakos, Kennee Switzer, Mikaela Rakos, Andrew McIntosh, Emily McIntosh Ambinder and the McIntosh Clan spread far and wide, Brian Verne, Alexis Fischer, Alice Alpert, Diane Wetzel, Emily Hopper, Zachary Beily, Divya Vohra, Nathaniel Seelen, Fiona Hecksher, Adolfo Bailon and Sydney Clark, Will Longo and Mary Heskel for the roles they played during my life during these tumultuous times of exploration. Thanks to my long-time friends in the Smokin' Reed Saxtet alumni (Andrew Allegretti, Michael Feldman, and the Saxyderms network for adding joy through music – playing saxophone with you was the most consistent single activity I did besides remote sensing, labwork, flying on planes and driving or riding in cars for 5 years and did much to keep me in tune with my spirit.

Finally, I thank most of all my family, my parents James and Janet Mayes, my brother Gregory for supporting me and recognizing the value I place on people and relationships

over so many years. Thanks to my extended family as well for continued encouragement: my Uncles Barry and Michael Rigberg (and the entire Rigberg clan) grandmother Irene Mayes, Aunt Martha and Uncle Dave, Aunt Ellen, Aunt Mindy (and the entire Mayes Clan) for always reminding me of the big picture things in life.

I dedicate this thesis to two people. First, to Niwaeli Kimambo and her family for demonstrating perseverance, enthusiasm, love for life and generosity. Second, to Makenzie "Sawa kabisa" Pumla, who passed away before he could see this thesis completed, or come to the United States to meet President Obama. After an inopportune first meeting with him armed with a machete, Makenzie and his family befriended our research team, hosted us at their homes, and taught our research team much about the Miombo Woodland landscape from a Sukuma perspective. Mackenzie and many of his family members had an underlying spirit of curiosity and generosity that will forever serve me as a model for how to foster friendship and fellowship across cultures.

Mackenzie Pumla and Marc Mayes, November 2014, near Msiliembe Village, Uyui District, Tabora, Tanzania

TABLE OF CONTENTS

List of Tables

List of Figures

CHAPTER ONE

Nitrogen Cycle Patterns and Slow Recuperation during Regrowth in a sub-Saharan African Tropical Dry Forest (Miombo Woodland) Landscape

Marc Mayes[a,b], Jerry Melillo[b], Chris Neill[b,c], John Mustard[a], Cheryl Palm[d], Gerson Nyadzi[e]

a) Department of Earth, Environmental and Planetary Sciences, Brown University, Providence, Rhode Island, United States

b) The Ecosystems Center, Marine Biological Lab, Woods Hole, Massachusetts, United States

c) The Woods Hole Research Center, Falmouth, Massachusetts, United States

d) The Earth Institute, Columbia University, Palisades, New York, United States

e) Millennium Villages Project-Mbola, Tabora, Tanzania

[Submitted as a Letter to Nature Geoscience]

Tropical dry forests in eastern and southern Africa, which cover more than 2.5 M km^2 across several nations with the world's fastest-growing populations, are under heavy development pressures to meet the resource demands of more than 150 M people[1–3]. While conservation of mature and regrowth forests could help sustain biodiversity, wood and energy resources across the region, we lack science-based understanding of key ecosystem processes including nutrient cycling to guide forest landscape management and restoration[4–6]. Here we report on changes in the cycling of nitrogen (N), a plant-limiting nutrient, across a regrowth chronosequence spanning more than 100 years in the Tanzanian Miombo woodlands. Contrasting N cycle patterns of Neotropical forests[5–7], we find evidence that conditions of low ecosystem N-availability for trees persists across young to mature forest sites. Ammonium, not nitrate, is the dominant form of inorganic N available to trees with most of the ammonium becoming available to plants through soil organic matter decay during the wet season. While total N pools in the soil had no significant trends with forest regrowth along the chronosequence, total aboveground tree N pools increased at a relatively slow but constant rage (6 to 7 kg N ha^{-1} yr^{-1}). We found evidence that N fixation operates during regrowth and likely contributes, together with low levels of atmospheric N inputs, to the recovery of tree N pools. Our findings suggest that management to protect N-fixing trees and minimize ecosystem N losses by limiting fire, tree biomass removal and deadwood harvest, will be important for aiding the recovery of N during regrowth of African tropical dry forests amid changes in climate, such as shortening rainy seasons.

The Miombo Woodlands contain the largest tropical dry forest (TDF) regions in southern Africa (>2.5M km^2) and provide food, water, energy and income to > 150 M people[1,2] (Fig. S1.1). Up to 340 M people will live in the region and depend upon its natural resources by 2050, an increase of 190 M people which is larger than the present total population of western Europe[8]. Miombo TDFs are mosaics of mature forest, shifting cultivation and regrowing forests that have historically experienced high rates of disturbance from fire and long-term human use[1]. Growing demands for agricultural land and resources such as timber and wood-derived fuels have driven increased forest disturbance, globally high clearing rates since 2000 and threaten trees valuable for use and ecological function[2,9,10]. Increasing disturbance and climate changes such as shorter rainy seasons [11] will likely reduce forest extent, productivity, services and capacity for regrowth.

Patterns of nutrient cycling during forest regrowth and recovery from disturbance that could guide Miombo conservation and management are not well understood. Forest landscape restoration programs that include management for natural regeneration alongside agricultural development are expanding across southern and eastern Africa and have potential to maintain these forests and their services[12,13]. Improved knowledge of ecosystem processes, such as the recovery and maintenance of nutrient cycling during forest growth, can inform decisions regarding management strategies to conserve Miombo forest areas.

Established paradigms predict that phosphorus (P) ultimately limits productivity in tropical forests on highly weathered soils [6,14]. More recent experiments and regrowth sequences in Neotropical humid and dry forests indicate that the supply of plant-available soil mineral N (ammonium - NH_4^+ and nitrate – NO_3^-) in soil limits forest regrowth in initial decades, but that this limitation diminishes as forests mature [5,6,15,16]. Because Miombo TDFs are open woodlands with mixed tree-grass cover and frequent fire, it is unclear if they exhibit low-N conditions as found in tropical savannas such as the Brazilian cerrado, or more rapid recovery of N availability with regrowth as seen in other tropical forests[6,16,17]. Decades of research that indicate N availability varies between wet and dry seasons in dry tropical environments[18], and limits agricultural productivity in southern Africa[19] also suggest that N availability could limit rates of Miombo forest regrowth.

There are reasons to suspect that Miombo Woodlands have low N supplies relative to tree N demand, and that land use and climate change pressures may negatively affect N availability for forest growth. A substantial fraction (about 40%) of Miombo woodlands grow on sandy to sandy loam soils that are low in organic matter, and experience strong water and nutrient limitation[20–23]. Sandy to sandy loam soil textures limit buildup of soil organic matter that stores soil N[23,24]. Erratic rainfall distribution and seasonally dry conditions make extended periods of low soil moisture common and and limit decomposition and release of organic matter through the mineralization process[23–25]. Fire can further retard soil N buildup and exacerbate N loss through volatilization[1,26]. It is unclear what processes contribute significant N inputs to ecosystems as forest regrow, such as N fixation or atmospheric deposition.

Here we report on changes in the cycling of nitrogen (N) across a regrowth chronosequence spanning more than 100 years in the Tanzanian Miombo Woodlands. We evaluated indicators of ecosystem N availability from regrowth to mature forests, and between wet and dry seasons, across a 12-site forest chronosequence in Miombo woodlands of Tabora region, Tanzania (Fig. S1.1). Tabora has a mean annual temperature of 23.9^{0}C, and mean annual precipitation of 770 mm that falls Nov-May with a six-month dry season. Central Tabora has a population of 2.3M (2012) that is growing rapidly. It experienced net 15% forest area loss between 1995-2011, and forest areas that had regrown since 1995 comprised 16% of forest cover by 2011.[27].

We identified forest chronosequence sites with a combination of remote sensing [27], field visits and interviews with local people about land use and fire. All sites had > 3 yr since fire, comparable (~20-yr) history of maize cultivation prior to regrowth, flat topography (slope <2%) and sandy soils (>70% sand). We studied indicators of ecosystem N availability including soil total organic N, soil mineral N (NH_4^+ + NO_3^-), foliar N concentrations, foliar and soil $\delta^{15}N$, leaf area and leaf specific mass. We inventoried trees, measured diameter at breast height (dbh) and used Miombo-specific allometric equations and wood chemistry to estimate stem wood carbon (C) and N pools. We sampled leaves from a N-fixing tree (*Pterocarpus angolensis (Pa)*) and two non-N fixers to assess patterns of N fixation across sites. We used foliar N, specific leaf area and the difference in leaf-area measured between wet and dry seasons (dLAI), to estimate N demand for canopy leaf production across sites. We sampled soils in wet and late dry seasons to determine seasonal N availability and conducted 14-day (14d) laboratory incubations to quantify an index of potential soil N mineralization supply rates (Nmin potentials).

Multiple indicators showed lack of N cycle recovery over the first four decades of regrowth and low ecosystem N availability relative to aboveground tree N pools (Fig. 1.1). Soil total N stocks (0.59-0.98 Mg N ha^{-1} to 15 cm depth) (Fig 1.1a, Table S1.1) were low and did not increase with forest age. Ammonium-dominated soil extractable mineral N (Fig. 1.1b) and indicated that microbes and plants competed for a low supply of mineralized N[25]. Soil mineral N (NH_4^+ + NO_3^-) concentrations did not increase with site age across regrowth classes, and were significantly lower in 10-24 yr sites (Tukey HSD, $p = 0.021$) and 30-40 yr sites ($p = 0.026$) compared to mature sites in ANCOVA analyses (Fig. 1.1c) (see Table S1.6). Fourth, foliar and soil $\delta^{15}N$ lacked positive trends with increasing site age that would be indicative of increasing ecosystem N availability by 40 years of regrowth[6,20,28].

Compared to trends in soil N, N demand for tree canopy leaf production (Fig. 1.1e-f) increased six-fold with regrowth. Foliar N concentrations (Fig. 1.1g) did not increase across regrowth sites or indicate increasing N availability after 40 years of regrowth (Tables S1.4, S1.6). Mature forest sites of ~100 yr , however, did have significantly higher soil mineral N concentrations than regrowth sites (Fig. 1.1c) (Fig. S1.3, Table S1.2). In sum, the data suggested that N cycle recovery occurred slowly in Miombo TDFs, and that it took longer than 40 years for soil N availability to increase significantly above that of 10-24 and 30-40 yr regrowth sites.

Wet-dry season differences in N mineralization potentials were similar in magnitude to the age effects. For mature forests, wet season N mineralization potentials (average 5.54 kg N ha^{-1} $14d^{-1}$ ± 0.51 s.e.m.) were 3 times higher than the potentials measured in the dry season (average 1.98 kg N ha^{-1} $14d^{-1}$ ±1.03 s.e.m.) (Fig. S1.3, Table S1.2). For regrowth sites, wet season Nmin potentials (average 3.03 kg N ha^{-1} $14d^{-1}$ ± 0.31 s.e.m) were about 2 times higher than the dry season (average 1.54 kg N ha^{-1} $14d^{-1}$) (Table S1.2).

Net trends in ecosystem N resource pools across regrowth and mature forests (Table 1) showed clearly that trees accrue significant quantities of N, while there was no clear trend in surface soil N pools. From 3-4 yr sites to 30-40 yr sites, total aboveground tree N pools increased by a factor of 10 (8.0 – 11 kg N ha^{-1} yr^{-1} rate). From 40 yr regrowth to mature forests, tree N pools increased by 5.6 kg N ha^{-1} yr^{-1}. For both these periods, there were no significant net changes in soil total N or estimates of annual N mineralization (5-11% of total soil N pools – see Table S1.3). A question that emerges from the N budget terms above is where are trees acquiring 100s of kg N on decadal timescales, given the lack of clear trends in soil supplies?

Tree acquisition of several hundreds of kg of N across the chronosequence could come from two possible sources: recycling and redistribution of N from soil to vegetation over time, or through new inputs to the ecosystem, including N deposition and N fixation. Our data indicated that N fixation continued to operate across regrowth and mature forests, and contributed N inputs to tree and associated ecosystem-scale N accumulation. Foliar $\delta^{15}N$ from a large canopy N-fixing tree, *Pterocarpus angolensis (Pa)* was < 0 per mil across all regrowth and mature forest sites, indicating active N fixation (Fig. 1.2a, Table S1.5)[29]. This was consistent with past findings in Tanzania that *Pa* has root nodules with nitrogenase activity in Tanzania[30]. Foliar N concentrations of *Pa* were also significantly higher than non-N fixers across all sites (Fig. 1.2b, Table S1.5). Estimates of probable rates of N fixation in the dry tropics (2-6 kg N ha^{-1} yr^{-1})[31] are however lower than the tree N accumulation we observed. N deposition inputs could contribute ecosystem N inputs making their way to trees, although modeled deposition rates (3-5 kg N ha^{-1} yr^{-1})[32] for southern Africa are also low relative to the total tree N accumulation. Redistribution of N from soil to vegetation likely contributes to tree N accumulation as well. The variability in total soil N pools is large enough to accommodate some N redistribution to tree pools, but not the total amount we measured accumulating in trees by 100 yr (650 kg N ha^{-1}) without new ecosystem inputs. Further study of soil-vegetation N cycle exchanges at higher temporal resolution, soil N pools and tree rooting behavior with depth, measurements of basal area of N-fixing trees species in the over-story and understory, the functioning of free-living fixation and N deposition are all required to further constrain contributions of these N sources that power tree N accumulation with regrowth.

Several results have direct consequences for Miombo Woodland TDF management and conservation. Ammonium-dominated soil N pools across the chronosequence are a strong signal that N remains in limited supply young to mature Miombo forest sites[25]. Soil mineral N readily available for plant uptake did not recover by 40 yr of regrowth, while tree biomass accumulation accounted for all increases in total ecosystem N pools through the first decades of regrowth, while. This suggests that land management for forest regrowth should minimize ecosystem N losses by carefully managing fire, and discouraging the removal of tree biomass in regrowth sites, including cutting of live stems and removal of deadwood. Our findings also indicate that protection of N-fixing tree species could be an important part of strategies to maintain N in Miombo TDFs. *Pa,* a large (>15 m tall) canopy dominant tree, is an endangered species poached for its high-value timber[10]. Conservation of regrowth and mature forest areas will face challenges from development pressures also targeting these soils for agriculture[9]. Findings of reduced mineral N potentials in dry compared to wet seasons suggest that if climate change shortens rainy seasons in Miombo regions[11] and droughts (e.g. Zambian drought during the 2015-16 El Nino) become more common, N availability from mineralization might be reduced and could impact forest regrowth rates. More research is needed on African TDF ecosystem processes to understand limits to forest regrowth, including the dynamics of soil moisture variability and N mineralization, and the timing of soil N uptake by trees. With over 190 M more people projected to be living in and depending upon resources of Miombo TDF regions by 2050, proactively managing forest landscapes to maintain N supply to forest trees to maximize forest regrowth could contribute to more sustainable production of wood and other forest-based resources.

Methods Summary:

We studied N cycling indicators across mature and regrowth forest sites in Miombo Woodlands of Tabora province in western Tanzania (Figure S1.1). Climate is seasonally dry tropical, with MAT 25C and MAP 700-900 mm yr^{-1} falling November – April. We sampled 12 sites for foliar, canopy and soil measurements: 9 regrowth sites aged 3 yr. (2 sites), 4 yr., 10 yr., 16 yr., 24yr, 30 yr. and 40 yr. (2 sites), and 3 mature forest sites > 100 yr. Field sites were laid out as 50 m x 50 m plots in woodlands or regrowth sites on village or privately owned land in coordination with local authorities and land owners. We took foliar samples in the mid-wet season from a canopy N-fixing tree, *Pterocarpus angolensis* (family Fabaceae), and two non-N-fixing species, a common Miombo canopy dominant *Brachystegia spiciformis* (family Caesalpiniaceae) and a local pioneer species, *Terminalia sericea* (family Combretaceae), found on-site. Canopy data and soils were sampled in 4 circular subplots (10 m radius) located via a stratified random sampling design with one subplot in each 25 x 25 m quadrant of the main plot. We took optical measures of leaf-area using a LICOR-2200 at six points per subplot, during wet season maximum (Mar-Apr 2015) and mid-dry season (Jul 2015) minimum leaf cover conditions to calculate dLAI (wet-dry) as an estimate of the area of annual leaf production. We sampled soils at the center of each subplot at 0-5 cm and 5-15 cm depths in wet (Mar-Apr '15) and late dry seasons (Sep-Oct '15). Soils were sieved (2 mm) and composited for laboratory analyses of soil moisture (gravimetric moisture) and 24-hr potassium chloride (KCL) extractions. Soil KCl extracts were kept frozen and analyzed for mineral N (ammonium and nitrate) via spectrophotometric analyses. We assessed soil N mineralization via 14-day aerobic laboratory incubations in a dark room at ambient temperature (~28 C), begun on the same day as sampling, with repeat KCl extracts performed after 14 days. Wood biomass N was calculated using tree inventory data across sites and published values for wood percent N in Miombo trees (0.57% - see Supplementary Figure 2). One-factor ANOVA was used to test effects of site age on canopy dLAI and N demand. ANOVA or ANCOVA with Tukey's Honest Significant Difference tests, or Kruskal-Wallis tests with Wilcoxon rank-sum tests were used to assess effects of site age and tree species (foliar data) or depth (soil) on foliar and soil data respectively. We followed procedures established by Davidson et al. (2007) for assessing N cycling indicators across regrowth chronosequences, assessing effects of site age as rank and the logarithm of site age on N cycling indicators, and repeating analyses on data excluding mature forests to test for trends among regrowth sites alone.

References:

1. Frost, P. *The Ecology of Miombo Woodlands*. *The Miombo in Transition: Woodlands and Welfare in Africa* (Center for International Forestry Research, 1996).

2. Rudel, T. K. *et al.* The national determinants of deforestation in sub-Saharan Africa. *Philos. Trans. R. Soc. Lond. B. Biol. Sci.* **368,** 20120405 (2013).

3. Hansen, M. C. *et al.* High-resolution global maps of 21st-century forest cover change. *Science* **342,** 850–3 (2013).

4. Poorter, L. *et al.* Biomass resilience of Neotropical secondary forests. *Nature* **530,** (2016).

5. Waring, B. G., Becknell, J. M. & Powers, J. S. Nitrogen, phosphorus, and cation use efficiency in stands of regenerating tropical dry forest. *Oecologia* 887–897 (2015). doi:10.1007/s00442-015-3283-9

6. Davidson, E. a *et al.* Recuperation of nitrogen cycling in Amazonian forests following agricultural abandonment. *Nature* **447,** 995–998 (2007).

7. Hedin, L. O., Brookshire, E. N. J., Menge, D. N. L. & Barron, A. R. The Nitrogen Paradox in Tropical Forest Ecosystems. *Annu. Rev. Ecol. Evol. Syst.* **40,** 613–635 (2009).

8. United Nations, Department of Economic and Social Affairs, P. D. *World population prospects: key findings and advance tables.* **1,** (2015).

9. Searchinger, T. D. *et al.* High carbon and biodiversity costs from converting Africa's wet savannahs to cropland. *Nat. Clim. Chang.* **5,** 481–486 (2015).

10. Schwartz, M. W., Caro, T. M. & Banda-Sakala, T. Assessing the sustainability of harvest of Pterocarpus angolensis in Rukwa Region, Tanzania. *For. Ecol. Manage.* **170,** 259–269 (2002).

11. Lyon, B. & Dewitt, D. G. A recent and abrupt decline in the East African long rains. *Geophys. Res. Lett.* **39,** 1–5 (2012).

12. Chazdon, R. L. Beyond Deforestation : Restoring Degraded Lands. *Communities* **1458,** 1458–1460 (2008).

13. WRI. AFR100: Africa Restoring 100 Million Hectares of Deforested and Degraded Land by 2030. (2016). Available at: http://www.wri.org/our-work/project/AFR100/about-afr100.

14. Chadwick, O. a, Derry, L. a, Vitousek, P. M., Huebert, B. J. & Hedin, L. O. Changing sources of nutrients during four million years of ecosystem development. *Nature* **397,** 491 – 497 (1999).

15. Davidson, E. A. *et al.* Nitrogen and Phosphorus Limitation of Biomass Growth in a Tropical Secondary Forest. *Ecol. Appl.* **14,** S150–S163 (2004).

16. Saynes, V., Hidalgo, C., Etchevers, J. D. & Campo, J. E. Soil C and N dynamics in primary and secondary seasonally dry tropical forests in Mexico. *Appl. Soil Ecol.* **29,** 282–289 (2005).

17. Bustamante, M. M. C. *et al.* 15 N Natural Abundance in Woody Plants and Soils of Central Brazilian Savannas (Cerrado). *Ecol. Appl.* **14,** 200–213 (2004).

18. Wang, L., Manzoni, S., Ravi, S., Riveros-Iregui, D. & Caylor, K. Dynamic interactions of ecohydrological and biogeochemical processes in water-limited systems. *Ecosphere* **6,** art133 (2015).

19. Vitousek P.M. et al. Nutrient imbalances in agricultural development. *Science (80-.).* **324,** 1519–1520 (2009).

20. Martinelli, L. a. *et al.* Nitrogen stable isotopic composition of leaves and soil: Tropical versus temperate forests. *Biogeochemistry* **46,** 45–65 (1999).

21. Churkina, G. & Running, S. W. Contrasting Climatic Controls on the Estimated Productivity of Global Terrestrial Biomes. *Ecosystems* **1,** 206–215 (1998).

22. Fisher, J. B., Badgley, G. & Blyth, E. Global nutrient limitation in terrestrial vegetation. *Global Biogeochem. Cycles* **26,** n/a–n/a (2012).

23. Palm, C., Sanchez, P., Ahamed, S. & Awiti, A. Soils: A Contemporary Perspective. *Annu. Rev. Environ. Resour.* **32,** 99–129 (2007).

24. Schmidt, M. W. I. *et al.* Persistence of soil organic matter as an ecosystem property. *Nature* **478,** 49–56 (2011).

25. Schimel, J. & Bennett, J. Nitrogen mineralization: challenges of a changing paradigm. *Ecology* **85,** 591–602 (2004).

26. Stromgaard, P. Immediate and long-term effects of fire and ash- fertilization on a Zambian miombo woodland soil. **41,** 19–37 (1992).

27. Mayes, M. T., Mustard, J. F. & Melillo, J. M. Forest cover change in Miombo Woodlands: modeling land cover of African dry tropical forests with linear spectral mixture analysis. *Remote Sens. Environ.* **165,** 203–215 (2015).

28. Amundson, R. Global patterns of the isotopic composition of soil and plant nitrogen. *Global Biogeochem. Cycles* **17,** 1031 (2003).

29. Shearer, G. & Kohl, D. H. Natural15N abundance as a method of estimating the contribution of biologically fixed nitrogen to N2-fixing systems: Potential for non-legumes. *Plant Soil* **110,** 317–327 (1988).

30. Högberg, P. Nitrogen-fixation and nutrient relations in savanna woodland trees (Tanzania). *J. Appl. Ecol.* **23,** 675–688 (1986).

31. Houlton, B. Z., Wang, Y.-P., Vitousek, P. M. & Field, C. B. A unifying framework for dinitrogen fixation in the terrestrial biosphere. doi:10.1038/nature07028

32. Lamarque, J.-F. Multi-model mean nitrogen and sulfur deposition. *Atmos. Chem. Phys. Discuss* **13,** 6247–6294 (2013).

Supplementary information: 3 figures, 7 tables.

Acknowledgements We thank staff of Tanzania Western Zone Agricultural Research Institute at Tumbi, Tabora (Fabian Bagayrama, Peter Matata, Kassim Massibuka, Ismail Raishidi, Temba Gilbert), members of the Millennium Villages Project-Tabora Office (Kagya Eliezer) and New York staff (Claire Ward), and Tabora Development Foundation Trust (Dick Mlimuka, Maganga, Sadiki Omari) for their assistance with project logistics, locating field sites, translation, field and laboratory work. We thank the Tanzania Forest Service, Tanzania Forest Research Institute (TAFORI) and Tanzania Army Anti-Poaching Unit for help securing site access, and locals of villages in Uyui District, Tabora, Tanzania for their time discussing land use history and permission sampling forests on village land. We also thank faculty and staff at Marine Biological Lab Ecosystems Center for assistance with sample processing and loaning of field instruments (PIE-LTER). The project was funded by the US National Science Foundation Partnerships for International Research and Education (PIRE) program, project title "Ecosystems and Human Well-Being" (Award # 0968211) PI Chris Neill. Additional research and dissertation support was provided to Marc Mayes from Brown University. The project was completed with permission and cooperation from the Tanzania Commission on Science and Technology (COSTECH Permit Nos. 2013-261-NA-2014-199 and 2015-183-ER-2014-199).

Author contributions: M.T.M. led project design, field work, laboratory work, analysis and writing of the paper. J.M.M., J.F.M. and C.N. advised the project and participated in writing the paper. C.P. and G.N. assisted with fieldwork and participated in writing the manuscript, and G.N. coordinated in-country research logistics and permissions.

TABLES: CHAPTER ONE

Table 1.1 Nitrogen (N) in surface soils and aboveground tree biomass across a forest regrowth chronosequence in the Miombo Woodlands, Tabora Tanzania. Site age effects on N resources were tested via ANOVA and log-linear age models and are indicated in superscript as significant^{i} or insignificant^{0} ($p < 0.05$). During regrowth (3-4 to 30-40 yr), N resource pools in aboveground woody biomass and canopy leaves increased significantly by rates of 8.1-11.1 kg N ha^{-1}. Soil N resources showed no significant trends with site age. By column, quantities with different superscript letters were different (Tukey Honest Significant Difference).

	Soils	Trees		
Site age class (n sites)	Total soil organic N^{o} 0-15 cm	^N in woody biomass^{i}	N demand for canopy leaf biomass^{i}	^Total N wood + canopy leaves^{i}
	kg ha^{-1}	kg N ha^{-1}	kg N ha^{-1} (yr^{-1})	kg N ha^{-1}
3-4 yr (3)	970 (216)	9.75 (3.98)^{c}	11.6 (7.40)^{b}	21.3 (9.2)^{c}
10-24 yr (3)	594 (52)	53.7 (4.94)^{b}	27.3 (10.4)^{b}	81.0 (14.1)^{bc}
30-40 yr (3)	981 (188)	252 (35.3)^{ab}	67.9 (6.6)^{ab}	320 (47.9)^{ab}
Mature (3) > 100 yr	857 (103)	568 (158)^{a}	86.1 (8.7)^{a}	654 (160)^{a}

Table S1.1 Physical and chemical characteristics of soils across a Miombo forest regrowth chronosequence by depth. Values listed are averages with standard error of the mean in parentheses. Accompanies Figure 1.1.

Age class	N sites	Depth (cm)	Bulk density g cm^{-3}	C g kg^{-1}	N g kg^{-1}	$\delta^{15}N$ o/oo	C:N ratio (mol)	SOC Mg ha-1	Total N Mg ha-1
3-4 yr	3	0-5	1.60 (0.05)	5.80 (1.28)	0.49 (0.13)	4.62 (0.68)	14.0 (0.67)	4.60 (0.89)	0.390 (0.092)
		5-15	1.57 (0.05)	4.63 (1.07)	0.37 (0.01)	4.82 (0.91)	14.5 (0.62)	7.22 (1.50)	0.581 (0.125)
		0-15	na	na	na	na	na	11.8 (2.37)	0.970 (0.216)
10-24 yr	3	0-5	1.52 (0.09)	4.14 (0.13)	0.30 (0.02)	3.14 (0.51)	15.9 (0.61)	3.16 (0.25)	0.233 (0.027)
		5-15	1.61 (0.03)	3.11 (0.07)	0.22 (0.01)	4.00 (0.37)	16.3 (0.67)	5.01 (0.15)	0.360 (0.025)
		0-15	na	na	na	na	na	8.17 (0.40)	0.594 (0.052)
30-40 yr	3	0-5	1.56 (0.07)	9.35 (2.36)	0.61 (0.14)	2.73 (0.43)	17.6 (0.45)	7.30 (1.83)	0.479 (0.111)
		5-15	1.63 (0.01)	4.81 (0.95)	0.31 (0.05)	3.62 (0.37)	18.1 (1.17)	7.85 (1.48)	0.502 (0.079)
		0-15	na	na	na	na	na	15.2 (3.30)	0.981 (0.188)
Mature >100 yr	3	0-5	1.54 (0.07)	7.58 (1.43)	0.53 (0.08)	3.51 (0.23)	16.5 (1.12)	5.88 (1.31)	0.412 (0.075)
		5-15	1.59 (0.02)	3.97 (0.40)	0.28 (0.02)	3.83 (0.68)	16.6 (1.00)	6.30 (0.61)	0.445 (0.036)
		0-15	na	na	na	na	na	12.2 (1.90)	0.857 (0.103)

Table S1.2 Soil mineral N (ammonium - NH_4^+ plus nitrate – NO_3^-) concentrations and N mineralization potentials from 14-day lab incubations across a Miombo forest regrowth chronosequence (accompanying Figure 1.b-c and Figure S1.3).

Age class *n=3 sites*	Depth cm	Soil N concentration (NH4+NO3) mg kg^{-1} soil (dry season)	NH_4^+: NO_3^- (dry season)	Soil N mineralization potential (14d lab) NH4+NO3 kg ha^{-1} $14d^{-1}$ (wet season)	Soil N mineralization potential (14d lab) NH4+NO3 kg ha^{-1} $14d^{-1}$ (dry season)
3-4	0-5	2.36 (1.1)	55.1 (19.5)	0.59 (0.12)	0.36 (0.20)
	5-15	1.27 (0.4)	22.1 (11.1)	2.12 (0.81)	1.14 (0.46)
	0-15			2.71 (0.90)	1.51 (0.60)
10-24	0-5	1.73 (0.30)	65.6 (21.0)	0.72 (0.25)	0.37 (0.14)
	5-15	0.92 (0.19)	27.8 (6.55)	2.92 (0.30)	0.82 (0.49)
	0-15			3.64 (0.55)	1.19 (0.61)
30-40	0-5	1.71 (0.24)	61.9 (26.0)	1.03 (0.33)	0.56 (0.07)
	5-15	0.94 (0.16)	30.7 (8.29)	1.67 (0.64)	1.36 (1.01)
	0-15			2.70 (0.95)	1.92 (1.08)
Mature >100	0-5	4.00 (0.67)	54.5	1.89 (0.42)	0.76 (0.46)
	5-15	1.54 (0.04)	25.2 (5.14)	3.65 (0.13)	1.22 (0.57)
	0-15			5.54 (0.51)	1.98 (1.03)

Table S1.3 Estimates of annualized soil N mineralization rates. N mineralization rates obtained from 2-week lab incubations in wet and dry seasons were scaled to a hypothetical year with 50% weighting between wet and dry season weeks.

	Soil N resources 0-15 cm		
Site age class (n sites)	Total soil organic N° kg ha^{-1}	Est. annualized soil mineral N potentials° (NH_4^+ + NO_3^-) kg N ha^{-1} yr^{-1}	Est. percent total soil N mineralized per year (%)
3-4 yr (3)	970 (216)	54.9 (8.17)	5.7
10-24 yr (3)	594 (52)	62.8 (13.5)	11
30-40 yr (3)	981 (188)	60.1 (11.4)	6.1
Mature (3) > 100 yr	857 (103)	97.9 (15.9)	11

Table S1.4 Average foliar chemistry and canopy data grouped by forest regrowth age class. (accompanying Fig. 1.1e-g).

Age Class yr (n trees)	Foliar N g kg-1	Foliar C:N mol	LAI_{wet} Mar-Apr '15	LAI_{dry} July '15	$LAI_{wet-dry}$	Canopy N kg N ha^{-1}
3-4 (11)	24.9 (1.8)	23.5 (1.7)	0.63 (0.30)	0.21 (0.02)	0.41 (0.28)	11.6 (7.4)
10-24 (18)	21.9 (1.4)	27.7 (1.9)	1.80 (0.50)	0.61 (0.05)	1.19 (0.48)	27.3 (10.4)
30-40 (12)	22.3 (2.1)	27.6 (3.1)	3.35 (0.36)	0.81 (0.04)	2.53 (0.40)	67.9 (6.6)
Mature >100 (12)	25.8 (2.2)	24.3 (2.2)	4.81 (0.03)	1.38 (0.09)	3.43 (0.06)	86.1 (8.7)

Table S1.5 Foliar data grouped by tree species and forest regrowth age class (accompanying Fig. 2).

Species	Age class yr	N trees	Foliar %C	Foliar N g kg^{-1}	C:N mol	d^{15}N ($^{o}/_{oo}$)	SLA g m^{-2}
Mninga	3-4	3	46.7 (0.3)	30.8 (2.6)	17.9 (1.6)	-0.16 (0.54)	102 (11.0)
Pterocarpus	10-24	6	47.2 (0.2)	28.7 (0.6)	19.3 (0.4)	-1.16 (0.24)	93.9 (7.7)
angolensis,	30-40	4	46.4 (0.3)	29.6 (0.6)	18.3 (0.4)	-1.31 (0.21)	81.2 (1.8)
fam. Fabaceae	Mature	4	48.5(0.32)	32.9 (2.0)	17.4 (0.8)	-0.94 (0.54)	82.8 (5.2)
Mtundu	3-4	4	48.4 (0.4)	26.3 (1.5)	21.7 (1.3)	3.01 (1.02)	112 (7.7)
(Brachystegia	10-24	6	49.6 (0.4)	22.5 (0.7)	25.9 (0.8)	1.83 (0.56)	104 (10.8)
Spiciformis,	30-40	4	47.9 (0.7)	24.4 (1.1)	23.1(0.9)	1.71 (0.40)	114(3.8)
fam. Caesal.	Mature	4	50.1 (0.9)	25.1 (2.2)	23.7 (1.6)	1.62 (0.70)	99.1 (12.3)
Mzima	3-4	4	47.2 (0.3)	18.9 (1.3)	29.4 (2.0)	4.15 (2.45)	142 (6.8)
Terminalia	10-24	6	46.8 (0.3)	14.5 (0.5)	37.9 (1.2)	0.81 (0.11)	153(9.2)
Sericea,	30-40	4	46.2 (0.3)	13.1 (0.6)	41.5 (1,9)	0.54 (0.63)	144 (13.1)
fam. Combretaceae	Mature	4	48.6 (1.2)	19.4 (3.9)	31.8 (4.2)	1.42 (0.54)	125 (12.7)

Table S1.6 Model summaries of forest site age and other co-variate effects on N cycle indicators (accompanying Fig. 1.1, Table 1.1 and Fig. S1.3).

Dependent variable	---Age as rank--- (model type in parentheses) [other factors in brackets]	---Log age---	Mature forests excluded ---Log Age or Kruskal-Wallis ---
Foliar ^{15}N	Kruskal-Wallis **Age** **Chi2 = 16.4, p <0.001** **Species** **Chi2 = 80.2, p <0.001**	NA (data not transformable to normal)	Kruskal-Wallis **Age** **Chi2 = 8.13, p = 0.017** **Species** **Chi2 = 28.4, p < 0.001**
Foliar %N	Kruskal-Wallis Age Chi2 = 3.94, p = 0.3485 **Species** **Chi2 = 36.0, p < 0.001**	NA (data not transformable to normal)	Kruskal-Wallis Age Chi2 = 1.39, p = 0.500 **Species** **Chi2 = 32.8, p < 0.001**
dLAI wet-dry season	(One-factor ANOVA) **Age** **P = 0.015** **R2 = 0.772, p = 0.015**	**Age** **P <0.001** **R2 = 0.859, p <0.001**	**Age** **P < 0.001** **R2 = 0.706, p = 0.011**
Gross Canopy N demand	(One-factor ANOVA) **Age** **p = 0.008** **R2 = 0.815, p = 0.009**	**Age** **p <0.001** **R2 = 0.821, p < 0.001**	**Age** **p = 0.015** **r2 = 0.6693**
Soil NO3- : NH4 (dry season)	(Kruskal-Wallis) Age **Depth** p = 0.516 **p = 0.008**	NA (data not transformable to normal)	Age depth p = 0.676 p = 0.085 chi2 chi2 0.785 2.97
Soil NH4:NO3- (dry season	Model 1: One-factor ANOVA Age P = 0.8041 *ns Model 2 – ANCOVA Age+depth+temp+moist Age Moisture P = 0.608 p = 0.051 **Depth** Temp. **P = 0.003** p = 0.603 *Model r2 = 0.417* *P = 0.035*	Model 1: age alone Age P = 0.698 *ns Model 2 – ANCOVA Age+depth+temp+moist Age Moisture P = 0.389 p = 0.084 **Depth** Temp. **P = 0.003** p = 0.908 *Model r2 = 0.432* *P = 0.012*	Model 1: age alone Age P = 0.435 *ns Model 2 – ANCOVA Age+depth+moist_temp Age Moisture P = 0.325 p = 0.101 **Depth** Temp. **p = 0.008** p = 0.453
Soil NO3+NH4 – N mg kg-1 soil	Model 1: One-factor ANOVA	Model 1: age alone Age	Model 1: age alone Age

(dry season)	Age p = 0.115 r^2 = 0.1388 Model 2 ANCOVA – age + depth [temp+moist co-variates] **Age** **Depth** **p = 0.015** **p = 0.003** *model* *r2 = 0.584 p = 0.001*	p = 0.183 r^2 = 0.037 *model not significant Model 2: age and depth Age **Depth** p = 0.108 **p = 0.002** *model* r^2 = 0.357, p = 0.004	p = 0.997 *model not significant Model 2: age and depth Age **Depth** p = 0.995 **p = 0.010** *model* r^2 = 0.357 (p = 0.004)
Soil Total Nitrogen 0-5, 5-15 cm depths	Model 1: One-factor ANOVA Age p = 0.088 *model p = 0.0876, *ns Model 2: ANCOVA – age + depth [temp + moist co-variates] Age Depth p = 0.068 p = 0.097 *model* *r^2 = 0.213 p = 0.018*	Model 1 Age p = 0.807 r^2 = 0.040 *model p = 0.807 *ns Model 2: age and depth Age p = 0.802 Depth p = 0.13 *model p = 0.325 *ns	Model 1: age alone Age p = 0.743 *model not significant Model 1: age alone Age p = 0.743 *model not significant Model 2: age and depth Age p = 0.735 Depth = 0.173 *model not significant
Soil N min 0-15 cm: Wet and Dry Season Combined	ANOVA – Season + Age **Season** Age **p = 0.002** p = 0.205 *model* *r^2 = 0.359, p = 0.013*	Age + Season Season Age **p = 0.003** p = 0.185 *model* *r^2 = 0.327, p = 0.006*	Age + Season **Season** Age **P = 0.031** 0.964 *Model* *r^2 = 0.178, p = 0.090*
Soil d15N 0-5 cm, 5-15 cm depths	Model 1: One-factor ANOVA Age p = 0.0728 *model not significant Model 2: ANCOVA – age + depth [temp + moist co-variates] **Age** Depth **p = 0.033** p = 0.084 Temp. (dry season) **p =0.037** *model* *r^2 = 0.399 p = 0.018*	Model 1 **Age** **p = 0.026** *r^2 = 0.169* Model 2: age + depth+temperature (dry season) **Age p = 0.001** Depth p = 0.013 **Temperature – dry season** **p = 0.014** *model* *r^2 = 0.4033, p = 0.004*	Model 1 **Age** **p = 0.006** *r^2 = 0.3404* Model 2: age + depth + temperature (dry season) **Age p < 0.001** Depth p = 0.173 **Soil temp. p < 0.050** **model not significant* *model* *R^2= 0.540, p = 0.003*
Soil Organic	Model 1: One-factor	Model 1	Model 1: age alone

Carbon 0-5 cm, 5-15 cm depths	ANOVA Age $p = 0.099$ *model not significant Model2: ANOVA – age+depth Age Depth $p = 0.079$ $p = 0.092$ *$r^2 = 0.236, p = 0.057$*	Age $p = 0.983$ *model not significant Model 2: age and depth Age $p = 0.982$ Depth $p = 0.013$ *model $p = 0.313$ *ns	Age $p = 0.497$ *model not significant Model 2: age and depth Age $p = 0.483$ Depth $p = 0.164$ **model not significant*
Annualized soil mineral N production potentials 0-15 cm ($NH_4^+ + NO_3^-$)	Model: One-factor ANOVA-age Age $P = 0.14$ $R^2 = 0.280, p = 0.141$ *model not significant	Model: Age Age $P = 0.0791$ $r^2 = 0.204, p = 0.079$ *model not significant	Model: Age Age $P = 0.8046$ $R^2 = -0.132, p = 0.8046$ *model not significant
Aboveground tree N: N in woody biomass (log transformed prior to analysis)	Model: One-factor ANOVA- age Age $P < 0.001$ *$R^2 = 0.864, p < 0.001$*	Model: Age Age $P < 0.001$ $R^2 = 0.824, p < 0.001$	Model: Age Age $P = 0.002$ $R^2 = 0.749, p = 0.002$
Aboveground tree N: Total (woody biomass + canopy leaves) (log transformed prior to analysis	Model: One-factor ANOVA-age Age $P < 0.001$ $r^2 = 0.839$ $p < 0.001$	Model: Age Age $P < 0.001$ $R^2 = 0.819, p < 0.001$	Model: Age Age $P = 0.002$ $R^2 = 0.717, p = 0.002$

Table S1.7 Comparisons of foliar chemistry results among tree species and forest regrowth age classes (accompanying Fig. 2).

Variable	Test	Result
Foliar d15N	**-Kruskal-Wallis, species** Wilcox MT vs MZ Wilcox MT vs MN Wilcox MN vs MZ	**Kruskal-Wallis chi-squared = 45.725, df = 11, p-value = 3.616e-06** **W = 244, p-value = 0.008714** **W = 0, p-value = 4.408e-10** **W = 3, p-value = 3.085e-09**
	-Kruskal-Wallis, class Wilcoxon *Regrowth site comparisons* Wilcox C01 vs C02 Wilcox C01 vs. C03 Wilcox C02 vs C03 *Regrowth to mature site comparisons* Wilcox C01 vs VIL Wilcox C02 vs VIL Wilcox C03 vs VIL	**Kruskal-Wallis chi-squared = 8.6771, df = 3, p-value = 0.03 391** **W = 154, p-value = 0.0125** **W = 107, p-value = 0.01057** W = 118, p-value = 0.6921 **W = 99, p-value = 0.04388** W = 96, p-value = 0.6315 W = 56, p-value = 0.3777
	Species vs. class interactions Mninga *Regrowth site comparisons* C01.MN vs C02.MN C01.MN vs C03.MN C02.MN vs C03.MN *Regrowth to mature site comparisons* C01.MN vs C04.MN C02.MN vs. C04.MN C03.MN vs C04.MN Mzima *Regrowth site comparisons* C01.MZ vs C02.MZ C01.MZ vs C03.MZ C02.MZ vs C03.MZ *Regrowth to mature site comparisons* C01.MZ vs C04.MZ C02.MZ vs C04.MZ C03.MZ vs C04.MZ mtundu	 **W = 18, p-value = 0.02381** W = 12, p-value = 0.05714 W = 16, p-value = 0.4762 W = 10, p-value = 0.2286 W = 11, p-value = 0.9143 W = 4, p-value = 0.3429 **W = 24, p-value = 0.009524** **W = 16, p-value = 0.02857** W = 17, p-value = 0.3524 W = 14, p-value = 0.1143 W = 5, p-value = 0.1714 W = 2, p-value = 0.1143

	Regrowth site comparisons C01.MT vs C02.MT C01.MT vs C03.MT C02.MT vs C03.MT *Regrowth to mature site comparisons* C01.MT vs C04.MT C02.MT vs C04.MT C03.MT vs C04.MT	 W = 21, p-value = 0.06667 W = 15, p-value = 0.05714 W = 14, p-value = 0.7619 W = 14, p-value = 0.1143 W = 14, p-value = 0.7619 W = 9, p-value = 0.8857
Foliar %N	**Kruskal-Wallis, species** Wilcox MT vs MZ Wilcox MT vs MN Wilcox MN vs MZ	**Kruskal-Wallis chi-squared = 35.997, df = 2, p-value = 1.52 5e-08** **W = 300, p-value = 1.597e-06** **W = 283, p-value = 2.509e-06** **W = 293, p-value = 1.644e-07**
	Kruskal-Wallis, class Wilcox *Regrowth site comparisons* C01 vs C02 C01 vs C03 C02 vs C03 *Regrowth to mature site comparisons* C01 vs VIL C02 vs VIL C03 vs VIL	Kruskal-Wallis chi-squared = 3. 2937, df = 3, p-value = 0.3485 W = 127, p-value = 0.2204 W = 77, p-value = 0.5254 W = 104, p-value = 0.8841 W = 63, p-value = 0.8801 W = 72, p-value = 0.1345 W = 48, p-value = 0.1782
	Species&class interactions Wilcox mninga C01.MN vs C02.MN C01.MN vs C03.MN C02.MN vs. C03.MN *Regrowth to mature site comparisons* C01.MN vs C04.MN C02.MN vs C04.MN C03.MN vs. C04.MN Mzima *Regrowth site comparisons* C01.MZ vs C02.MZ C01.MZ vs C03.MZ C02.MZ vs C03.MZ *Regrowth to mature site*	Kruskal-Wallis chi-squared = 4 0.964, df = 11, p-value = 2.444e -05 W = 12, p-value = 0.5476 W = 8, p-value = 0.6286 W = 6, p-value = 0.257 W = 6, p-value = 1 W = 3, p-value = 0.06667 W = 3, p-value = 0.2 **W = 24, p-value = 0.00952** **W = 16, p-value = 0.02857** W = 20, p-value = 0.1143

	comparisons C01.MZ vs C04.MZ C02.MZ vs C04.MZ C03.MZ vs C04.MZ mtundu *Regrowth site comparisons* C01.MT vs C02.MT C01.MT vs C03.MT C02.MT vs C03.MT *Regrowth to mature site comparisons* C01.MT vs C04.MT C02.MT vs C04.MT C03.MT vs C04.MT	 W = 11, p-value = 0.4857 W = 5, p-value = 0.1714 **W = 0, p-value = 0.0285** W = 21, p-value = 0.06667 W = 12, p-value = 0.3429 W = 6, p-value = 0.2571 W = 10, p-value = 0.6857 W = 8, p-value = 0.4762 W = 8, p-value = 1

FIGURES: CHAPTER ONE

Figure 1.1 Indicators of N cycling show low ecosystem N availability and lack of recovery relative to tree N demand along a Miombo forest regrowth chronosequence.

a-g, (a) soil total organic N; **(b)** soil ammonium:nitrate ratio; **(c)** soil extractable mineral N (nitrate + ammomium) concentration by depth; **(d)** foliar $\delta^{15}N$; **(e)** wet-dry season leaf-area difference (dLAI); **(f)** N demand for canopy leaf production; **(g)** foliar mass percentage N. Error bars indicate s.e.m. for data within each group. Forest age effects are significant in analyses of variance, covariance or kruskal-wallis tests for soil extractable mineral N, foliar $\delta^{15}N$, dLAI and canopy N demand ($P < 0.05$, see Supplementary Table 3 for all P values). Soil, foliar and canopy indicators (**a-d, g**) showed no increase in ecosystem N availability with regrowth, and contrasted significant increases in indices of tree demand for N for primary production during regrowth (**e, f**). See Supplementary Tables S1.5 and S1.6 for age and other effects on dependent variables.

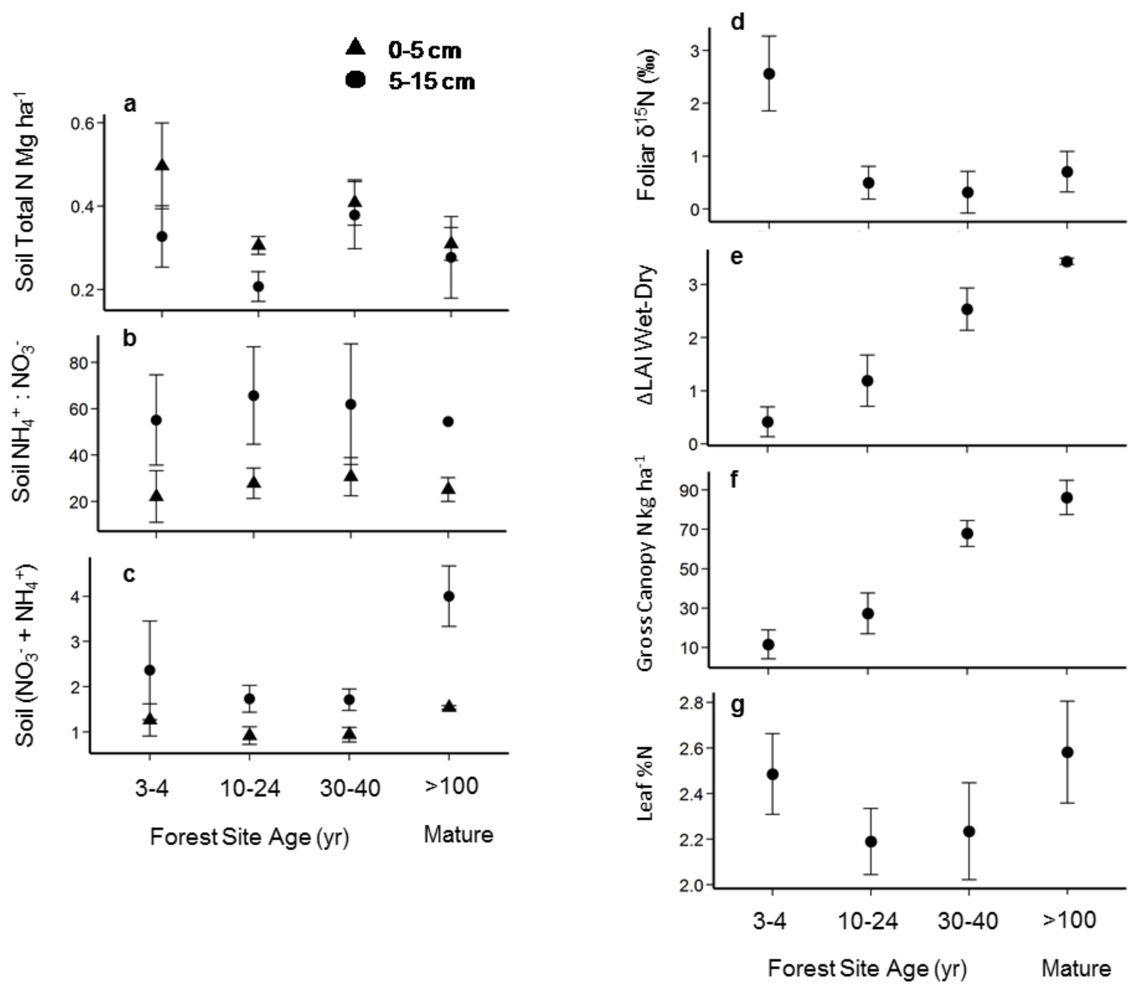

Figure 1.2 Differences in foliar N cycle indicators among an N-fixing and non N-fixing tree species across a Miombo forest regrowth chronosequence.

a-b, (a) Foliar $\delta^{15}N$ (**a**); Foliar N concentration (**b**) Error bars indicate s.e.m. for data within each species-site group. The N-fixing tree is *Pterocarpus angolensis* (*Pa*); the non-N fixing trees are *Brachystegia spiciformis* (*Bs*) and *Terminalia sericea* (*Ts*). Indicators showed significant differences by species (P < 0.05 in Kruskal-Wallis tests, see Supplementary Table 6). The N-fixer had significantly lower foliar $\delta^{15}N$ <0 per mil (a) and higher %N (b) compared to non-N fixers grouped among all regrowth and mature forest classes. *Ts* showed significantly lower foliar %N in 30-40 yr sites than mature forest sites (P < 0.05 in Kruskal-Wallis tests, see Supplementary Table S1.7).

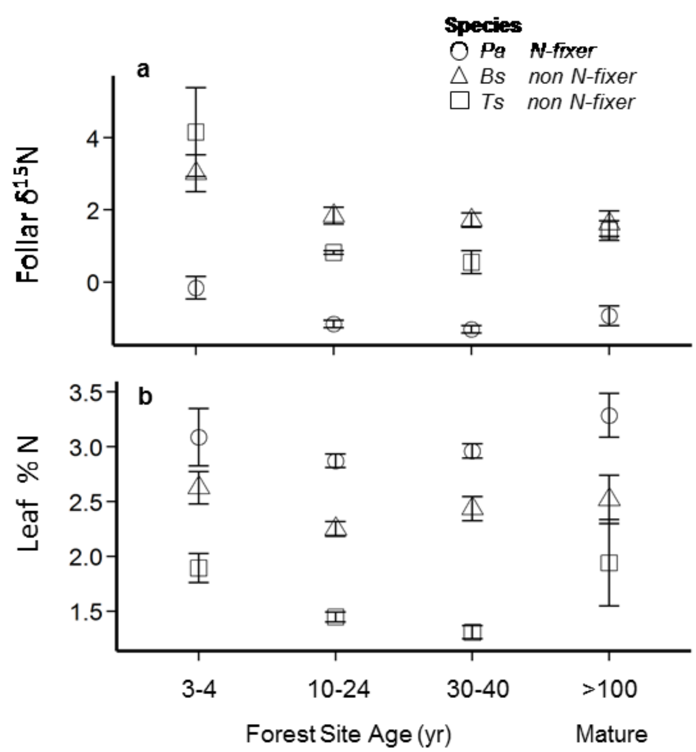

Figure S1.1 Location of Miombo Woodlands, Tabora, Tanzania and forest regrowth chronosequence field sites. **a-c, (a)** Miombo Woodlands are shown in green (dry tropical forest-containing regions in sub-Saharan Africa subset from the Nature Conservancy Ecoregions dataset, http://maps.tnc.org/gis_data.html). The national boundary of Tanzania is shown in black, and Tabora Province shown in solid black; **(b)** The Tabora woodlands studied here are located in the center of Tabora Province, with field sites indicated by yellow dots against a June 2014 Landsat 8 false-color image.

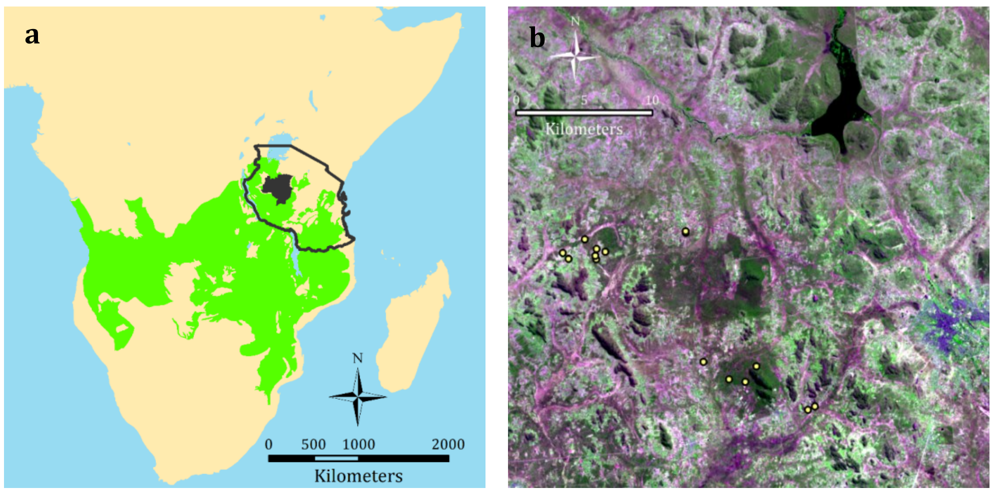

Landsat 8 – June 2015.
Yellow dots indicate field sites.
False color combination:
Red – Band 6 (1.65 um)
Green – Band 5 (0.86 um)
Blue – Band 7 (2.21 um)

Figure S1.2 Carbon stock accumulation with regrowth site age. Carbon stocks were assessed via methods similar to Williams et al. (2008)[1], by sampling all stems >5 cm diameter-at-breast-height in four 10 m-radius subplots distributed in a stratified random manner within 50 x 50 m field sites (see Methods). Four sets of allometric equations from three Miombo sites (Zambia[2], Mozambique[3], Tanzania[4] and the pan-Dry Tropics (Brown et al. 1989, ref. 1) were used to calculate stem biomass and C stocks and single-model C stock accumulations (grey lines below). Model results were averaged to produce C stocks with uncertainties for each site (green dots, error bars s.e.m. of four model-calculations) and an average linear C stock accumulation curve to regrowth sites aged 40 yr. N accumulation with regrowth was calculated using an average of published Miombo tree percent N values (Chidumayo 1993, ref. 5).

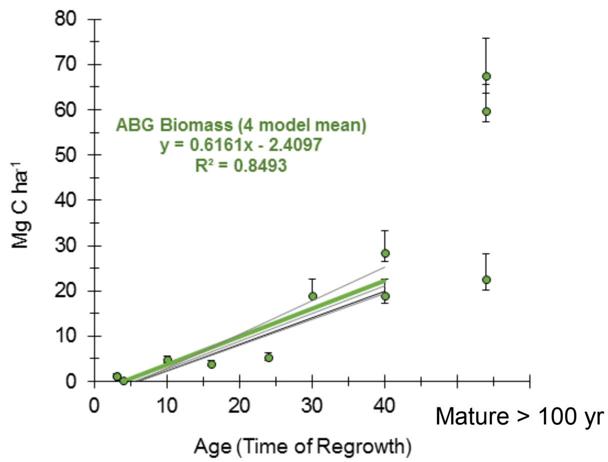

References for allometric equations:

1. Williams, M. *et al.* Carbon sequestration and biodiversity of re-growing miombo woodlands in Mozambique. *For. Ecol. Manage.* **254,** 145–155 (2008).

2. Chidumayo, E. . Estimating tree biomass and changes in root biomass following clear-cutting of Brachystegia-Julbernardia (miombo) woodland in central Zambia. *Environ. Conserv.* **41,** 54–63 (2014).

3. Ryan, C. M., Williams, M. & Grace, J. Above- and belowground carbon stocks in a Miombo wooodland landscape of Mozambique. *Biotropica* **43,** 423–432 (2011).

4. Malimbwi, R. E., Solberg, B. & Luoga, E. Estimate of biomass and volume inmiombo woodland at Kitulangalo Forest Reserve , Tanzania. *J. Trop. For. Sci.* **7,** 230–242 (1994).

5. Chidumayo, E. N. Phenology and nutrition of miombo woodland trees in Zambia. *Trees* **9,** 67–72 (1993).

Figure S1.3 Soil N (NH_4^+ + NO_3^-) mineralization potentials (Nmin) in 14-day lab incubations, compared across Miombo forest regrowth chronosequence sites in wet and dry seasons. **a-b,** Lab-measured potential soil N(NH_4^+ + NO_3^-) mineralization production potentials for 0-15 cm in the **(a)** 2015 wet season (March-April) and **(b)** 2015 dry season (Sep-Oct). Error bars show group s.e.m. In ANOVA, Nmin differed significantly by season ($p = 0.032$); wet season Nmin rates averaged across all forest sites (average 3.65 kg N ha^{-1} 14 d^{-1} ± 0.47 s.e.m) were more than double those of dry season Nmin rates (average 1.65 kg N ha^{-1} 14 d^{-1} ± 0.38 s.e.m.) ($P < 0.05$, Tukey HSD tests, see Supplementary Table S1.2 and S1.7). Within the wet season (**a**), Nmin rates showed a lack of trend among regrowth forest sites. Wet season Nmin rates among regrowth sites (average 3.02 kg N ha^{-1} 14 d^{-1} ± 0.31 s.e.m.) were > 50% lower and significantly different than mature forest Nmin rates (average 5.54 kg N ha^{-1} 14 d^{-1} ± 0.51 s.e.m.) ($P < 0.05$, Wilcoxon sum rank tests, see Supplementary Table S1.2 and S1.7).

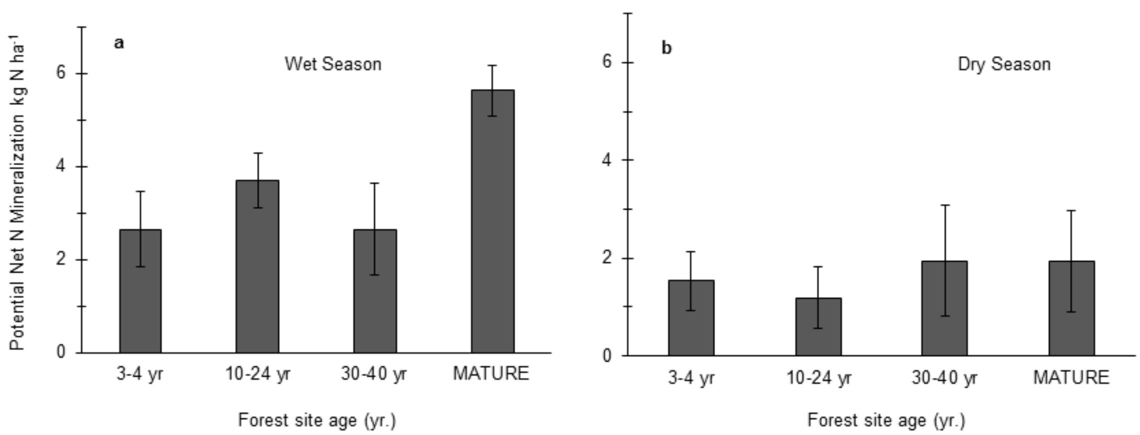

CHAPTER TWO

GOING BEYOND THE GREEN:

SENESCED VEGETATION MATERIAL PREDICTS BASAL AREA AND BIOMASS IN REMOTE SENSING OF TREE COVER CONDITIONS IN AN AFRICAN TROPICAL DRY FOREST (MIOMBO WOODLAND) LANDSCAPE

Marc Mayes[a,b], John Mustard[a], Jerry Melillo[b], Christopher Neill[b,c], Gerson Nyadzi[d]

a) Department of Earth, Environmental and Planetary Sciences, Brown University, Providence, Rhode Island, United States

b) The Ecosystems Center, Marine Biological Lab, Woods Hole, Massachusetts, United States

c) The Woods Hole Research Center, Falmouth, Massachusetts, United States

d) Millennium Villages Project-Mbola, Tabora, Tanzania

[Prepared for Submission as an Original Article to Environmental Research Letters]

Abstract

In sub-Saharan Africa, tropical dry forest and savanna landscapes cover over 2.5 million km^2, support livelihoods for millions in fast-growing nations, and have experienced high rates of tree cover changes amid increasing resource demands. To inform conservation efforts, there is a need for improved monitoring of forest and tree cover conditions across these landscapes. Existing satellite remote sensing methods poorly characterize land and tree cover in the African dry tropics. In this study, we tested the hypothesis that senesced vegetation land cover features would relate significantly to tree cover structure, and improve upon greenness-based methods for modeling tree cover from remotely sensed data in a Miombo Woodland landscape. Subsequently, we developed new basal area and biomass maps using senesced and green vegetation metrics calculated from Landsat data, and assessed their performance at field and landscape spatial scales. Across regrowth forest sites representing a low-high biomass gradient in a western Tanzanian Miombo landscape , we found that strong linear relationships ($p < 0.01$) of canopy cover to basal area ($r^2 = 0.815$) and biomass ($r^2 = 0.635$), and dominant NPV ground cover (>60%), mediated an inverse relationship between tree structure and exposure of NPV ground cover to the sky. This relationship in field data scaled to Landsat metrics of senesced vegetation (spectral mixture analysis (SMA)-non-photosynthetic vegetation (NPV) fractions), which showed strong ($p < 0.01$) inverse correlations to basal area (Pearson $r = -0.86$) and biomass ($r = -0.87$) that were equivalent or stronger than direct correlations of land cover and tree structure to Landsat greenness metrics (SMA-green vegetation (GV) fractions, and the Normalized Difference Vegetation Index, NDVI)) ($r = 0.82$-0.85). Senesced vegetation

metric-based Landsat maps had absolute differences in biomass estimates from field data (mean 12 Mg ha^{-1}) that were 30% lower than greenness index-based Landsat maps (18-19 Mg ha^{-1}). For forest and non-forest land cover areas at landscape scales, senesced and green vegetation metrics estimated similar ranges of average basal area (13.0-16.0 m^2 ha^{-1}) and biomass (31.4-46.1 Mg ha^{-1}) for forest areas. However, for non-forest areas, Landsat SMA-NPV maps estimated average basal area (4.23 m^2 ha^{-1}) and biomass (7.14 Mg ha^{-1}) values that was higher and closer to field data from than green vegetation-based maps. At image validation sites spanning dense woodland, shorter-stature woody vegetation bordering seasonal drainages (mbuga) and cleared areas with known gradients in biomass (<10 – 150 Mg ha^{-1}) , the senesced vegetation metric modeled significant differences in biomass across all three tree cover types, while green vegetation metrics did not. Our results suggest senesced vegetation metrics at Landsat scales are a promising means for improved quantification of tree cover conditions across regrowth and ecological gradients in African TDF landscapes.

1. Introduction

Sub-Saharan Africa has among the world's largest tropical dry forest regions (>2.5 M km^2), which support biodiversity, water resources, food production and economic development for countries with the globe's fastest-growing populations (Campbell 1996). Land use and climate change pose significant threats for African tropical dry forests. Increasing demand for agricultural land and forest resources has driven high net deforestation rates since 2000 across sub-Saharan African countries including Tanzania and Zambia (Rudel *et al* 2013). Trees provide key resources to millions of people such as timber and wood-based fuels, including firewood and charcoal, which are a primary source of energy for an estimated 90% of SSA households (Chidumayo and Gumbo 2013). As smallholder farmers face unpredictable crop harvests because of increasingly variable rainfall, and changes such as shortening rainy seasons (Lyon and Dewitt 2012), forests and trees provide important income from off-farm activities such as sales of timber, commercial charcoal and honey production (Luoga *et al* 2000). Rainfall and temperature variability may also affect tree productivity and capacity for regrowth following disturbance, though much less is known about tree productivity responses to changing climate. Amid rising pressures on trees and forests, initiatives such as World Resource Institute's AFR100 landscapes are calling for increased attention to conservation of African TDFs and sustainable use of forest resources (WRI 2016).

Given pressures from land use and climate change, improved capacity to monitor tree structure, forest conditions and change at landscape to continental-scales in African dry tropical landscapes is needed to guide land management for conservation and sustainable use. Remote sensing offers synoptic, repeatable means of measuring forest and tree structure and recent satellite-derived products such as Global Forest Watch forest change maps are promising developments (Hansen *et al* 2013). However, current global-scale methods do not adequately quantify tree and forest structure variability (e.g. stem size distributions and density, basal area, biomass) in African TDF landscapes. For Global Forest Watch data, accuracy assessments showed a 48% false-negative rate in detection of forest cover loss in SSA, and a 52% false negative rate across tropical forests globally (Tyukavina *et al* 2015). The resulting area of mischaracterized forest cover and forest cover change is likely quite large. Other global land cover map products (GlobCover at 300 m resolution, MODIS land cover version 5) show high rates of disagreement particularly in Africa (Fritz *et al* 2011). Recent moderate-resolution optical (Landsat, 30 m pixel) and radar-based assessments (ALOS-PALSAR, 12-25m pixel scale) show that the majority of forest change events occur at small spatial scales of <2 ha (Ryan *et al* 2012, Mayes *et al* 2015). At these spatial scales, there is poor understanding of how tree structure varies across important landscape-scale gradients such as forest age and disturbance history, and this has precluded detailed study of forest condition beyond forest cover at landscape scales in the region.

One major challenge for characterizing tree structure in African and other tropical dry forest areas with optical remote sensing is relating the land cover features these data measure – materials comprising the land surface such as green vegetation or exposed substrate – to tree structure across forest and non-forest areas and landscape gradients on the ground. Forest areas – including a mix of closed and open canopy woodlands - have complex canopy, stem and land cover structure because of varied edaphic conditions (e.g. landscape position and soil type) and the chronic disturbances of fires and human activities over long timescales(Frost 1996). There is large variability in mature forest basal area (5-30 m^2 ha^{-1}) and aboveground biomass (50-150 Mg ha^{-1}) (Williams *et al* 2008, Kalaba *et al* 2013a, McNicol *et al* 2015, Chidumayo 2013). Land cover and land use disturbances add further complexity. Today, African dry forest landscapes are mosaics of forest, shifting agricultural fields and village areas with patch sizes from 0.5-5 ha. Forest loss, degradation and regrowth occur across large regions at small spatial scales reflective of localized land use, as well as over large areas in the case of factors such as cattle grazing and fire, with variable effects on forest structure (Frost 1996).

An important step to understanding tree structure-land cover relationships on the ground in African dry forest landscapes is examining how multiple types of land cover features relate to tree structure. Greenness-related field (e.g. leaf-area index (LAI)) and satellite measures (e.g. normalized difference vegetation index, NDVI) underlie many widely used global methods for optical remote sensing of tree structure (Hansen *et al* 2013, Baccini *et al* 2012). However, past studies in African dry forests have found that greenness measures such as NDVI alone have correlated only moderately to canopy and forest structure (Ribeiro *et al* 2008, Halperin *et al* 2016). Non-*green* land cover components, such as woody stem density and canopy structure, or patterns in leaf litter, senesced grass or exposed substrate, can also relate to forest structure. Studies of tree structure with remote sensing in North American Pacific Northwest, Russian and Brazilian forests have found non-green land cover metrics correlated as well or better to aspects of tree structure than greenness measures (Sabol *et al* 2002, Adams *et al* 1995, Healey *et al* 2005). While a few studies have collected tree inventories to assess forest structure changes across regrowth chronosequences in African dry forests (Williams *et al* 2008, Kalaba *et al* 2013b, Chidumayo 2013, McNicol *et al* 2015), none have collected field data on green and non-green canopy and land cover features alongside tree stem inventories to study how they relate on the ground.

Another challenge to quantifying tree and forest structure in African dry forests is testing how field data on land cover, forest and tree structure in African dry forests relate to remotely sensed observations. This need is akin to developing an appropriate "calibration curve" on a laboratory instrument that spans an expected range of analyte concentrations for a set of samples taken from a given environment or population. African TDFs occupy the low end (50-250 Mg C ha^{-1}) of typical global tropical forest biomass ranges (200-500 Mg C ha^{-1}) (Baccini *et al* 2012, Aber and Mellilo 1991). The combination of prevalent open-canopy conditions and shorter-stature trees (<15 m) yield a forest structure for which global and continental scale-oriented forest remote sensing approaches are not well calibrated. Globally or pan-tropically-oriented remote sensing methodologies, such as those behind Global Forest Watch data products, exclude identification of forests with trees < 5m height and only count forest loss or gain areas as those with changes from >50% to 0% canopy cover or vice versa (Hansen et al. 2013). The calibration sites and training data must represent generalized mature forest structures and signatures of change across a range of conditions spanning continents and climate zones. Recent work has focused on refining remote sensing approaches for African forests at large, but focuses its attention on continental-scale forest structure gradients from Congolese rainforests to South African grasslands defined by climatological factors (Hansen *et al* 2016). This work does not address how forest structure and land cover vary and relate to within-landscape gradients such as forest regrowth age, management, or disturbance intensities.

Our goals in this paper are to characterize tree structure, land cover features and their relationships to each other across regrowing, mature and disturbed forest sites, and sites reflecting landscape-scale gradients in tree cover types in an African dry forest landscape. We quantify relationships between land cover and tree structure features on the ground, and between field and Landsat satellite-derived metrics of senesced and green vegetation materials quantified by vegetation indices (NDVI) and spectral mixture analyses (SMA), which physically models land cover features (Adams and Gillespie 2006, Adams *et al* 1995, Chambers *et al* 2013, Mayes *et al* 2015). We test a hypothesis that exposure of senesced vegetation ground cover features, modulated by tree canopy cover, relates inversely to tree basal area and biomass. Subsequently, we produce new satellite-derived maps of tree basal area and aboveground biomass and assess their results by comparisons to field data and known landscape-scale trends in tree cover structure.

2. Methods

2.1 Study area

Our study landscape is located in central Tabora Province, western Tanzania (5.0^{O}S, 32.8^{O}E) (figures 2.1-2.2). Tabora is located in the northeastern Miombo Woodlands, which although often classified as a tree-grass savanna ecosystem, has extensive tree cover-dominated regions that constitute the largest area (2.5M km^2) of dry forest in sub-Saharan Africa (Frost 1996) (figure 2.1). Tree cover includes dense forest and woodland areas with canopy cover 50-100%, and areas of sparse canopy cover (<20%) in tree-grass savanna regions, located in clay-textured peripheries of seasonal drainages at low landscape positions, called mbuga (figure 2.2b-c) (Frost 1996). Mean annual temperature is 23.9 ^{O}C and mean annual precipitation is 770 mm (2000-2009), with 90% falling between November and May. In 2012, Tabora had a population of 2.3 M and experienced high rates of forest turnover and net deforestation from the mid 1990s-2010s , caused by pressures from agricultural development, urbanization and growing timber and wood-based fuel demands that are common throughout the Miombo Woodland region (Mayes *et al* 2015, URT 2014, Schwartz and Caro 2003, Chidumayo and Gumbo 2013). Forests in the study region fall under a variety of management regimes, including nationally managed reserves (Igombe Forest Reserve) and village-managed forest areas (figure 2.2a). Of standing forest cover in the region in 2011, an estimated 16% consists of regrowth since 1995(Mayes *et al* 2015). Because crop and woodland phenology make the early to mid-dry season the optimal time to quantify forest and non-forest land cover variability for scaling to satellite remote sensing at landscape scales (Mayes *et al* 2015), we organized field and satellite remote sensing studies contemporaneously in June-July 2015. At this time, agricultural areas are harvested, while woodland trees retain moderate canopy leaf cover, which maximizes the landscape-scale variability in green and non-green land cover materials with which to test our hypothesis.

2.2 Field site locations and layout

We collected data on land and tree cover structure from 18 sites spanning a forest regrowth chronosequence of ages 3 yr to maturity (>100 yr) in the early to mid-dry season (July 2015) (figure 2.2a, figure S2.1). Of mature forest sites, three were under national jurisdiction of the Tanzania Forest Service in Igombe Forest Reserve and three were in village-managed areas (figure 2.2a). Given mostly flat topography and long-term shifting cultivation in the region, time since abandonment of cultivation was one of the most prevalent gradients along which forest characteristics varied at landscape scales that we could sample in a repeatable and stratified manner. We chose field sites using a combination of remote sensing, field visits and interviews with local people about land use and fire history. All sites had > 3 yr. since fire, recent (20-yr) prior history of maize cultivation, flat topography (slope < 2%) and sandy (>70%) soils.

At each field site, we established a 0.5 ha (50 x 50 m) plot located as far as possible from boundaries such as roads or field edges. We measured forest structure, canopy and land cover in a spatially aligned manner within four circular sub-plots of 10 m radius, located using a stratified random sampling design in each quadrant of field sites (Williams *et al* 2008). For forest/tree cover structure, we inventoried stem basal diameter and diameter-at-breast-height (dbh) at 1.3 m) for all trees > 5 cm dbh in the sub-plots. Allometric relationships specific to the Miombo and global dry tropics were used to convert stem sizes to biomass (table 2.1). Basal area and biomass were summed across all plots and normalized to the sum of sub-plot areas to calculate tree basal area and biomass density over an approximately 1/8 –ha area (Williams *et al* 2008). For canopy structure data, we took two types of data. First, we measured plant-area index (PAI) data using an LAI-2200 photosensor (LiCOR, Lincoln, NE) at 1.3 m. Second, we took spherical densitometer (gridetched convex hemispherical mirror) surveys of cover to account specifically for what materials comprised canopy cover following a classical United States Forest Service method (Strickler 1959, Korhonen *et al* 2006). Mounting the densitometer on a stand at 1.3 m height, we tallied and summed counts of four classes of material at 17 points in a wedge-shaped subset of the mirror area in four cardinal directions: green leaf, senesced leaf, woody material and open sky (no material). We took these data (a total of 68 counts per point at 7 points) within the sub-plots with readings at plot centers and at 5 m intervals along three 10 m radii oriented at compass bearings of 0^{0}, 120^{0} and 240^{0}. We averaged the proportions of cover calculated at 7 points for a final measurement of the cover in a subplot, and averaged the subplot averages to compute a plot cover total. For ground cover data, at the same 7 points were canopy data were taken, we used a modified point-line transect method and tallied, summed and averaged proportions of the following land cover materials: leaf litter, green grass, senesced grass, woody litter, roots/stems, charred organic matter, ash, and bare substrate. The point-line transect method has been used widely in measuring land cover in semi-arid regions and has been shown to scale successfully between ground and satellite data (Pilliod and Arkle 2013, Elmore *et al* 2000).

2.3 Satellite data and image analysis methods

For satellite data, we acquired six Landsat 8 OLI surface reflectance-corrected scenes from June-July 2015 from the NASA/USGS ESPA processing system covering the area of Tabora Province. Landsat 8 images were processed to surface reflectance using the L8SR algorithm (Vermote *et al* 2016). Using the six traditional visible, near-infrared and shortwave infrared optical bands with 30 m spatial resolution, we conducted spectral mixture analyses (SMA) using field-validated endmembers (EM) to model land cover. SMA is an established satellite image analysis technique that models pixel reflectance values as linear multiplicative sums of the reflectance of known materials, subject to constrains that the sum of the fractions must equal 1.0 and there are no negative values, and acts as a physical modelling technique that estimates the proportion of known materials that comprise landscape surfaces (Adams and Gillespie 2006). We used a fixed-endmember SMA approach, using single endmembers for four materials consistent with categories used for canopy and ground cover data: green vegetation (GV), non-photosynthetic vegetation (NPV), substrate and shade, which were chosen from georeferenced field sites with high proportions of these materials, and successfully used for forest change mapping in Tabora, Tanzania (Mayes *et al* 2015) (figure S2.2). Outputs of SMA are images with pixel values from 0-1 representing modeled proportions of endmember materials comprising land cover surfaces. We calculated normalized difference vegetation index (NDVI) images to compare how a more common greenness-based measure for land cover performed against SMA for representing Miombo TDF land cover. To deal with image variability from scene to scene, we normalized EMs and NDVI to scene summary statistics by calculating Z-scores on a per-pixel basis.

2.4 Statistical analysis of field-satellite data relationships and assessment of basal area and biomas maps

We quantified and assessed differences in field data on forest structure, canopy and land cover variables and satellite data among sites and site age groups using analysis of variance (ANOVA and Tukey's HSD means comparisons, $p < 0.05$) and ordinary least-squares linear regression. We developed and applied log-linear models to predict tree structure (basal area, biomass) from satellite data using three Landsat-derived indices: two of the SMA output images (Landsat SMA-NPV and SMA-GV) and NDVI. Landsat SMA-NPV, SMA-GV and NDVI values were extracted for 3x3 pixel regions chosen over GPS points for field sites. Of the 18 field sites, 17 were used to develop linear models – one site (S07, mature village forest) showed evidence of moderate burned area on the ground that confounded its SMA results (table S2.1). Using these models, we mapped basal area and biomass maps in a 275,000-ha well-known training region in central Tabora Province (figure 2.2).

We assessed map performance in three ways. First, we compared the senesced and green vegetation metric-based Landsat map estimates of tree structure to data at field sites, specifically the direction and absolute values of differences between remotely sensed biomass and field biomass data. Second, we calculated the average tree structure (basal area and biomass) modeled by the senesced and green vegetation metric-based approaches for region-wide forest and non-forest land cover classes, delineated by a Landsast SMA-based thresholding method developed for the Miombo that accounted for land cover phenological variability (Mayes *et al* 2015). Then, we compared the modeled forest and non-forest land cover tree structure to field data for mature forest, and young regrowth (3-4 and 10-24 yr) sites respectively. Third, we compared the sensitivity of the three remote sensing approaches to tree structure for dense woodland, mbuga woody vegetation and areas largely cleared of trees in nationally managed (Igombe Reserve) and village-managed (Millennium Villages Project) regions. To do this, we selected 35-40 image validation points for dense, sparse and cleared areas (little to no tree cover) separate from our field sites, using knowledge from the field and Google Earth imagery from 2013 onward to verify site conditions. We conducted analysis of variance (ANOVA) for tree biomass estimates, modeled by the three remote sensing approaches for each region, using tree cover type (dense woodland, mbuga and cleared) and remote sensing index as independent variables, with the goal of assessing the degree to which SMA-NPV, SMA-GV or NDVI-based models could differentiate tree structure across known gradients at landscape scales.

3. Results

3.1 Field-measured forest structure and land cover

Forest (tree) structure showed significant differences among age and disturbance classes (ANOVA, $p < 0.05$, figure 2.3) . Basal area, biomass, stem density, height and volume all increased significantly with increasing site age, and mature forests varied between village-managed and national reserve-managed sites (figure 2.3, table 2.2). Basal area differed among all regrowth age classes (3-4 yr, 10-24 yr, 30-40 yr) ($p < 0.05$) and village-managed mature forests (figure 2.3a). Biomass and biomass carbon trends were similar to basal area (figure 2.3b, table 2.2). Regrowth sites of 3-4 yr ages had significantly lower biomass than all other regrowth and mature sites ($p < 0.05$. Biomass at 10-24 yr sites was significantly greater than 3-4 yr sites and significantly less than mature forests. Biomass of 30-40 yr sites was intermediate and did not differ significantly between 10-24 yr regrowth and mature sites. Disturbed forest sites (aged 6-19 yr) had lower biomass, basal area and stem density than mature and older (30-40 yr) regrowth sites, and similarly aged regrowth sites (10-24 yr), but differences were not significant from 10-24 yr regrowth sites. Though highly variable within groups and not significantly different from each other, village-managed forest field sites had higher stem density, basal area and biomass than nationally-managed forest field sites (table 2.2, figure 2.3).

Total plant canopy area (plant-area index, PAI) and open-sky fraction tallied from spherical densitometer measures differed significantly by regrowth site age categories

(ANOVA, $p < 0.05$), with PAI increasing and open-sky fraction decreasing with increasing site age (figure 2.4a, 2.4c). Amid overall canopy area changes, woody material fractions had weak trends and green leaf material fractions had no significant trend or differences with site age (figure 2.4b). Below these canopy structure changes, ground cover was dominated by leaf litter and senesced grasses across all sites (>60%) (figure 2.4d). In continuous relationships between land cover and forest structure on a per-site basis, overall canopy area (PAI) had a strong, direct linear relationship to basal area ($r^2 = 0.815$, $p < 0.01$) and biomass ($r^2= 0.635$, $p < 0.01$) (figure 2.5a) and canopy open sky fraction showed a strong, inverse linear relationship to basal area ($r^2 = 0.763$, $p <0.01$) and biomass ($r^2 = 0.552$, $p = 0.002$) (figure 2.5b). No significant relationship existed between the proportion of green leaf area in the canopy to basal area ($r^2 = 0.105$, $p = 0.103$) or biomass ($r^2 <0.01$, $p = 0.330$) (figure 2.5c).

3.2 Satellite-modeled land cover and field-satellite data relationships

Landsat SMA successfully modeled land cover with low root-mean square error (<0.01) and greater than 90% of pixels with reasonable endmember proportions greater than 0 or less than 1 in the training region over central Tabora (table 2.3). The SMA-NPV fraction comprised the highest mean proportion of land cover materials per pixel (0.40 ± 0.15 s.e.m.) and the highest sensitivity to varying land cover mixtures (table 3). Mean per-pixel green vegetation fractions of land cover were lower (0.15 ± 0.07 s.e.m.)) and less variable across the landscape.

Non-photosynthetic vegetation (NPV) measures had equal or stronger relationships among land cover, forest structure and satellite data than green vegetation measures across sites. The senesced vegetation-related metrics between field-measured land cover and satellite data had stronger relationships than green vegetation metrics between field-measured land cover and satellite data. Landsat SMA-derived NPV had a significant positive linear relationships with open-sky fraction of the canopy ($r^2 = 0.632$, $p < 0.001$), coherent with increasing exposure of NPV ground cover (figure 2.6a). Positive linear relationships occurred but were not as strong between canopy PAI and Landsat SMA-derived GV ($r^2 = 0.514$, $p < 0.001$) and NDVI ($r^2 = 0.484$, $p < 0.001$) (figure 2.6b-c). Pearson correlations among forest structure and senesced land cover features (Landsat SMA-NPV) were as strong or stronger than forest structure correlations to greenness metrics (Landsat SMA-GV and NDVI) (figure 2.7). For green vegetation features, as forest basal area and biomass increased, canopy area (PAI) grew and overall green material increased as part of increased canopy cover. Thus, despite showing inconsistent trends with regrowth as a proportion of canopy cover alone (figure 2.3b), the green vegetation satellite metrics had direct relationships to total canopy area (figures 2.6b-2.6c) and forest structure (figure 2.7b-2.7c, 2.7e-f). Log-linear regression models showed significant relationships among scene-normalized (Z-score) NPV and green satellite metrics (Landsat SMA-GV and NDVI), and tree basal area and biomass (table 2.4). Correlation coefficients of Landsat-NPV-based relationships to basal area and biomass were slightly higher than Landsat SMA-GV or NDVI-based ones.

3.3 Landsat-derived basal area and biomass maps

In satellite metric-derived maps of basal area and biomass, >90% of pixels were modeled within published ranges for basal area (0-35 $m^2\ ha^{-1}$) and biomass (0-200 $Mg\ ha^{-1}$) in Miombo forests (table 2.5). Relative to data at field sites, SMA-NPV maps estimated biomass with mean absolute value errors of 12 $Mg\ ha^{-1}$, 30% lower than mean absolute errors for SMA-GV (19 Mg ha^{-1}) and NDVI maps (18 Mg ha^{-1}) (table S2.1-S2.2). For all metrics, satellite maps produced biomass estimates closest to field data for mature forest, 30-40 yr regrowth and disturbed forest site classes (table S2.1). All metrics overestimated biomass at 3-4 and 10-24 yr regrowth site classes, with SMA-NPV metrics showing the closest estimates to field values, but field values themselves were smaller than the field-satellite map error rates for all metrics (table S1).

At landscape scales between forest and non-forest land cover, all metrics estimated mean forest basal area and biomass to be 300% larger than non-forest land cover areas (figure 2.8-2.9, table 2.6). Among metrics, SMA-NPV maps estimated higher basal area and biomass than SMA-GV and NDVI maps for both forest and non-forest land cover. Forest land cover biomass estimates were 2-3 times the mean absolute errors between satellite estimates and ground data at field sites. The SMA-NPV-based maps' scene-wide means (and standard errors) for non-forest area basal area (4.23 ± 4.01 m^2 ha^{-1}) and biomass (7.14 ± 11.2 Mg ha^{-1}) were in the middle of the range of field-measured basal area and biomasses for 3-4 and 10-24 yr regrowth sites (table 2.2, figure 2.9). The SMA-GV and NDVI maps modeled mean basal areas and biomass for non-forest areas scene-wide at the low end of the range of 3-4 and 10-24 yr field sites (table 2.2, figure 2.9). However, non-forest area biomass estimates (3-7 Mg ha^{-1}) were below the values of mean absolute errors between satellite estimates and ground data at field sites.

In analyses of satellite metric performances across image validation points, both tree cover type and remote sensing index showed significant relationships to remote biomass estimates (table 2.7). For Igombe Reserve and village-managed areas, the SMA-NPV maps significantly differentiated the biomass for all three tree cover types - dense woodland, mbuga woody vegetation and remnant woody biomass in cleared areas (figure

2.10, table S2.3). The greenness indices differentiated biomass only for dense woodlands, but not among mbuga and cleared areas (figure 2.10, table S2.3). SMA-NPV and greenness indices modeled similar biomass estimates for dense woodland validation points (at Igombe Reserve, 115-130 Mg ha^{-1}; in the Millennium Village area, 85-95 Mg ha^{-1}) and cleared area validation points (at Igombe Reserve, 4-8 Mg ha^{-1}; in the Millennium Village area, 2 Mg ha^{-1}). However for mbuga woody biomasses, SMA-NPV estimates (23-24 Mg ha^{-1} at Igombe Reserve and Millenium Village areas) were roughly 3-4 times larger than those of greenness indices (at Igombe Reserve, 8.5-9.5 Mg ha^{-1}; in the Millennium Village area, 6.4-6.9 Mg ha^{-1}) (table S2.3).

4. Discussion

4.1 Senesced vegetation land cover features relate strongly to forest structure

Characterization of early-dry season land cover features across regrowth and mature forest sites yielded practical new insights for optical remote sensing of tree structure at landscape scales in Tabora. There were clear relationships between tree stem structure and total canopy cover across sites, shown by independent measurements: PAI (photosensor) correlated directly to basal area and biomass, and open-sky fraction (spherical densiometer), correlated inversely. There was also persistently high NPV comprised of senesced grass and leaf litter on the ground. The net effect of dominant NPV ground cover and strong canopy cover trends with tree basal area and biomass was that canopy cover-mediated exposure of NPV ground materials emerged as a land cover pattern that related strongly to tree structure. There was not a significant relationship between tree structure and the proportion of green leaf cover in the canopy at this time of year. As opposed to total canopy cover, which is comprised of significant proportions of woody material controlled by long-term tree growth, green leaf cover is affected by more factors that could confound its relationship to basal area and biomass in the early dry season. These include variable phenology across individual trees and tree species, and landscape-driven edaphic factors such as topographic position and soil moisture. At the scales of field plots, land cover and tree structure data corroborated our hypothesis that total canopy cover would control exposure of NPV that varied inversely with basal area and biomass.

4.2 Field-measured land cover-forest structure patterns scale to Landsat SMA analyses

Land cover relationships to tree structure in field data provided the basis to test if our hypotheses about land cover-tree structure relationships scaled to Landsat-derived metrics. Indeed, SMA-derived NPV fractions at scales of about 1 ha (3x3 30 m pixel groups averaged over field sites) showed inverse relationships to basal area and biomass, driven by the net land cover signal of canopy-mediated NPV exposure. This non-green land cover signal was stronger than Landsat SMA-green vegetation fraction and NDVI relationships to basal area and biomass. Despite poor canopy green leaf proportion-tree structure relationships in the field, Landsat-scale greenness metrics still correlated to basal area and biomass at 1 ha spatial scales. Though this study was oriented to compare the performance of non-green and green land cover variables separately for modeling forest structure, its results indicate non-green and green land cover could be used in combination to model tree basal area and biomass across African TDF landscapes. Other recent studies have shown the value of using not only multiple land cover metrics, but also ancillary data on landscape variables to map aspects of tree structure in African TDF landscapes (Halperin *et al* 2016).

4.3 Senesced vegetation-based indices model basal area and biomass with lower error relative to field sites and higher sensitivity to variable tree cover types than green vegetation-based indices

All senesced and green vegetation metric-based maps estimated landscape-scale ranges of tree basal area and biomass that matched published Miombo Woodland tree inventories (basal area 0-35 m^2 ha^{-1} ; biomass 0 – 150 Mg biomass ha^{-1} or 0-70 Mg ha^{-1} biomass carbon (C) ha^{-1}) estimating C as 47% of woody biomass (Frost 1996, Williams *et al* 2008, Kalaba *et al* 2013). All metrics also captured large differences in tree structure of forest and non-forest land cover, >10 m^2 ha^{-1} in basal area and > 30 Mg biomass ha^{-1}. These results indicate that SMA-NPV, SMA-GV fraction images, or NDVI calculated from 30 m Landsat scale-optical remote sensing data in the early dry season all are capable of representing broad tree cover structure trends at landscape scales in an African dry forest environment. Similar approaches may be transferrable for coarse landscape-scale forest structure monitoring in other global tropical dry forests, or using other optical remote sensing data sources such as the new Sentinel-2 sensors.

The performance assessments we were able to complete for senesced and green vegetation metric-based biomass maps at field sites, and across gradients in tree cover type via image validation points were imperfect, but illustrative of the advantages senesced vegetation-based metrics demonstrated over green vegetation metrics for mapping tree structure particularly for low-biomass tree cover areas. With unlimited resources, the best validation of our methods would use additional tree inventory data collected from field sites on the ground, distributed either among regrowth forest sites or major tree cover types, as independent sites against which to test model estimates. More field data would also help to improve the calibration dataset and verify that the relationships we found among land cover and tree structure across 17 sites holds for a larger dataset. At the scale of individual field sites, both field data for biomass and satellite estimates varied widely (5%-100 %+) relative to average values for site categories. This serves as a caution for using the methods described in this paper for site-specific forest or tree cover monitoring, as opposed to monitoring of larger areas, at least until the variability of tree structure and land cover on the ground as well as satellite metrics is characterized at more sites.

However, with the limited field data available, the back-comparison of model estimates to field site measurements of biomass, and the image validation point analyses together suggested the SMA-NPV senesced vegetation metric estimated aboveground tree biomass values more accurately and with greater sensitivity to biomass variability across different tree cover types than the greenness metrics. With overall mean absolute value differences in biomass estimates from field sites of 12 Mg ha^{-1} across all sites, the SMA-NPV metric could in theory be capable of resolving biomass variability or change of 20-25 Mg ha^{-1}, using a guideline of only estimating biomass variability or change at twice or more than the magnitude of the metric's error or uncertainty. With mean absolute value differences in map-field biomass estimates of >18 Mg ha^{-1}, the greenness measurements would have a resolving power of detecting biomass variability or change at rates of 35-40 Mg ha^{-1}. The image validation point analyses further demonstrated the "edge" in accuracy and sensitivity that SMA-NPV metrics showed over greenness metrics for biomass estimation at a broader landscape scale. From past Miombo Woodland research, woody biomass at the periphery of mbuga or clayey-soil (vertisol) drainage regions in Miombo landscapes has been measured at 15-30 Mg ha^{-1} , which is between that of 10-24 (10 Mg ha^{-1}) and 30-40 yr regrowth forest sites (40 Mg ha^{-1}) (Frost 1996, Woollen *et al* 2012). In both the nationally-managed Igombe Reserve and village-managed regions of interest, the SMA-NPV metric estimated similar mean biomass around mbuga peripheries at 24 Mg ha^{-1}, significantly different from mature forests (>80 Mg biomass $ha^{-1-)}$ and cleared areas (<5 Mg ha^{-1}). In contrast, the greenness metrics modeled mbuga periphery woody biomass of about 5-10 Mg ha^{-1}, a significant underestimate relative to past studies, which further did not significantly differentiate mbuga woody biomass from cleared area biomass. These comparisons indicate that the SMA-NPV senesced vegetation metric showed better accuracy and precision for modeling tree biomass relative to the green vegetation metrics, particularly in intermediate to low-biomass areas like the mbuga peripheries and 10-24 and 30-40 yr regrowth sites.

Notably, biomass estimates for Igombe Reserve and the village-managed forest areas, quantified by data from field sites and image validation points showed different comparative trends. Though it was not a goal of this study to evaluate impacts of national versus local management on forest condition, the results highlight useful considerations about field site selection and the value-added of remote sensing approaches, with quantified uncertainties, toward addressing questions about management effects on forests at landscape scales. At the field sites we were able to access for tree inventories, village-managed forests had higher mean biomass (100 ± 28 Mg ha^{-1}) than nationally-managed forest sites (76 ± 9.0 Mg ha^{-1}) (figure 2.3, table S2.1). However, in image validation point analyses covering broader areas, the Igombe Reserve dense woodland points' mean biomass estimates (115-130 Mg ha^{-1}) were larger than village-managed dense woodlands (88-92 Mg ha^{-1}). These discrepancies likely reflect field measurement biases related to the nature of sites that were accessible for tree inventories between the Igombe Reserve and village areas, and differences in land-use pressures or management policy effects on forest structure between the regions. With fewer roads in Igombe Reserve, and safety concerns due to illegal settlement in the forest reserve, hiking to the most remote mature forest sites or dense woodlands was not possible or advisable. As forest protection was poorly enforced in the reserve, the sites we were able to access, closer to roads, likely reflect more disturbance pressure than much of the remote mature forest and dense woodland. In contrast, the forest sites we measured in villages were often under informal but strong use agreements among surrounding villages to not clear or disturb forest cover. We had asked village residents about measuring the most intact remaining forests. Thus, our sites probably represented among the less disturbed forest and dense woodland areas among the broader population of remnant and regrowth dense woodland in village areas. The number of sites in this study was small, and certainly additional field sites would be needed to evaluate village versus national management policies, and the resulting regional land-use pressures, on forest structure. However, remote sensing offers a way to get around logistical difficulties of site access and biases, and provides a more synoptic assessment of forest resources at landscape scales than can often be accomplished with field inventories.

Given the performance assessments, Landsat-scale tree structure maps generated by methods such as those in this study may be useful for a number of forest and tree cover monitoring applications. All indices may be suitable for monitoring biomass changes from clearing or moderate to severe degradation of mature or 30-40 yr regrowth Miombo forest at scales of Landsat pixels (0.25 ha+) , due to land uses such as timber or tree harvesting for wood-fuel production, whose impacts to tree structure are large (>30-50 Mg ha^{-1}) (Luoga *et al* 2002). As part of such applications, further research is needed to assess how temporal variability of land cover metrics at satellite scales affects biomass estimates at no-change sites of high and low forest biomass. The SMA-NPV indices show promise over greenness metrics for monitoring biomass changes of smaller magnitudes in lower to moderate tree biomass areas (20-30 Mg ha^{-1}), perhaps associated with monitoring regrowth, agroforestry or forest restoration projects. Given the uncertainties, none of the remote sensing approaches could be considered accurate for estimating biomass variability or change below or between ranges of the 3-4 and 10-24 yr regrowth field sites (<10 Mg ha^{-1}).

This study highlights three key opportunities for further work to improve knowledge of land cover-tree structure relationships, and use of optical remote sensing to monitor forest and tree cover conditions in African dry tropical landscapes. First, there is great need for more field data on tree structure and land cover in African dry tropical landscapes to enable more rigorous accuracy assessment of remote sensing products. Second, given the mean absolute errors between maps and field data and their implications for reasonable detection of forest structure variability and change, there is a need to further refine remote sensing methods to monitor smaller biomass changes and tree structure variability in low-biomass regions. Other SMA approaches that characterize land cover at sub-Landsat pixel scales, such as multiple-endmember spectral mixture analyses (MESMA) or use of automated SMA methods such as the Carnegie Landsat Analysis System (CLAS) could be useful for such efforts (Roberts *et al* 1998, Asner *et al* 2009). Data-fusion approaches that merged optical with active remote sensing data (e.g. radar, LiDAR) have proved effective for mapping tree structure in African dry tropical forests and across the global tropics for larger areas (Ribeiro *et al* 2008, Baccini *et al* 2012, Saatchi *et al* 2011), and may also be useful within landscapes. High resolution (< 1m) remote sensing observations of tree structure, such as those from small drones (UAS), may also prove useful for improved scaling between field and satellite data (Tang and Shao 2015, Paneque-Galvez *et al* 2014). Three, further integration of repeat local community monitoring and scientific research on land cover-forest structure relationships is an opportunity to improve forest monitoring capabilities and inform assessment of local management effects on forest and tree cover condition.

5. Conclusions

In this study, we have found that senesced vegetation land cover features in the early dry season relate significantly to tree structure at scales of field and satellite data in the western Tanzanian Miombo Woodlands, offering an alternative to monitoring tree structure across African TDF landscapes that is particularly effective for low-biomass areas. In field data, we found that canopy cover-mediated exposure of non-photosynthetic vegetation (NPV) on the ground (senesced litter and grass cover) had strong inverse correlations to tree basal area and biomass across a gradient of young to mature and disturbed forest sites. In contrast, there was no significant relationship between the proportion of green leaf material in tree canopies to tree structure. In analyses of Landsat data over field sites, including spectral mixture analyses (SMA) and NDVI, metrics for senesced vegetation cover (SMA-NPV fractions) had inverse relationships to land cover and tree structure that were comparable to or stronger than direct correlations of greenness measures (SMA-vegetation, NDVI) to tree structure. Basal area and biomass maps based on Landsat metrics for senesced (SMA-NPV) and green vegetation(SMA-vegetation fraction, NDVI) performed similarly for high-biomass forested areas, but senesced vegetation-based maps produced more reasonable ranges of basal area and biomass estimates in non-forest areas. While more field data is needed to validate the landscape-scale tree structure estimates of these pilot maps, our results demonstrate that senesced vegetation metrics at Landsat scales are a promising means for improved quantification of tree structure conditions and change in African TDF ecosystems.

Acknowledgements

We thank staff of Tanzania Western Zone Agricultural Research Institute at Tumbi, Tabora (Fabian Bagayrama, Peter Matata, Kassim Massibuka, Ismail Raishidi, Temba

Gilbert), members of the Millennium Villages Project-Tabora Office (Kagya Eliezer) and New York staff (Claire Ward), Tabora Development Foundation Trust (Dick Mlimuka, Moses Maganga, Sadiki Omari) for their assistance with project logistics, locating field sites, translation, field and laboratory work. We thank the Tanzania Forest Service, Tanzania Forest Research Institute (TAFORI) and Tanzania Army Anti-Poaching Unit for help securing site access, and locals of villages in Uyui District, Tabora, Tanzania for their time discussing land use history and permission sampling forests on village land. We also thank faculty and staff at Marine Biological Lab Ecosystems Center for assistance with sample processing and loaning of field instruments (PIE-LTER). The project was funded by the US National Science Foundation Partnerships for International Research and Education (PIRE) program, project title "Ecosystems and Human Well-Being" (Award # 0968211) PI Chris Neill. Additional research and dissertation support was provided to Marc Mayes from Brown University. The project was completed with permission and cooperation from the Tanzania Commission on Science and Technology (COSTECH Permit Nos. 2013-261-NA-2014-199 and 2015-183-ER-2014-199). M. Mayes was also supported by a Dissertation Fellowship at Brown University during completion of the research.

References

Aber J A and Mellilo J M 1991 *Terrestrial ecosystems*

Adams J B and Gillespie A R 2006 *Remote Sensing of Landscapes with Spectral Images: A Physical Modeling Approach* (New York: Cambridge University Press)

Adams J B, Sabol D E, Kapos V, Almeida Filho R, Roberts D A, Smith M O and Gillespie A R 1995 Classification of multispectral images based on fractions of endmembers:

Application to land-cover change in the Brazilian Amazon *Remote Sens. Environ.* **52** 137–54

Asner G P, Knapp D E, Balaji A and Paez-Acosta G 2009 Automated mapping of tropical deforestation and forest degradation: CLASlite *J. Appl. Remote Sens.* **3** 033543 Online: http://remotesensing.spiedigitallibrary.org/article.aspx?doi=10.1117/1.3223675

Baccini a., Goetz S J, Walker W S, Laporte N T, Sun M, Sulla-Menashe D, Hackler J, Beck P S a., Dubayah R, Friedl M a., Samanta S and Houghton R a. 2012 Estimated carbon dioxide emissions from tropical deforestation improved by carbon-density maps *Nat. Clim. Chang.* **2** 182–5 Online: http://dx.doi.org/10.1038/nclimate1354

Campbell B M 1996 *The Miombo in Transition : Woodlands and Welfare in Africa* vol 72 Online: http://books.google.com/books?hl=en&lr=&id=rpildJJVdU4C&oi=fnd&pg=PR9&dq=The+Miombo+in+Transition+:+Woodlands+and+Welfare+in+Africa&ots=FMsmiYa2th&sig=_hEtp4U1rk54Sn8tgXWfkMD-v-8

Chambers J Q, Negron-Juarez R I, Marra D M, Di Vittorio A, Tews J, Roberts D, Ribeiro G H P M, Trumbore S E and Higuchi N 2013 The steady-state mosaic of disturbance and succession across an old-growth Central Amazon forest landscape *Proc. Natl. Acad. Sci.* **110** 3949–54

Chidumayo E N 2013 Forest degradation and recovery in a miombo woodland landscape in Zambia: 22 years of observations on permanent sample plots *For. Ecol. Manage.* **291** 154–61 Online: http://dx.doi.org/10.1016/j.foreco.2012.11.031

Chidumayo E N and Gumbo D J 2013 The environmental impacts of charcoal production in tropical ecosystems of the world: A synthesis *Energy Sustain. Dev.* **17** 86–94 Online:

http://dx.doi.org/10.1016/j.esd.2012.07.004

Elmore A J, Mustard J F, Manning S J and Lobell D B 2000 Quantifying Vegetation Change in Semiarid Environments: Precision and Accuracy of Spectral Mixture Analysis and the Normalized Difference Vegetation Index *Remote Sens. Environ.* **73** 87–102

Fritz S, See L, McCallum I, Schill C, Obersteiner M, van der Velde M, Boettcher H, Havlík P, Achard F, A A S, O A, S B E and B A, P B, al B S et, al C X et, L D G A J, Agency) E (European S, al F J et, al F J et, al F M et, L F S and S, L F S and S, al F S et, al F S et, al F S et, Observations) G (Group on E, C G, al G C et, al H et, al H M et, al L L et, R M M and S, al M P et, al M I et, al N K et, A P R, al Q T et, al R D P et, S S L and F, al S L et, Interior U D of, al V P H et, al W C et and al Y L et 2011 Highlighting continued uncertainty in global land cover maps for the user community *Environ. Res. Lett.* **6** 044005 Online: http://stacks.iop.org/1748-9326/6/i=4/a=044005?key=crossref.e37ea06a1a56e58be6fbd1f907045b97

Frost P 1996 *The Ecology of Miombo Woodlands* ed B M Campbell (Bogor, Indonesia: Center for International Forestry Research) Online: http://books.google.com/books?hl=nl&lr=&id=rpildJJVdU4C&pgis=1

Halperin J, LeMay V, Coops N, Verchot L, Marshall P and Lochhead K 2016 Canopy cover estimation in miombo woodlands of Zambia: Comparison of Landsat 8 OLI versus RapidEye imagery using parametric, nonparametric, and semiparametric methods *Remote Sens. Environ.* **179** 170–82

Hansen M C, Potapov P, Goetz S J, Turubanova S, Tyukavina A, Krylov A, Kommareddy A and Egorov A 2016 Mapping tree height distributions in Sub-Saharan Africa using Landsat 7 and 8 data *Remote Sens. Environ.* Online:

http://dx.doi.org/10.1016/j.rse.2016.02.023

Hansen M C, Potapov P V, Moore R, Hancher M, Turubanova S a, Tyukavina a, Thau D, Stehman S V, Goetz S J, Loveland T R, Kommareddy a, Egorov a, Chini L, Justice C O and Townshend J R G 2013 High-resolution global maps of 21st-century forest cover change. *Science* **342** 850–3 Online: http://www.ncbi.nlm.nih.gov/pubmed/24233722

Healey S P, Cohen W B, Zhiqiang Y and Krankina O N 2005 Comparison of Tasseled Cap-based Landsat data structures for use in forest disturbance detection *Remote Sens. Environ.* **97** 301–10

Kalaba F K, Quinn C H, Dougill A J and Vinya R 2013a Floristic composition, species diversity and carbon storage in charcoal and agriculture fallows and management implications in Miombo woodlands of Zambia *For. Ecol. Manage.* **304** 99–109

Kalaba F K, Quinn C H, Dougill A J and Vinya R 2013b Floristic composition, species diversity and carbon storage in charcoal and agriculture fallows and management implications in Miombo woodlands of Zambia *For. Ecol. Manage.* **304** 99–109 Online: http://dx.doi.org/10.1016/j.foreco.2013.04.024

Korhonen L, Korhonen K T, Rautiainen M and Stenberg P 2006 Estimation of forest canopy cover: A comparison of field measurement techniques *Silva Fenn.* **40** 577–88

Luoga E J, Witkowski E T F and Balkwill K 2002 Harvested and standing wood stocks in protected and communal miombo woodlands of eastern Tanzania *For. Ecol. Manage.* **164** 15–30

Luoga E J, Witkowski E T F and Balkwill K 2000 Subsistence use of wood products and shifting cultivation within a miombo woodland of eastern Tanzania, with some notes on commercial uses *South African J. Bot.* **66** 72–85

Lyon B and Dewitt D G 2012 A recent and abrupt decline in the East African long rains *Geophys. Res. Lett.* **39** 1–5

Mayes M T, Mustard J F and Melillo J M 2015 Forest cover change in Miombo Woodlands: modeling land cover of African dry tropical forests with linear spectral mixture analysis *Remote Sens. Environ.* **165** 203–15

McNicol I M, Ryan C M and Williams M 2015 How resilient are African woodlands to disturbance from shifting cultivation? *Ecol. Appl.* 150407011925001 Online: http://www.esajournals.org/doi/abs/10.1890/14-2165.1

Paneque-Galvez J, McCall M K, Napoletano B M, Wich S A and Koh L P 2014 Small drones for community-based forest monitoring: An assessment of their feasibility and potential in tropical areas *Forests* **5** 1481–507

Pilliod D S and Arkle R S 2013 Performance of Quantitative Vegetation Sampling Methods Across Gradients of Cover in Great Basin Plant Communities *Rangel. Ecol. Manag.* **66** 634–47

Ribeiro N S, Saatchi S S, Shugart H H and Washington-Allen R A 2008 Aboveground biomass and leaf area index (LAI) mapping for Niassa Reserve, northern Mozambique *J. Geophys. Res.* **113** G02S02 Online: http://doi.wiley.com/10.1029/2007JG000550

Roberts D A, Gardner M, Church R, Ustin S, Scheer G and Green R O 1998 Mapping Chaparral in the Santa Monica Mountains Using Multiple Endmember Spectral Mixture Models *Remote Sens. Environ.* **65** 267–79

Rudel T K, Rudel T, DeFries R, Rudel T, Uriarte M, Hansen M, Brink A, Hugh D, Chidumayo E, Mayaux P, Fisher B, Sayer J, Harcourt C, Collins N, Debroux L, Hart T, Kaimowitz D, Karsenty A, Topa G, Corden W, Neary J, Wunder S, Chidumayo E, Gumbo D, Malaisse F, Binzangi K, Rudel T, Asner G, Defries R, Laurance W, Grainger A, Hansen M, Stehman S, Potapov P, Harris N, Kauppi P, Ausubel J, Fang J, Mather A, Sedjo R, Waggoner P, Saatchi S, Ernst C, Philippe M, Astrid V, Catherine B, Musampa C, Pierre D, Peterson R and Janzen D 2013 The national determinants of deforestation in sub-Saharan Africa. *Philos. Trans. R. Soc. Lond. B. Biol. Sci.* **368** 20120405 Online: http://www.ncbi.nlm.nih.gov/pubmed/23878341

Ryan C M, Hill T, Woollen E, Ghee C, Mitchard E, Cassells G, Grace J, Woodhouse I H and Williams M 2012 Quantifying small-scale deforestation and forest degradation in African woodlands using radar imagery *Glob. Chang. Biol.* **18** 243–57 Online: http://doi.wiley.com/10.1111/j.1365-2486.2011.02551.x

Saatchi S S, Harris N L, Brown S, Lefsky M, Mitchard E T A, Salas W, Zutta B R, Buermann W, Lewis S L, Hagen S, Petrova S, White L, Silman M and Morel A 2011 Benchmark map of forest carbon stocks in tropical regions across three continents *Proc. Natl. Acad. Sci.* **108** 9899–904 Online: http://www.pnas.org/cgi/doi/10.1073/pnas.1019576108

Sabol D E, Gillespie A R, Adams J B, Smith M O and Tucker C J 2002 Structural stage in Pacific Northwest forests estimated using simple mixing models of multispectral images *Remote Sens. Environ.* **80** 1–16

Schwartz M W and Caro T M 2003 Effect of selective logging on tree and understory regeneration in miombo woodland in western Tanzania *Afr. J. Ecol.* **41** 75–82

Strickler G S 1959 Use of the densiometer to estimate density of forest canopy on permanent sample plots *US Dep. Agric. Pacific Northwest For. Range Exp. Stn.* 5

Tang L and Shao G 2015 Drone remote sensing for forestry research and practices *J. For. Res.* **26** 791–7 Online: http://link.springer.com/10.1007/s11676-015-0088-y

Tyukavina A, Baccini A, Hansen M C, Potapov P V, Stehman S V, Houghton R A, Krylov A M, Turubanova S and Goetz S J 2015 Aboveground carbon loss in natural and managed tropical forests from 2000 to 2012 *Environ. Res. Lett. Environ. Res. Lett* **10** 74002–74002 Online: http://iopscience.iop.org/1748-9326/10/7/074002

URT 2014 *Basic Demographic and Socio-Eonomic Profile Statistical Tables, Tanzania Mainland* (Dar es Salaam) Online: http://www.tanzania.go.tz/egov_uploads/documents/Descriptive_tables_Tanzania_Mainland_sw.pdf

Vermote E, Justice C, Claverie M and Franch B 2016 Preliminary analysis of the performance of the Landsat 8/OLI land surface reflectance product *Remote Sens. Environ.*

Williams M, Ryan C M, Rees R M, Sambane E, Fernando J and Grace J 2008 Carbon sequestration and biodiversity of re-growing miombo woodlands in Mozambique *For. Ecol. Manage.* **254** 145–55

Woollen E, Ryan C M and Williams M 2012 Carbon Stocks in an African Woodland Landscape: Spatial Distributions and Scales of Variation *Ecosystems* **15** 804–18

WRI 2016 AFR100: Africa Restoring 100 Million Hectares of Deforested and Degraded Land by 2030 Online: http://www.wri.org/our-work/project/AFR100/about-afr100

TABLES: CHAPTER TWO

Table 2.1 Allometric equations used to calculate tree biomass from field data.

Reference	Equation	Source country	Notes
Chidumayo 2013	log (B) = 2.553*log(dbh) – 2.563	Zambia	MAP 894 (44) mm yr^{-1} (1967-2009)
Ryan et al. 2011	log (B) = 2.601*log(dbh) – 3.629	Mozambique	MAP 850 (269) mm yr^{-1} (1956-1969, 1998-2007)
Malimbwi et al. 1994	log (B) = 2.603*log(dbh) – 2.959	Tanzania	MAP not reported. Study location along Dar es Salaam-Morogoro Road.
Brown et al. 1989	B = 34.47 – 8.067*(dbh) + 0.659*$(dbh)^2$	Pan-dry tropics	Global dry tropics

Table 2.2 Forest structure variability by regrowth site age class across a Miombo Woodland landscape in Tabora, Tanzania. Values by column not sharing letters differed significantly in analyses of variance (ANOVA) and Tukey's Honest Significant Difference tests ($p < 0.05$).

Forest site age yr	N sites	Stem Density Stems ha-1	Height m	Biomass C Mg ha^{-1}	Volume m^3 ha^{-1}
3-4	3	138 (50.6)^{c}	3.18 (0.74)^{c}	0.85 (0.35)^{d}	2.51 (1.04)^{d}
10-24	3	756 (108)^{ab}	5.05 (0.06)^{bc}	4.71 (0.43)^{bc}	14.4 (1.30)^{bc}
30-40	3	891 (154)^{a}	8.02 (0.41)^{ab}	22.1 (3.09)^{ab}	70.2 (9.84)^{ab}
Mature – Village >100	3	897 (104)^{a}	11.4 (0.97)^{a}	49.9 (13.9)^{a}	160 (44.9)^{a}
Mature – Reserve >100	3	531 (137)^{abc}	9.19 (1.57)^{a}	38.1 (4.49)^{a}	122 (14.8)^{a}
Disturbed* 6-19 yr	3	307 (37)^{bc}	4.06 (0.38)^{bc}	1.48 (0.34)^{cd}	4.29 (1.06)^{cd}

Table 2.3 Variability of land cover features assessed by linear spectral mixture analysis of Landsat 8 data in a Miombo Woodland landscape, Tabora, Tanzania.

Date	Endmember	Mean (±σ)	% < 0	% > 100
14 July 2015	Vegetation	0.154 (0.071)	0.969	0
	NPV	0.396 (0.151)	0.140	0.056
	Substrate	0.121 (0.091)	7.41	0
	Shade	0.328 (0.083)	0.011	0
	RMS	0.008 (0.002)		

Table 2.4 Linear relationships modeling forest structure variables with Landsat 8-derived senesced vegetation and green vegetation land cover metrics in a Miombo Woodland landscape, Tabora, Tanzania.

Forest structure variable	Relationship	r^2
Basal area (A, m^2 ha^{-1})	$\log(A+1) = 1.908 - 2.364*NPV_z$	0.67 ($p < 0.001$)
	$\log(A+1) = 1.465 + 2.167*VEG_Z$	0.64 ($p < 0.001$)
	$\log(A+1) = 1.661 + 0.825*NDVI_Z$	0.58 ($p < 0.001$)
Biomass (B, kg ha^{-1})	$\log(B) = 9.049 - 3.859*NPV_Z$	0.66 ($p < 0.001$)
	$\log(B) = 8.364 + 3.413*VEG_Z$	0.57 ($p <0.001$)
	$\log(B) = 8.658 + 1.325*NDVI_Z$	0.55 ($p < 0.001$)

$_Z$Scene-normalized vegetation index (Z-score).

Table 2.5 Tree cover structure model results for a Miombo Woodland landscape in Tabora, Tanzania, estimated from Landsat 8-derived senesced vegetation and green vegetation land cover metrics. Values show the percentage of the modeled area (2.47×10^5 ha, 2470 km^2) with basal area and biomass ranges within reported field data for Miombo Woodlands. Z subscripts indicate Z-score (scene-normalization) of land cover metrics (see Methods).

Model type	Basal area 0-35 m^2 ha^{-1} (% training area)	Biomass 0-150 Mg ha^{-1} (% training area)
NPV_Z	95.7	97.2
VEG_z	92.7	98.6
$NDVI_Z$	96.5	97.8

Table 2.6 Tree cover structure estimates for forest and non-forest land cover areas for a Miombo Woodland landscape in Tabora, Tanzania, estimated from Landsat 8-derived senesced vegetation and green vegetation land cover metrics. Values shown are means and standard errors in parentheses. Forest and non-forest land cover was delineated following a regional approach accounting for variable land cover phenology (Mayes *et al* 2015). Z subscripts indicate Z-score (scene-normalization) of land cover metrics (see Methods).

Model type	Land cover type	Basal area m^2 ha^{-1}	Biomass Mg ha^{-1}	Biomass carbon Mg C ha^{-1}
NPV_Z	Forest	16.0 (9.55)	46.1 (43.0)	23.1 (21.5)
	Non-Forest	4.23 (4.01)	7.14 (11.2)	3.57 (5.58)
VEG_Z	Forest	12.2 (9.28)	31.4 (36.8)	15.7 (18.4)
	Non-Forest	2.09 (1.99)	2.94 (3.81)	1.47 (1.91)
$NDVI_Z$	Forest	13.0 (9.48)	35.2 (41.3)	17.6 (20.6)
	Non-Forest	2.47 (1.28)	3.14 (1.93)	1.57 (0.96)

Table 2.7. Analysis of variance for linear regression models assessing effects of tree cover type and remote sensing index (remote index) on aboveground biomass in a Miombo Woodland landscape, Tabora, Tanzania.

Region of Interest	Linear Model Fit Tree Type + remote index	Factor	F-ratio	*P*
1. Igombe Forest Reserve National managent	$r^2 = 0.938$ $p < 0.001$	Tree cover type	2400	<0.001
		Remote index	10.2	<0.001
2. Millennium Villages Village management	$r^2 = 0.794$ $p < 0.001$	Tree cover type	685	<0.001
		Remote index	2.42	0.090

Table S2.1. Field-measured and remote sensing-based estimates for aboveground tree biomass, derived from Landsat 8 OLI-based models based on senesced and green vegetation land cover metrics. Data reported for all field sites, grouped by categories of forest site age, management and disturbance.

Site category	Site	Field Biomass Mg ha^{-1}	SMA-NPV-est biomass Mg ha^{-1}	SMA-GV-est. biomass Mg ha^{-1}	NDVI-est. biomass Mg ha^{-1}
Regrowth	S08	2.6	1.2	1.8	2.2
3-4 yr	S10	0.32	6.2	5.7	5.5
	S13	2.3	9.7	15.8	12.5
	Mean ± s.e.m.	*1.7 ± 0.7*	*5.7 ± 2.5*	*7.7 ± 4.2*	*6.8 ± 3.0*
Regrowth	S02	9.7	5.0	12	8.4
10-24 yr	S12	11	22	44	35.8
	S18	7.8	14	6.1	6.5
	Mean ± s.e.m.	*9.4 ± 0.9*	*14 ± 5.0*	*21 ± 12*	*17 ± 10*
Regrowth	S16	38	95	86.7	85
30-40 yr	S17	38	13	14.7	10
	S19	57	52	52.2	41
	Mean ± s.e.m.	*44 ± 6.2*	*53 ± 24*	*51 ± 21*	*46 ± 22*
Mature	S07	140	*not modeled	*not modeled	*not modeled
Village-mgd	S14	45	18	14.2	10
>100 yr	S15	120	113	145	140
	Mean ± s.e.m.	*100 ± 28*	*66 ± 48*	*80 ± 65*	*75 ± 64*
Mature	S04	94	108	40	48
Igombe	S05				
Reserve		66	54	25	27
>100 yr	S06	68	42	31	31
	Mean ± s.e.m.	*76 ± 9.0*	*68 ± 20*	*32 ± 4.4*	*36 ± 6.3*
Disturbed	S03	2.9	3.0	4.0	3.8
	S09	1.8	3.2	3.3	3.0
	S11	4.2	4.7	5.1	4.9
	Mean ± s.e.m.	*3.0 ± 0.7*	*3.6 ± 0.5*	*4.1 ± 0.5*	*3.9 ± 0.6*

Table S2.2. Absolute values of differences between field measured and remote sensing estimates for biomass, derived from Landsat 8 OLI-based models based on senesced and green vegetation land cover metrics.

Site category	Site	| Field – SMA NPV biomass | $Mg\ ha^{-1}$	| Field-SMA GV biomass | $Mg\ ha^{-1}$	|Field – NDVI biomass | $Mg\ ha^{-1}$
Regrowth	S08	1.4	0.77	0.31
3-4 yr	S10	5.9	5.4	5.2
	S13	7.5	13.5	10.3
	Mean ± s.e.m.	***4.9 ± 1.8***	*6.5 ± 3.7*	*5.3 ± 2.9*
Regrowth	S02	4.7	2.5	1.3
10-24 yr	S12	12	33	25
	S18	6.2	1.7	1.3
	Mean ± s.e.m.	***7.5 ± 2.1***	*13 ± 11*	*9.2 ± 7.9*
Regrowth	S16	57	49	47
30-40 yr	S17	25	23	28
	S19	5.1	4.4	15
	Mean ± s.e.m.	*29 ± 15*	***26 ± 13***	*30 ± 9.3*
Mature	S07	*not modeled	*not modeled	*not modeled
Village-managed	S14	27	31	35
>100 yr	S15	5.9	25	19
	Mean ± s.e.m.	***16 ± 11***	*28 ± 2.8*	*27 ± 7.6*
Mature	S04	14	54	46
Igombe Reserve	S05	12	42	39
>100 yr	S06	27	37	37
	Mean ± s.e.m.	***17 ± 4.6***	*44 ± 5.2*	*41 ± 2.8*
Disturbed	S03	0.1	1.1	0.89
	S09	1.4	1.5	1.2
	S11	0.5	0.91	0.75
	Mean ± s.e.m.	***0.7 ± 0.4***	*1.2 ± 0.2*	*0.9 ± 0.1*
Overall	Mean ± s.e.m.	**12 ± 3.5**	19 ± 4.6	18 ± 4.2

Table S2.3. Aboveground biomass estimates at image validation sites, modeled with senesced (SMA-NPV) and green vegetation (SMA-GV, NDVI) Landsat 8-based land cover indicators, for dense woodland, mbuga and cleared tree covert types in national reserve and village-managed Miombo landscape regions of Tabora, Tanzania. Validation sites for tree cover types were selected as 3x3 pixel areas from a 14 July 2015 Landsat 8 OLI image (see Methods). Region numbers correspond with numbered boxes in figure 2(a). Means comparison tests (Tukey HSD) for biomass were performed for each management region separately; values not sharing letters by region of interest differed significantly in Tukey HSD tests ($p < 0.05$). Accompanies figure 2.10.

Region of interest	Model type	Tree Cover Type	N sites	Biomass Mg ha^{-1}
1.Igombe Forest Reserve National management	Senesced Veg. SMA-NPV	Dense Woodland	38	130 ± 2.8^{a}
		Mbuga	40	24 ± 1.7^{c}
		Cleared	40	4.2 ± 0.5^{d}
	Green Veg. SMA-GV	Dense Woodland	38	115 ± 3.0^{b}
		Mbuga	40	8.5 ± 0.7^{d}
		Cleared	40	14 ± 2.9^{d}
	Green Veg. NDVI	Dense Woodland	38	130 ± 2.7^{a}
		Mbuga	40	9.5 ± 1.0^{d}
		Cleared	40	7.8 ± 1.2^{d}
2.Millennium Villages Village management	Senesced Veg. SMA-NPV	Dense Woodland	40	88 ± 5.0^{a}
		Mbuga	41	23.8 ± 1.8^{b}
		Cleared	38	2.0 ± 0.2^{c}
	Green Veg. SMA-GV	Dense Woodland	40	91 ± 5.1^{a}
		Mbuga	41	6.4 ± 0.5^{c}
		Cleared	38	1.9 ± 0.4^{c}
	Green Veg. NDVI	Dense Woodland	40	92 ± 5.6^{a}
		Mbuga	41	6.9 ± 0.6^{c}
		Cleared	38	2.0 ± 0.3^{c}

FIGURES: CHAPTER TWO

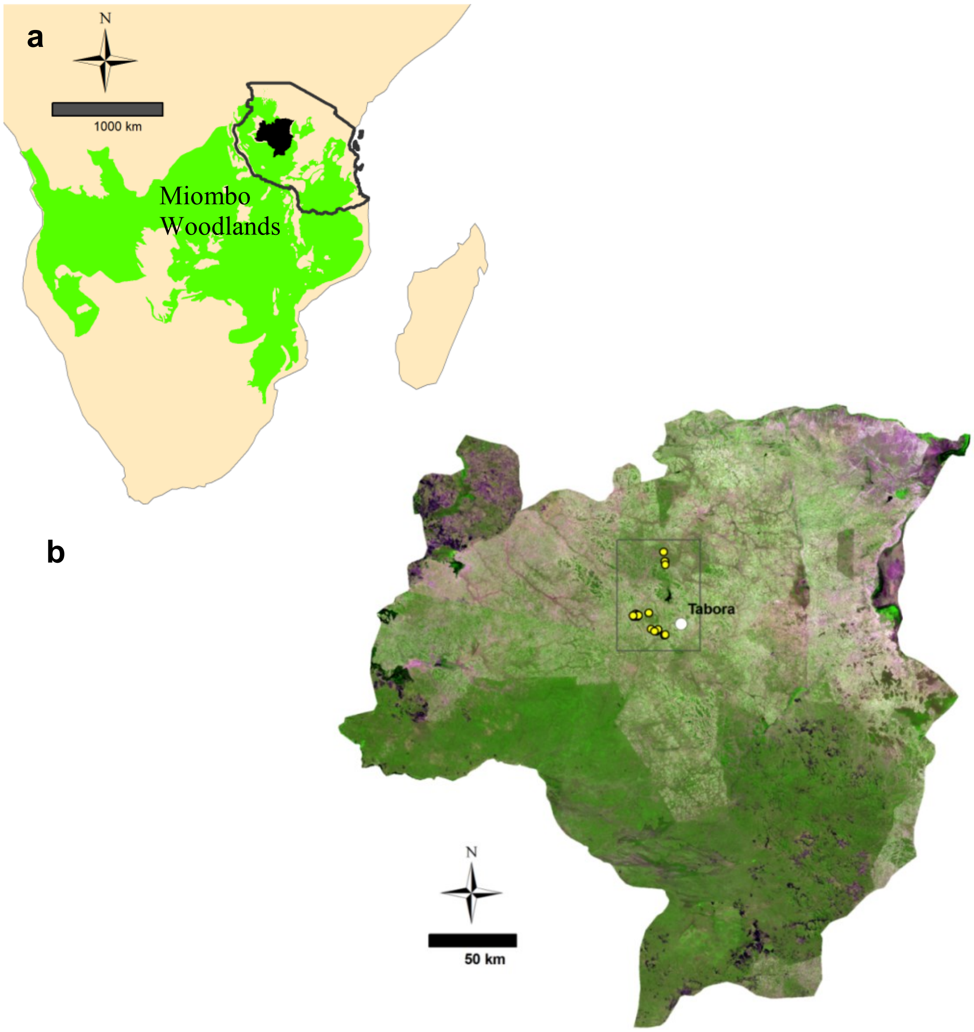

Figure 2.1. Location of the Tabora, Tanzania study area. (a) Tabora, Tanzania (black polygon) is located in the northeastern part of the Miombo Woodlands (green) which span 2.5 million km^2 across sub-Saharan Africa ecoregion. (b) Land cover of Tabora, Tanania shown in a Landsat 8 false-color image mosaic from June-July 2015 (red:green:blue colors showing Landsat 8 bands 6 (shortwave infrared, 1.57-1.65 um), 5 (near-infrared, 0.85-0.88 um), 7 (2.11-2.29 um). Tree cover-dominated TDF regions predominate to the south, shown in darker greens. Village areas dominate the northern half of the province and are a mix of shifting cultivation, mature and regrowth woodlands. Across Tabora region, more sparsely vegetated regions in brighter reds and pinks, burned areas in purple, and wet areas (e.g. reservoirs and welands) in black *(right-center)* The gray box shows the part of Tabora where field sites were located for this study (figure 2.2).

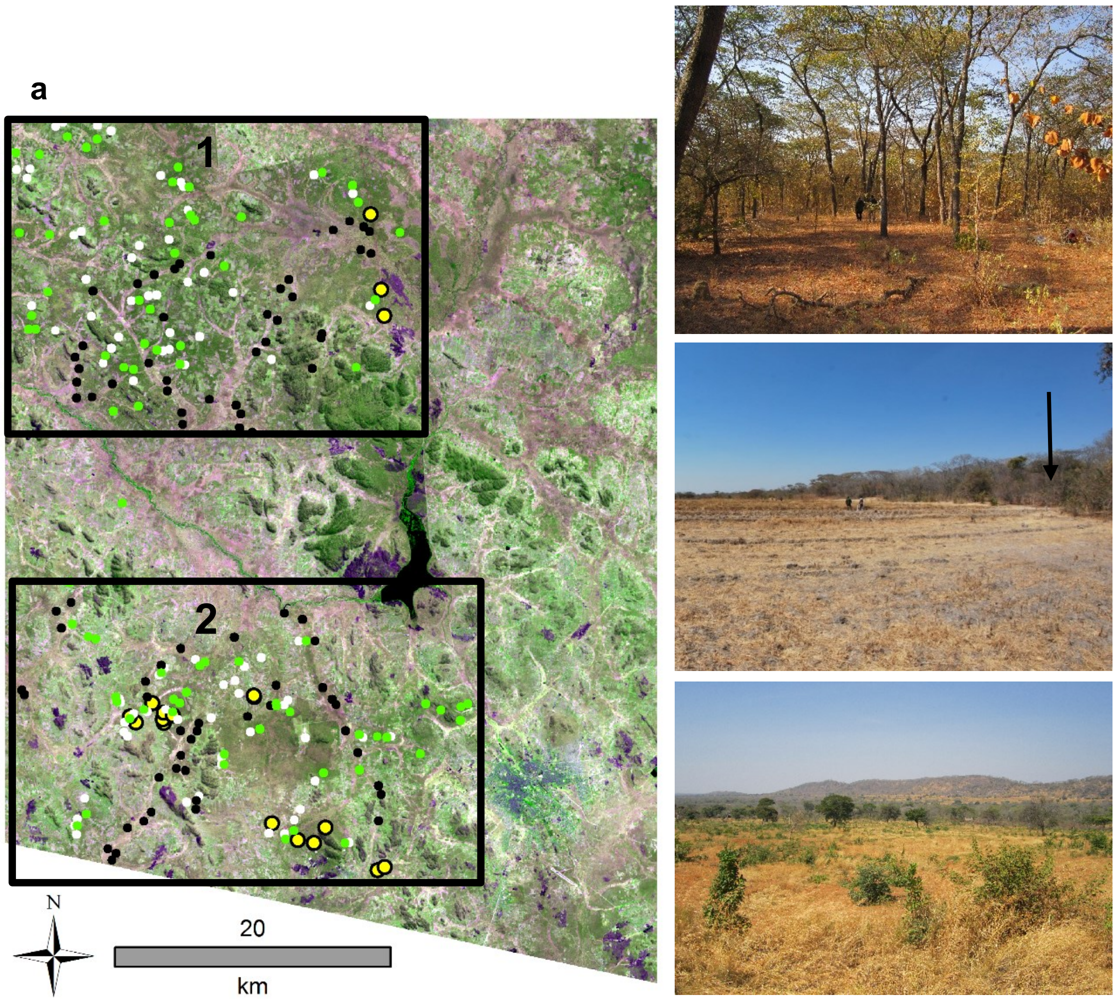

Figure 2.2. Locations of field sites and regions of interest for forest monitoring in Tabora Region, Tanzania. (a) Landsat 8 false-color image of the 2470 km^2 training area (gray box in figure 1), 14 July 2015, with red:green:blue showing bands 6 (shortwave infrared, 1.57-1.65 um), 5 (near-infrared, 0.85-0.88 um), 7 (2.11-2.29 um). Land surface areas with dense tree cover appear in darker greens, and with decreasing tree cover, the land surface appears increasingly pink or white. Dark-bordered yellow markers indicate field sites across a forest regrowth chronosequence, where tree inventory, land cover and ground data were sampled (18 total sites). Boxes 1 and 2 indicate two regions for forest monitoring with different land management regimes: 1-Igombe Forest, a nationally managed forest reserve; 2-The Millennium Villages Project-Mbola region, a locally-managed village landscape. (b) – (d) Photos of dense, sparse and low tree cover areas, indicated by green (dense), black (sparse) and white (low) markers on the map in (a). We selected 35-40 image-validation points across national and village-managed regions to assess the performance of tree structure maps. (b) Dense tree cover (locations indicated by green markers in (a)). (c) Sparse tree cover areas indicated by arrow, prevalent along seasonally flooding drainages (locally, mbuga or dambo) with high water tables and clay-textured soils (black markers in (a)). (d) Areas with low to no tree cover (white markers in (a)). The photos shown (M. Mayes) were taken in dry seasons 2015 (b,c) and 2012 (d) and used to illustrate land cover conditions, but field data was not collected at these locations. Representative photos of regrowth chronosequence sites where field data were taken are shown in figure S1.

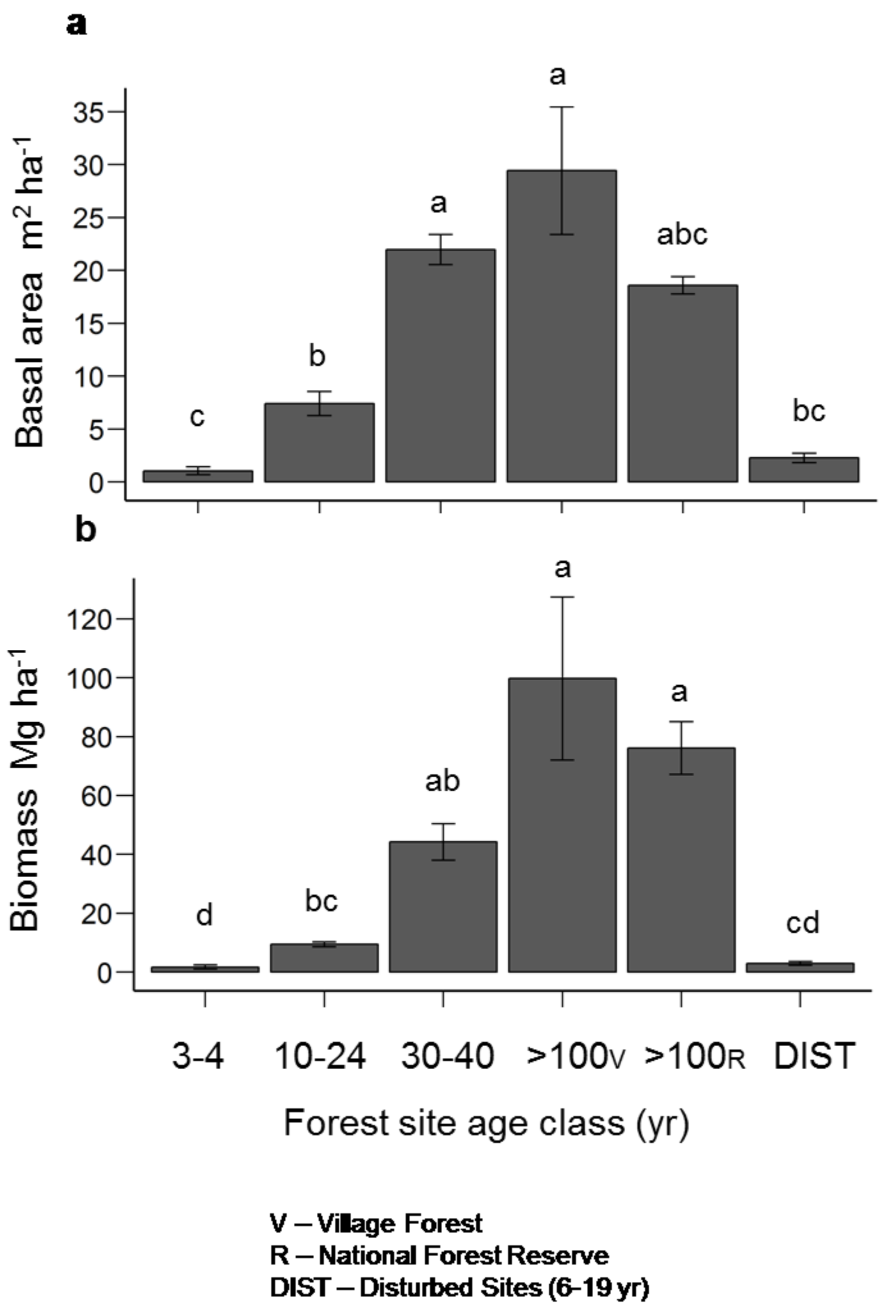

Figure 2.3. Forest structure across regrowth and mature Miombo tropical dry forest sites in Tabora, Tanzania. **(a)** Basal area relationships to forest site age class. **(b)** Biomass relationships to forest site age class. Letters indicate significant class differences in ANOVA and Tukey's Honest Significant Difference Tests ($p < 0.05$).

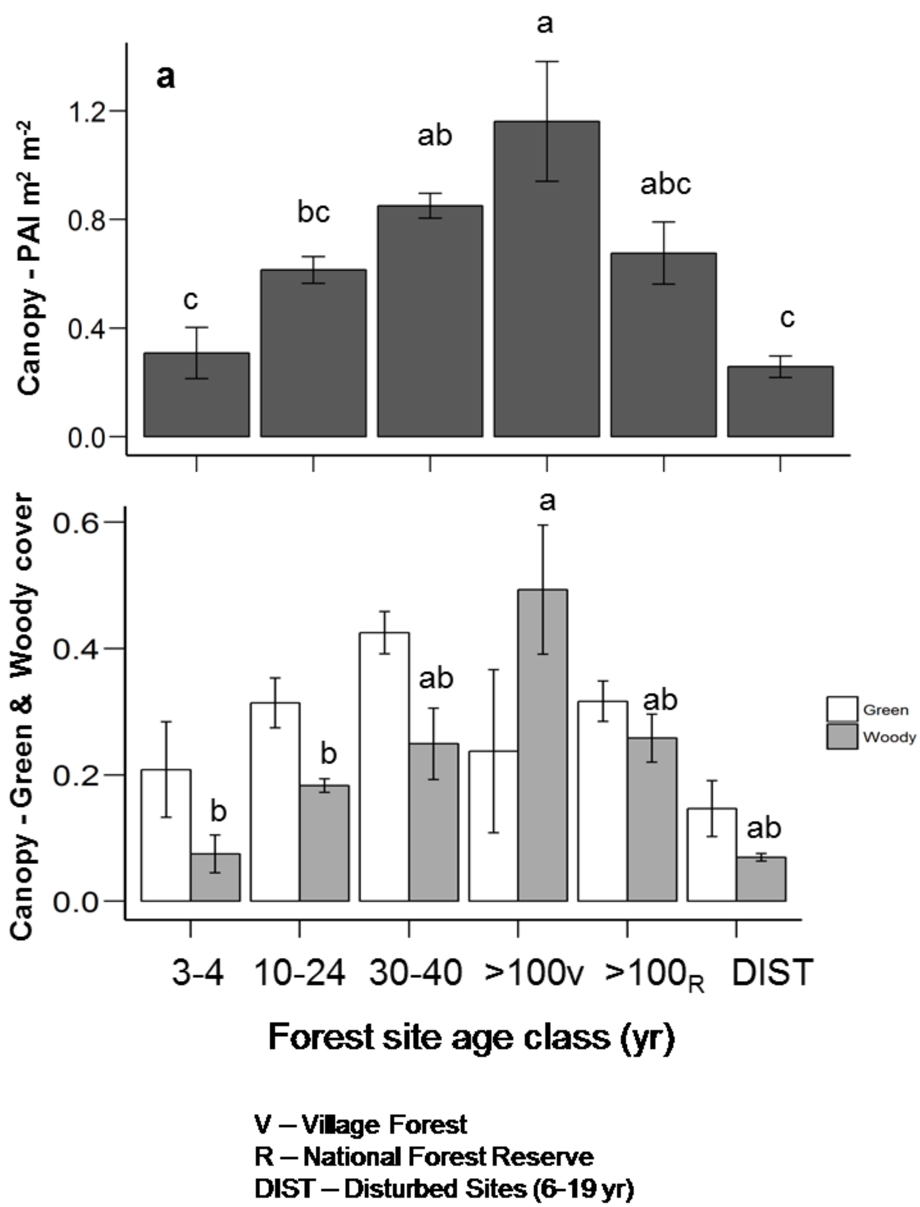

Figure 2.4. Land cover features from canopy and ground cover across regrowth and mature Miombo tropical dry forest sites in Tabora, Tanzania. **(a)** Canopy Plant-Area Index (PAI). **(b)** Proportions of Green Leaf and Woody Material comprising canopy cover measured by spherical densiometer. **(c)** Proportions of Open Sky area comprising canopy survey measurements by spherical densiometer. **(d)** Summed proportions of leaf litter and senesced grass comprising ground cover measured by point-line transect. Letters indicate significant class differences in ANOVA and Tukey's Honest Significant Difference tests ($p < 0.05$). Panels **(c)** and **(d)** follow on the next page.

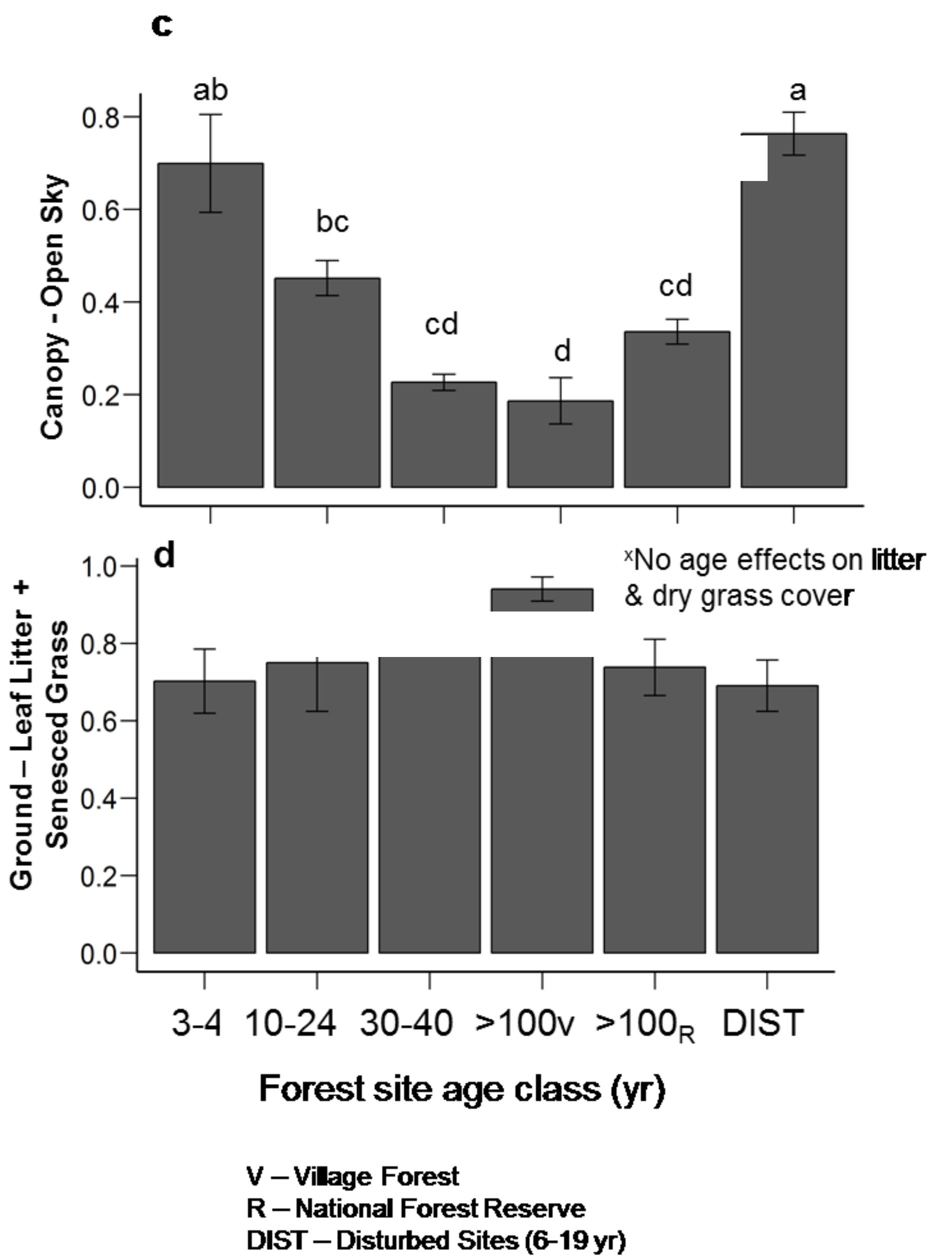

Figure 2.4 (cont). Land cover features from canopy and ground cover across regrowth and mature Miombo tropical dry forest sites in Tabora, Tanzania. Continued from previous page.

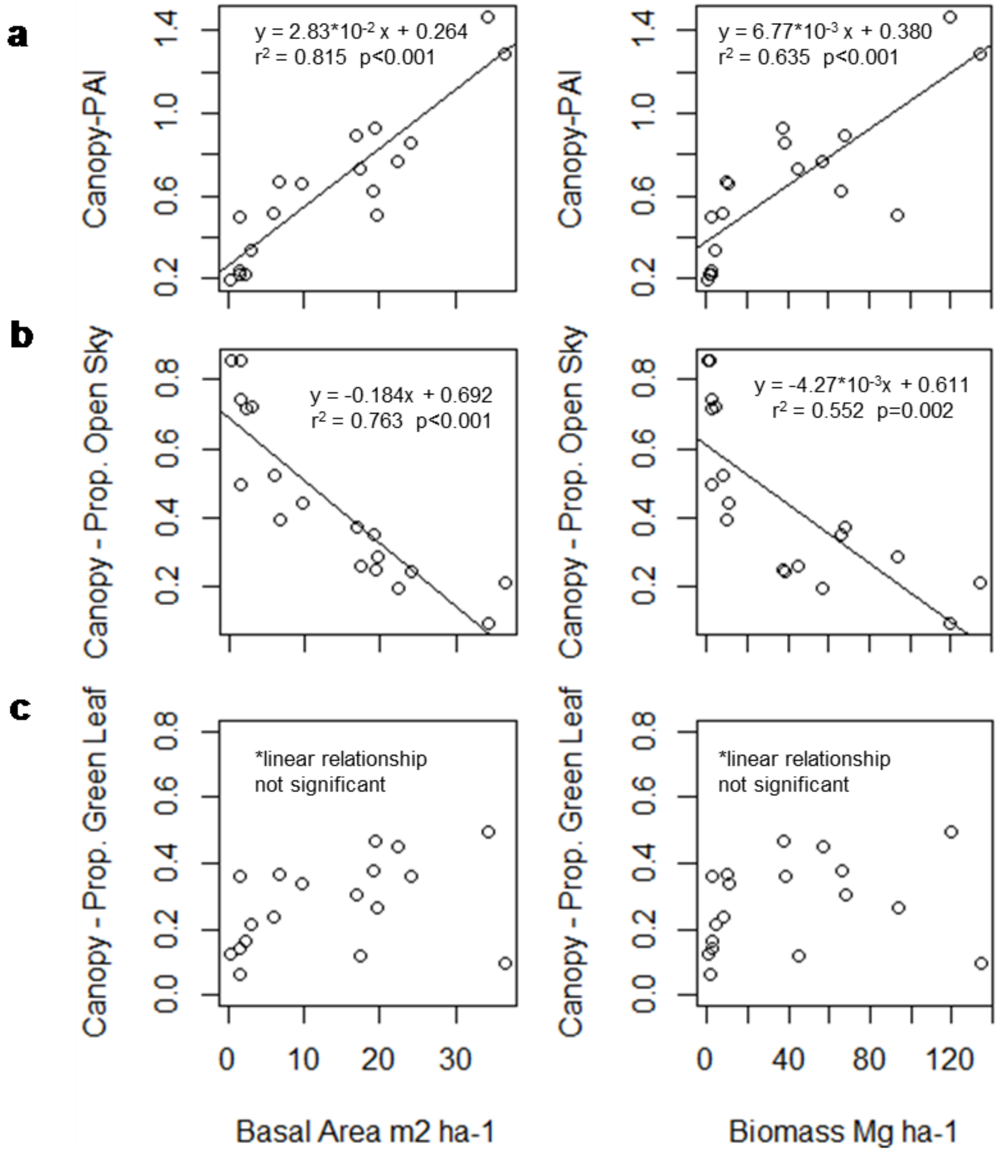

Figure 2.5. Linear Relationships among canopy and forest structure variables across Miombo Woodland forest sites in Tabora, Tanzania. Figure sub-panels consist of three rows. **(a)** Canopy Plant-Area Index (PAI) vs. basal area and biomass. **(b)** Canopy proportion open sky (spherical densiometer survey) vs. basal area and biomass. **(c)** Canopy proportion green leaf material (spherical densiometer survey) vs. basal area and biomass.

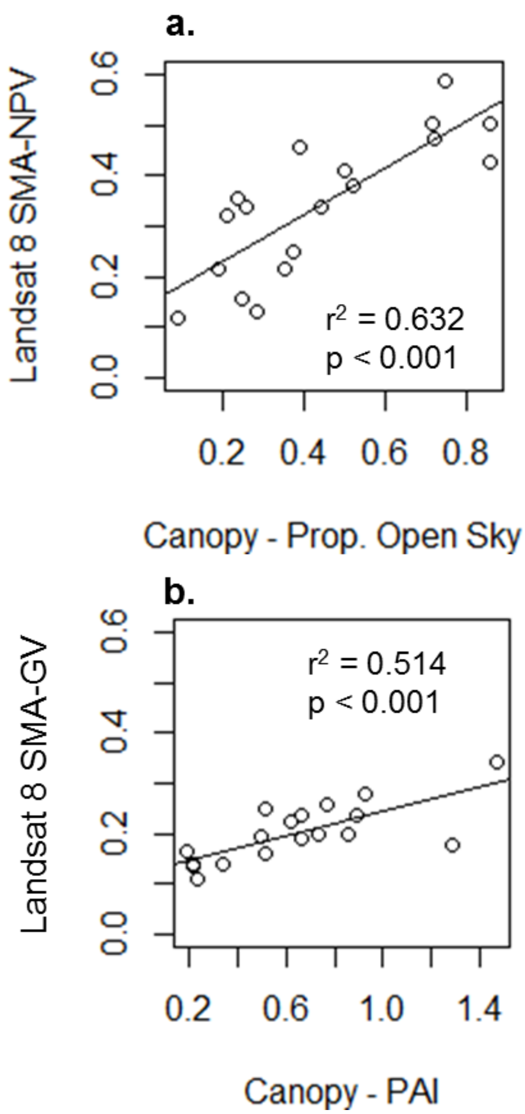

Figure 2.6. Linear relationships among field-measured canopy cover and Landsat-derived land cover metrics in a Miombo Woodland, Tabora, Tanzania. **(a)** Landsat SMA-NPV vs. canopy proportion open sky (spherical densiometer survey). **(b)** Landsat SMA-GV vs. canopy plant-area index (PAI). **(c)** Landsat NDVI vs. PAI.

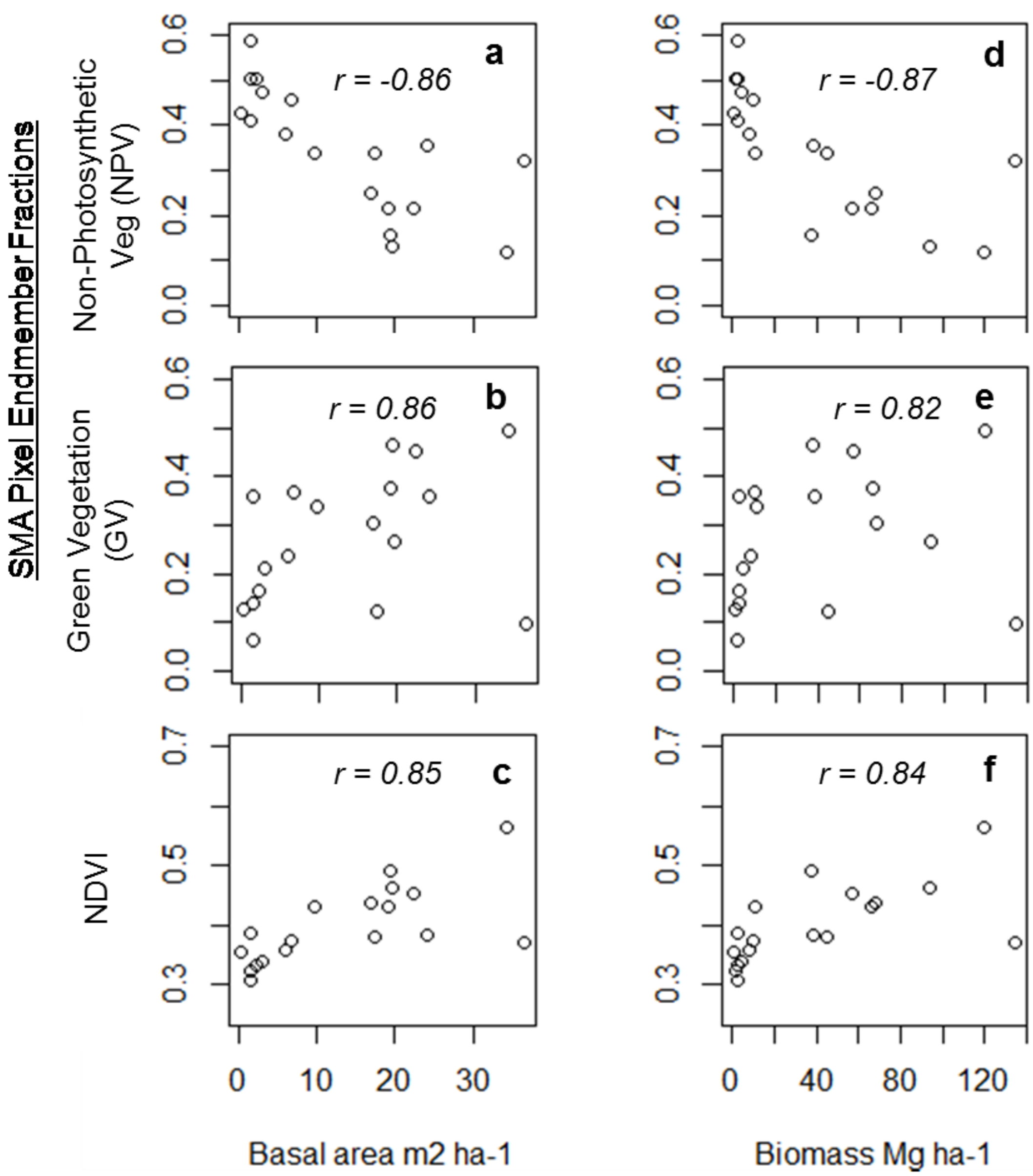

Figure 2.7. Pearson correlations among forest structure and Landsat-derived land cover metrics in a Miombo Woodland, Tabora, Tanzania. **(a)** Landsat SMA-NPV vs. basal area. **(b)** Landsat SMA-GL (Green Leaf) vs. basal area. **(c)** Landsat-NDVI vs. basal area. **(d)** Landsat SMA-NPV vs. biomass. **(e)** Landsat SMA-GL vs. biomass. **(f)** Landsat-NDVI vs. biomass. Pearson correlations are listed on figures ($p < 0.01$).

a

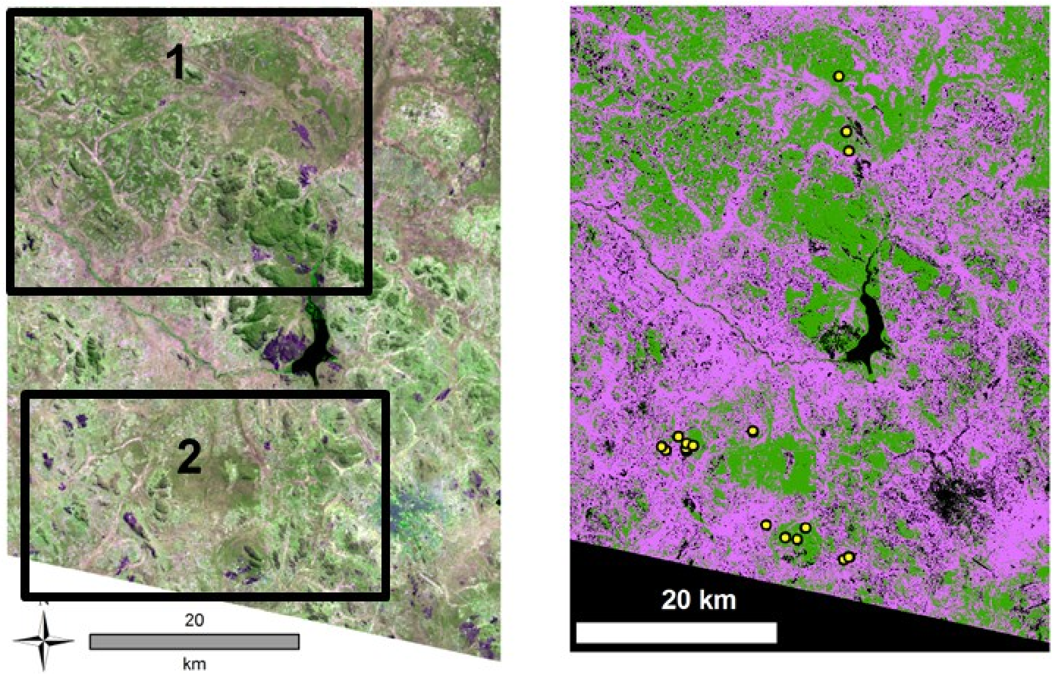

Figure 2.8. Basal area and biomass maps modeled by senesced vegetation and green vegetation Landsat 8-derived land cover metrics in a Miombo Woodland, Tabora, Tanzania. Figure extends for four pages. **(a)** Landsat 8 reflectance image (14 July 2015) (left) and land cover map created using SMA-based thresholding (Mayes *et al* 2015) showing forest in green, non-forest in magenta (right), and areas not mapped in black (water, urban, burned areas and scene edges). Regions of interest for forest monitoring are 1. Igombe Reserve and 2. Millennium Villages area (see Methods and figure 2). Yellow dots in land cover map show locations of field sites. **(b)** Basal area and biomass maps derived from Landsat SMA-NPV, a senesced vegetation land cover metric. **(c-d)** Basal area and biomass derived from green vegetation metrics: Landsat SMA-GV and **(d)** Landsat-NDVI.

b

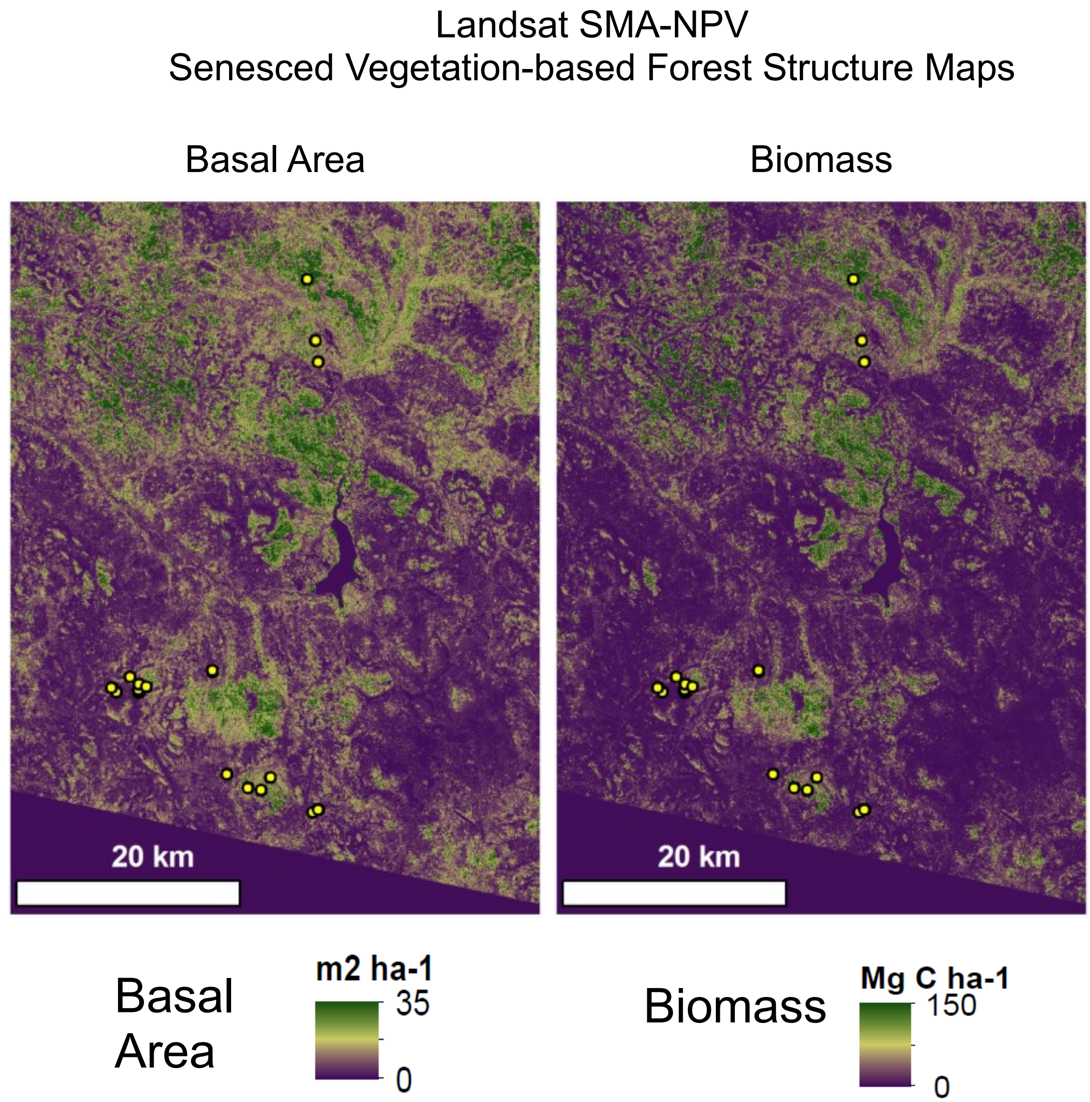

Figure 2.8 (cont). Basal area and biomass modeled by senesced vegetation and green vegetation Landsat 8-derived land cover metrics in a Miombo Woodland, Tabora, Tanzania. **(b)** Basal area and biomass maps derived from Landsat SMA-NPV, a senesced vegetation land cover metric.

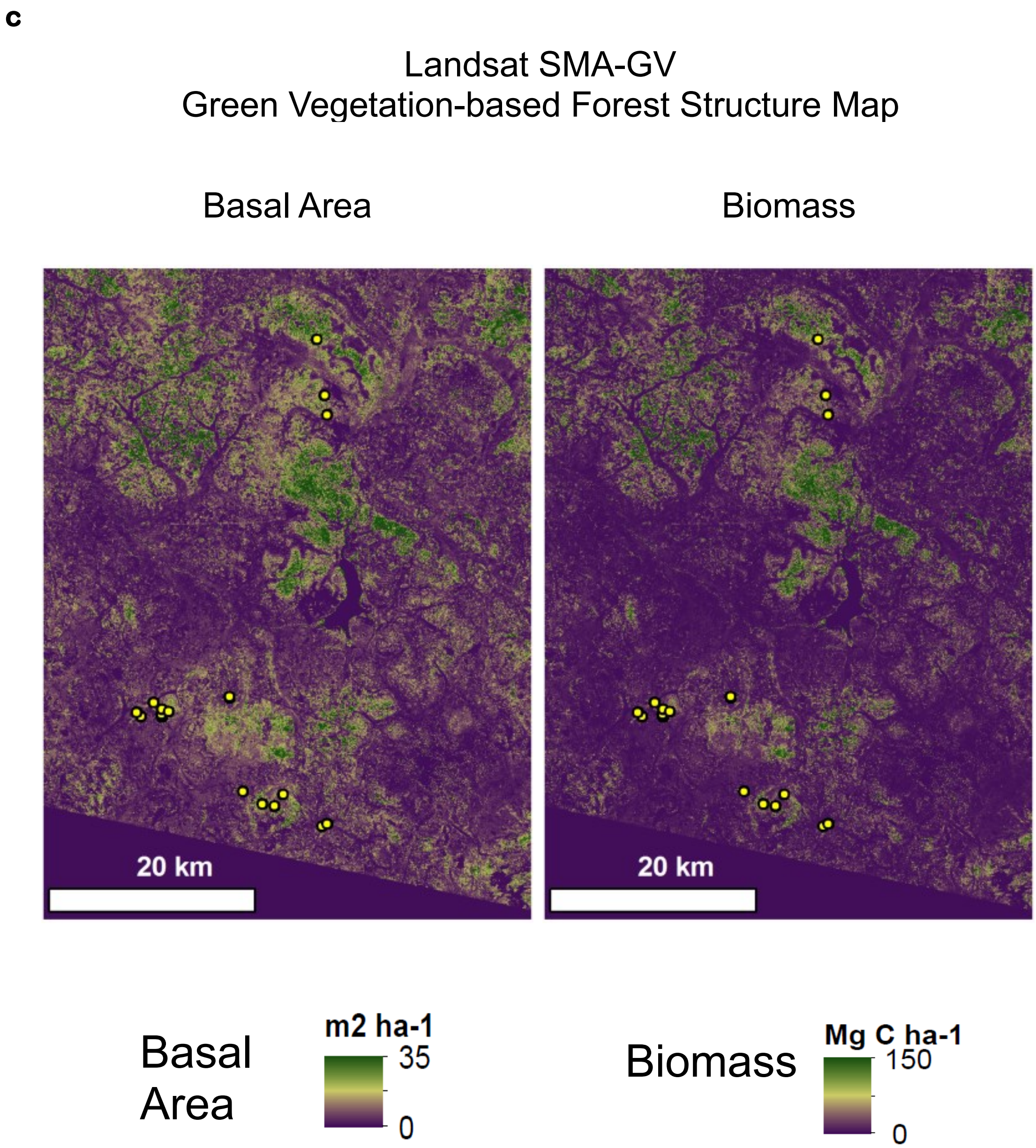

Figure 2.8 (cont). Basal area and biomass modeled by senesced vegetation and green vegetation Landsat 8-derived land cover metrics in a Miombo Woodland, Tabora, Tanzania. **(c)** Basal area and biomass derived from green vegetation metrics: Landsat SMA-GV.

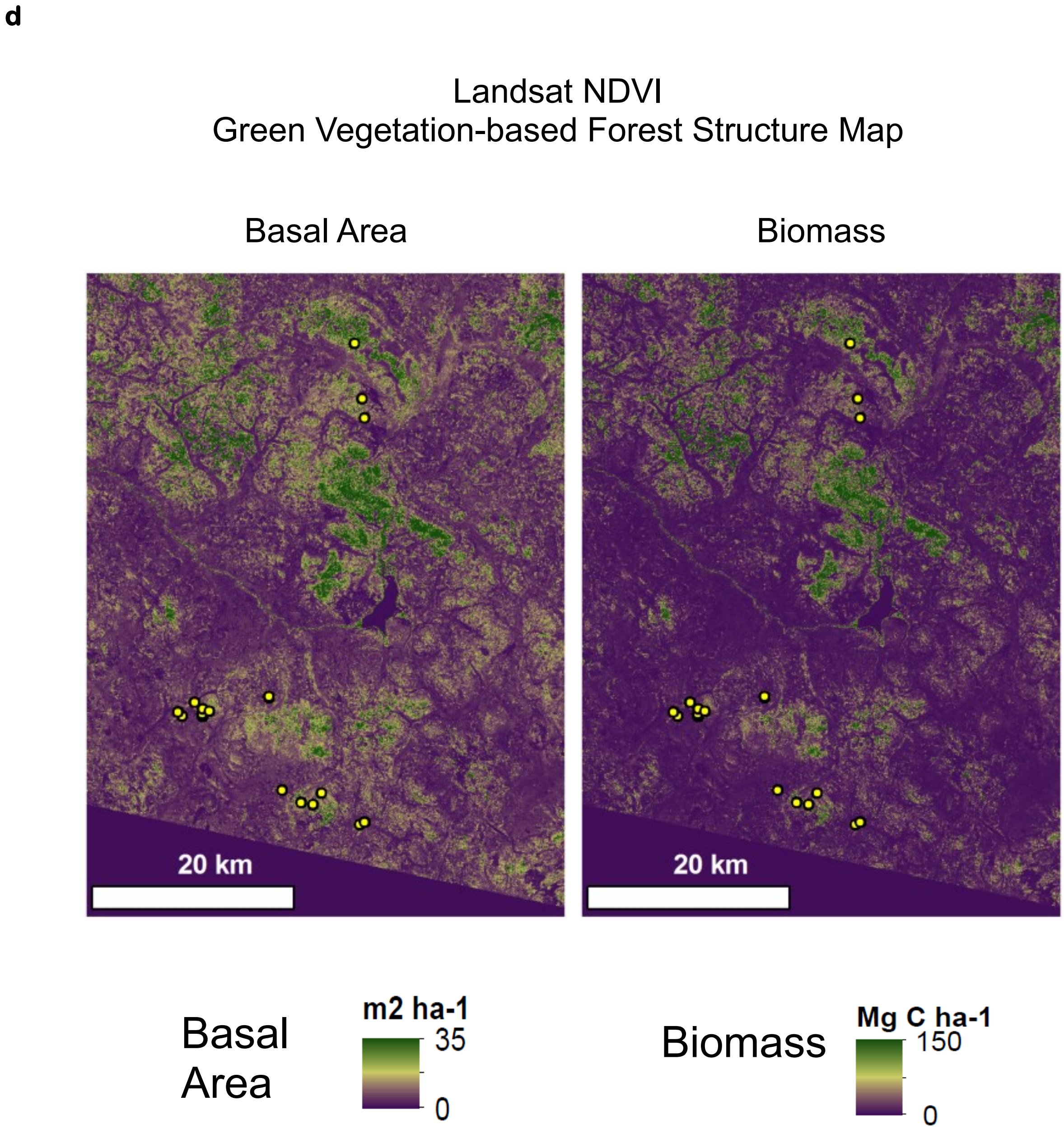

Figure 2.8 (cont). Basal area and biomass modeled by senesced vegetation and green vegetation Landsat 8-derived land cover metrics in a Miombo Woodland, Tabora, Tanzania. **(d)** Basal area and biomass derived from green vegetation metrics: Landsat SMA-NDVI.

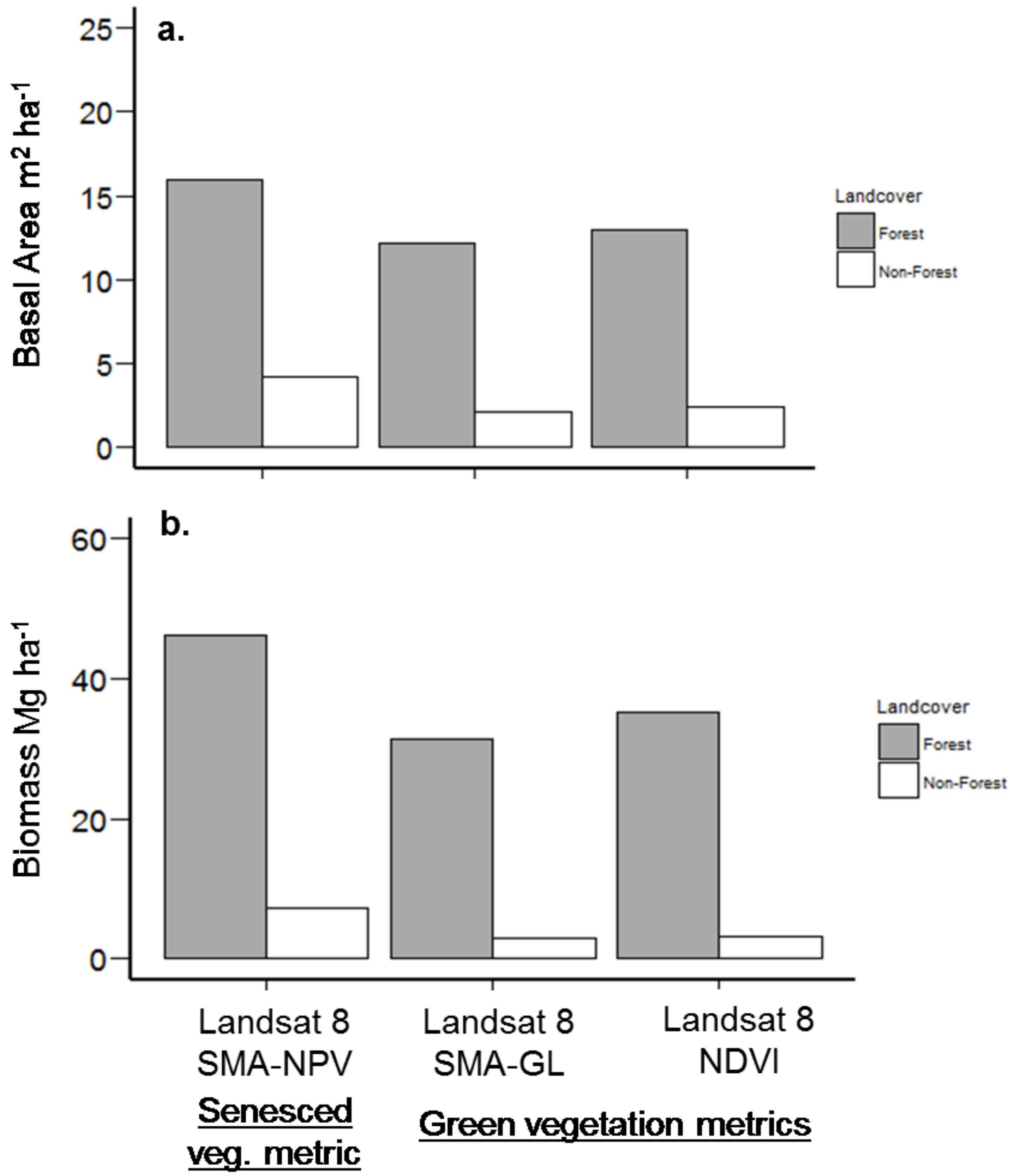

Figure 2.9. Estimates of tree structure for forest and non-forest land cover regions in a Miombo Woodland, Tabora Tanzania, modeled with three Landsat 8 land cover metrics. **(a)** Basal area estimates from Landsat SMA-NPV, Landsat SMA-GV and Landsat-NDVI. **(b)** Biomass estimates from Landsat SMA-NPV, Landsat SMA-GV and Landsat-NDVI.

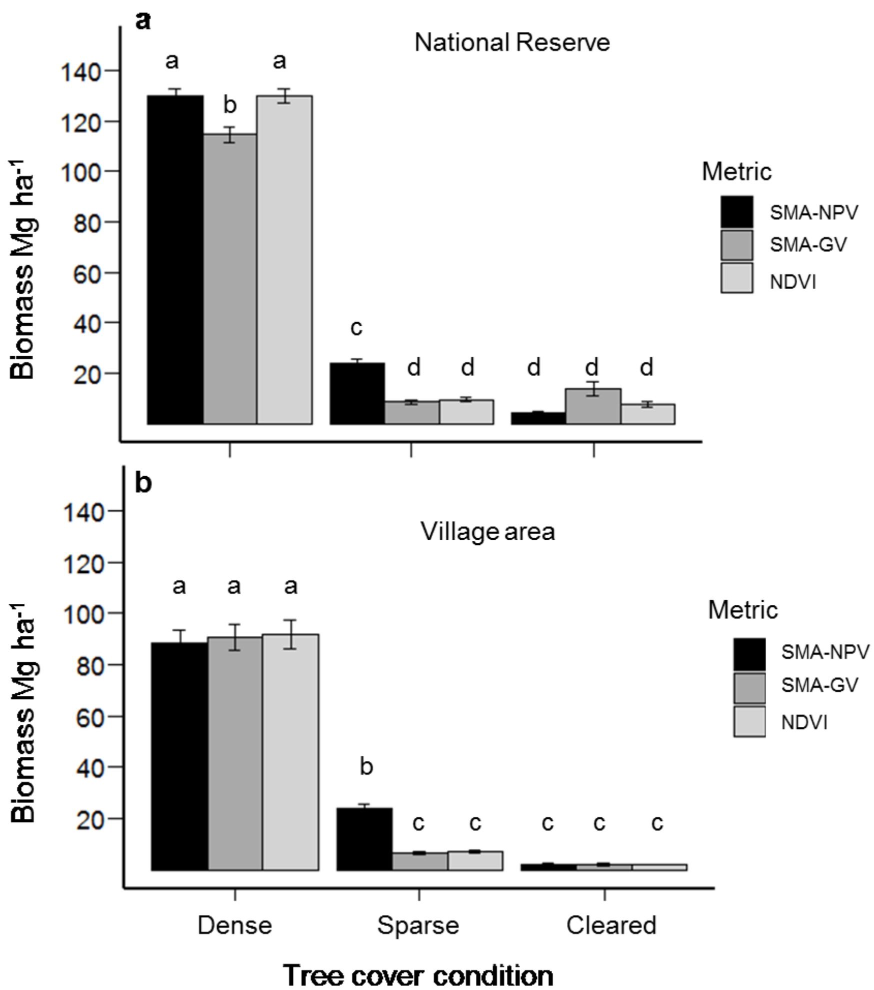

Figure 2.10. Aboveground biomass estimates for three tree cover types, modeled with senesced (SMA-NPV) and green vegetation (SMA-GV, NDVI) Landsat 8-based land cover indicators, at nationally managed forest reserve (Igombe Reserve) and village-managed (Millennium Village-area) Miombo landscapes in Tabora, Tanzania. Bars represent mean biomass estimates for groups of 38-41 image validation sites selected for each tree cover type as 3x3 pixel areas from a 14 July 2015 Landsat 8 OLI image (see Methods). Means comparison tests (Tukey HSD) for biomass were performed for each management region separately; values not sharing letters by region of interest differed significantly in Tukey HSD tests ($p < 0.05$).

Figure S2.1. Photos of representative field sites across the forest regrowth chronosequence from which tree inventory, land and ground cover data were collected in 2014-15. (a) A 3 yr regrowth site, representative of sites 3-4 yrs. (b) A 10 yr regrowth site, representative of sites 10-24 yrs. (c) A 30 yr regrowth site, representative of sites 30-40 yrs. (d) A mature forest site (Village area), representative of sites 50 to more than 100 years.

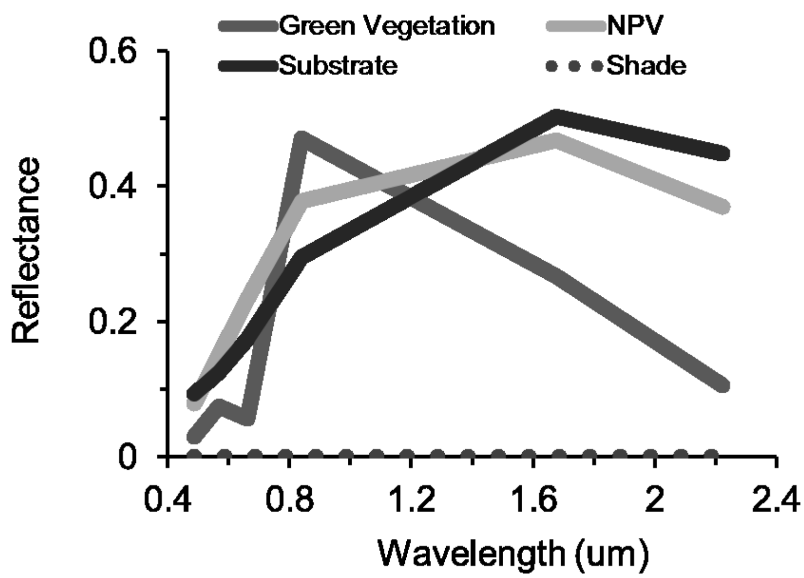

$$p_b = \sum [F_{EM} P_{EM,B} + E_b];\ \sum F_{EM} = 1$$

Figure S2.2 Spectral endmembers used for linear spectral mixture analysis of Landsat data and the governing equation for linear SMA analysis with a unit sum constraint**.** SMA models pixel reflectance (p_b) as multiplicative fractions of the reflectance spectra of known land cover materials or mixtures ($F_{em*}p_{em}$) plus an error term (E_b), with the constraint that all pixel fractions must sum to unity (1). The endmembers used to model green vegetation, non-photosynthetic vegetation (NPV) and substrate are Tabora-specific, selected from different time periods (May 2008 (green vegetation spectra) and July 2008 (NPV, substrate)) Landsat 5 data from pixels geolocated to calibration field sites with high proportions of these materials comprising ground cover (Mayes *et al.* 2015). Spectra were converted to Landsat 8 spectral resolution using Spectral Library Resampling tool

CHAPTER THREE

RELATING LANDSAT-DERIVED LAND COVER METRICS TO FOREST STRUCTURE FOR PREDICTING LANDSCAPE-SCALE BIOMASS PATTERNS ACROSS TWO MIOMBO WOODLAND REGIONS IN TANZANIA AND MOZAMBIQUE

Marc Mayes[a,b], John Mustard[a], Jerry Melillo[b], Christopher Neill[b,c], Casey Ryan[d], Emily Woollen[d], Mat Williams[d], Iain McNicol[d], Gerson Nyadzi[e]

a) Department of Earth, Environmental and Planetary Sciences, Brown University, Providence, Rhode Island, United States

b) The Ecosystems Center, Marine Biological Lab, Woods Hole, Massachusetts, United States

c) The Woods Hole Research Center, Falmouth, Massachusetts, United States

d) School of Geosciences, University of Edinburgh, Edinburgh, Scotland, United Kingdom

e) Millennium Villages Project-Mbola, Tabora, Tanzania

[Prepared for Submission as an Original Article to Remote Sensing of Environment]

Abstract

The Miombo Woodlands in sub-Saharan Africa contain among the world's largest contiguous tropical dry forests and are a global hot spot for forest changes (Campbell, 1996; Rudel et al., 2013). There is poor understanding of the heterogeneity of forest structure, or the extent and impacts of disturbance on forest condition beyond forest cover in Miombo Woodlands. Forest areas in Miombo Woodlands have lo

wer maximum biomass (<250 Mg ha^{-1}), sparser canopy cover (<50%) and high spatial variability compared to other global tropical forests (Aber & Mellilo, 1991; Frost, 1996). Increasing proportions of standing forest consists of recent regrowth and disturbed areas which have low biomass (<50 Mg ha^{-1}) (Chidumayo, 2013; Mayes, Mustard, & Melillo, 2015). This study presents one of the first cross-regional comparisons of field data on forest structure to land cover metrics quantified with Landsat data in the Miombo Woodlands. Its goals were to (1) identify relationships among optical remote sensing metrics of land cover and forest structure patterns useful for biomass monitoring, with a focus on low-biomass areas (<50 Mg ha^{-1}), within in two different Miombo forest regions (Tabora, Tanzania and Sofala, Mozambique); and (2) compare the performance of existing and new biomass maps produced from (1) for modeling tree biomass, particularly for low-biomass regions. Despite significantly different mature forest structure across regions and use of different Landsat sensors for each, we found strong positive correlations among Landsat 5 and 8-derived NDVI (greenness), NDMI (moisture) and forest structure (basal area, biomass) (range of Pearson r = 0.60-0.85, $p < 0.01$), and negative correlations between land cover brightness (sum of Landsat optical reflectance bands) and forest structure (range of Pearson r = -0.65-(-0.83). In both regions, we found that an existing 500 m pan-tropical biomass map (Baccini

et al., 2012) over-estimated aboveground biomass in low-biomass areas (<50 Mg ha^{-1}) by 10-60 Mg ha^{-1} (20 to +100%). Landsat-scale 30 m maps produced from regional land cover-forest biomass regressions produced absolute values and spatial patterns of biomass (0-200 Mg ha^{-1}) in both Tabora and Sofala more closely matching landscape gradients related to land use and ecological factors, though need further validation and methodological refinements. Our findings suggest successful pursuit of transferrable remote sensing relationships for Miombo landscapes should use multiple land cover metrics besides greenness measures, and appropriate representation of covariates affecting forest structure-land cover relationships in field datasets. The new 30 m biomass maps we developed provided new insight into landscape-scale biomass variability in Tanzania and Mozambique study regions, particularly at low-biomass areas, and offer ways forward for monitoring of forest condition beyond forest cover in these regions.

1. Introduction

The Miombo Woodlands cover more than 2.5 million square kilometers across sub-Saharan Africa (Campbell, 1996; Olson & Dinerstein, 2002). They provide biodiversity, terrestrial carbon storage, ecosystem services and livelihood benefits to over 150 million people in fast-growing countries (Campbell, 1996; Rudel et al., 2013; United Nations, Department of Economic and Social Affairs, 2015). The Miombo are mixed tree-grass savannas that have extensive areas of deciduous and semi-deciduous tropical dry forest (Frost, 1996). Miombo Woodlands are a global hot spot for forest changes, but they are among the most difficult regions globally in which to monitor forest changes at landscape scales using remote sensing (Hansen et al., 2013; Tyukavina et al., 2015). This is because of the heterogeneity of mature forest structure and land cover, the small spatial scales (often <1-2 ha) of land use and management, and complex effects of ecological and land use-related disturbance on land cover (Frost, 1996; Ryan et al., 2012; Williams et al., 2008). Current pan-tropical forest biomass mapping approaches (Baccini et al., 2012; Saatchi et al., 2011) lack calibration in Miombo regions where standing forest biomass is quite low (<50 Mg ha^{-1}). Improved understanding of land cover-satellite data relationships in areas of low aboveground tree biomass is becoming more important both for understanding landscape change in forest areas, where increasing proportions of standing Miombo consists of low-biomass recent regrowth, and non-forest areas, where strategies are needed to monitor reforestation and afforestation targets as part of larger sustainable land use and development programs (WRI, 2016).

This study tests relationships between field data on forest structure and land cover variables measured by Landsat satellites, and assesses the performance of new Landsat-based 30 m and existing MODIS-based 500 m biomass maps in low (<50 Mg ha^{-1}) and high (>50 Mg ha^{-1}) forest biomass areas across contrasting Tanzania and Mozambique study regions. Since a comprehensive review in the 1990s (Campbell, 1996) , there has been little new cross-comparison or synthesis of information on mature forest structure across different Miombo Woodland regions, nor attention to how relationships among field data on forest structure and satellite data on land cover vary between Miombo regions. For mature forests, past studies have reported wide ranges of basal areas (10 to > 30 m^2 ha^{-1}), aboveground tree biomass (40 to > 100 Mg ha^{-1}) and canopy cover (20% to > 80%) depending on rainfall, edaphic factors and disturbance history (Frost, 1996; Sankaran et al., 2005; Williams et al., 2008). Increasingly, large areas of Miombo forests do not reflect mature-forest conditions. Since the year 2000, high rates of regional forest loss and degradation have occurred amid increasing demands for agricultural land, timber, wood-derived fuels and other natural resources (Chidumayo & Gumbo, 2013; M C Hansen et al., 2013; Hosonuma et al., 2012). Clearing and degradation effects on forest structure can differ, depending on whether land-use drivers are related to resource use for building poles, charcoal, timber or other purposes (Banda, Schwartz, & Caro, 2006; Chidumayo, 2013; Luoga, Witkowski, & Balkwill, 2002). At the same time, forests and woodlands have strong capacity for regrowth and secondary forests attain biomass at the lower range of mature forest biomass within 2-3 decades (Chidumayo, 2013; Kalaba, Quinn, Dougill, & Vinya, 2013a; McNicol, Ryan, & Williams, 2015). Increasing proportions of Miombo consist of recent regrowth and low-biomass forest stands. In one western Tanzania case study, 16% of forest cover was estimated to have regrown in 20 years since 1995 (Mayes et al., 2015).

Given the range of forest conditions within landscapes, a primary challenge for relating field data on forest structure to satellite indicators is to obtain field data sets that represent a comprehensive range of the ground conditions across major landscape gradients, such as regrowth chronosequences or elevation. Recent studies have shown the importance of accounting for environmental co-variables such as elevation or soil type in the development of predictive relationships between satellite data and forest structure in Miombo systems (Halperin et al., 2016).

An additional challenge for remote sensing of forest structure is to understand the relationships and sensitivity of satellite (or airborne, drone/UAS system) metrics to forest structure and other land cover conditions, and how that sensitivity varies among different Miombo regions. Landsat satellite data, with a 40-yr archive and continued acquisition, widespread geographic coverage, and 30 m resolution matching spatial scales of disturbance and land use, are a versatile, readily available and current source of information on land cover across the Miombo. Optical data are becoming increasingly available and practical to use as part of forest monitoring as more well-calibrated, Landsat-style sensors come online (e.g. ESA Sentinel) and the use of other tools such as drones and UAVs increases for forest monitoring (Tang & Shao, 2015). As optical sensors, Landsat satellites (measuring reflectance at visible, near- and shortwave-infrared wavelengths 0.4-02.2 um) do not directly measure forest structure, but rather an integrated signal of land cover materials whose relationships to forest structure are poorly known across different Miombo regions. While past remote sensing estimates of forest biomass in the Miombo and globally have combined optical with active remotely sensed data such as RADARSAT, ALOS-PALSAR (radar) and ICESAT (LiDAR), the active data missions have had shorter lifespans and limited spatial coverage, restricting their use for monitoring forest change through time or over large areas (Baccini et al., 2012; Ribeiro, Saatchi, Shugart, & Washington-Allen, 2008; Ryan et al., 2012). Recent research has shown that global-scale forest biomass maps at coarse spatial resolution (500 m) struggle to capture within-landscape patterns in biomass variability across regions, where many sets of local land cover conditions fall outside calibration conditions represented in global studies (Rodríguez-Veiga, Saatchi, Tansey, & Balzter, 2016).

Past remote sensing studies focused in the Miombo have mainly focused on single case study landscapes (Halperin et al., 2016; Ribeiro et al., 2008). As a result, patterns between satellite land cover metrics and forest structure have not been cross-compared rigorously among different Miombo landscapes, contributing to the problem of limited transferability of optical satellite data relationships among regions (Foody, Boyd, & Cutler, 2003). Cross-regional study of relationships between forest structure and optical Landsat-style data is needed to help identify transferrable relationships or approaches for use of optical image data, alone or combined with other data types, to estimate forest structure with more repeatable methods across larger regions and through time.

It is unclear what individual or combinations of land cover features measured by Landsat-scale remotely sensed data show the strongest relationships to forest structure within and across different Miombo regions. Land cover features depend on the timing of image acquisition relative to the seasonality or phenological status of the landscape. For the Miombo, the early dry season is suited for optical differentiation of forest structure because herbaceous and understory vegetation has senesced, while most trees retain some green leaf cover (Frost, 1996; Fuller, Prince, & Astle, 1997). This maximizes spectral contrasts between woody vegetation, herbaceous vegetation and other landscape features. In past studies, greenness measures (such as Normalized Difference Vegetation Index, or NDVI) have related positively to tree biomass, leaf area and canopy cover as regions with more tree cover would have more green leaf area (Halperin et al., 2016; Ribeiro et al., 2008). However, the strength of these relationships has been variable and weaker for biomass than canopy cover and leaf area. Wetness measures (such as Normalized Difference Moisture Index, or NDMI) would in theory relate positively to tree cover, as tree-dominated areas have higher green leaf biomass and canopy water content relative to grass-dominated areas in the Miombo early dry season (Jin & Sader, 2005). Aside from their inclusion with multiple predictor variables in linear models, NDMI has not been evaluated for its exclusive power to predict forest structure. Albedo, or overall surface brightness, shows an inverse relationship to tree cover through the following mechanism. Grass, herbaceous vegetation and exposed substrate (soil and regolith) dominate non tree-covered areas in African tropical dry forests and woodlands (Sankaran et al., 2005). Senesced vegetation and substrate have much higher absolute reflectance in visible through shortwave infrared wavelengths, particularly in visible wavelengths (0.4-0.7 um) and shortwave infrared (~1.5-2.5 um) because they are much drier than remaining tree leaf and woody material. Trees also cast shadows, which darken surface albedo of tree stands. A measure of landscape brightness, such as the sum of reflectance values across visible through shortwave infrared bands, should thus be high over dry, senesced vegetation and exposed substrate and low over tree-covered areas, but has also not yet been tested individually against other measures for relationships to forest structure.

This study evaluates relationships among field data on forest structure and Landsat-derived land cover indicators, and develops new 30 m forest biomass maps for two contrasting Miombo Woodland case study regions in Tanzania and Mozambique. Its goals are to: (1) assess patterns among forest structure (basal area and biomass) and satellite-derived land cover indicators (greenness, moisture and albedo), and derive predictive relationships for forest biomass using satellite indicators that show the strongest relationships to forest structure in each region, and (2) critique performances of Landsat 30 m and MODIS/ICESat GLAS LiDAR 500 m forest biomass maps (Baccini et al., 2012) against field data and among forest regions of importance in each Miombo region. We test the hypotheses that forest basal area and biomass show direct relationships to satellite-derived greenness (NDVI) and wetness (NDMI) land cover indicators, and inverse relationships to a land cover brightness indicator (sum of reflectance across six Landsat visible , near and shortwave-infrared bands). We conduct multiple regression analyses to test what combinations of land cover indicators and environmental co-variates (elevation, soil type) best predict forest structure across regions. Finally, we compare new Landsat 30 m aboveground tree biomass maps to an existing global 500 m dataset, paying particular attention to whether the field-satellite data relationships we found lead to improvements in biomass estimates for low-biomass areas across landscapes of the two case study regions.

2. Methods

2.1 Study areas

The two Miombo Woodland study regions are located in Tabora, western Tanzania and Sofala, Mozambique, including the Gorongosa National Park area (Fig. 3.1, 3.2). They share a seasonally dry climatology with a unimodal rainy season, and soils that are highly weathered, nutrient-poor sands and sandy loams (Table 3.1). Miombo woodland vegetation dominates across large areas of all landscapes and includes trees of the genus *Brachystegia*, *Julbernardia, Pterocarpus, Combretum, Acacia* and *Albizia,* among others (Banda et al., 2006; Frost, 1996; Mayes et al., 2015; Ryan et al., 2012). Long-term, frequent disturbance by megafauna (historically), fire and human land use shaped the vegetation across both landscapes.

Terrain, vegetation structure and modern land-use pressures differ between the study regions. The Tabora, Tanzania region's landscape is generally flat except for punctuated small hills (Fig. 3.2). Miombo vegetation occurs in a range of patch sizes (<0.5 – 500 ha), including mature and regrowth forest areas, that vary in size and age based on soils, past disturbance and land use (Mayes et al., 2015) (Fig. 3.2). Grasslands (mbuga or dambo) occupy low-lying seasonally flooding drainages (Mayes et al., 2015). Local population growth rates are above 2% per year, and during the last 25 years, the area experienced a net 15% loss of forest cover (Mayes et al., 2015). One important regional question for forest monitoring is the status of biomass in forest reserves with differing management regimes and local use pressures. Igombe Reserve to the north is managed by national authorities (Tanzania Forest Service – TFS), and due to its locations near to roads, suffers from tree poaching and illegal settlement. Ugalla Reserve to the south is managed by a combination of village cooperative and national authorities, and is more remote from major roads.

The Sofala. Mozambique region's landscape, which includes Gorongosa National Park, spans the southern end of the East African Rift Valley across lowlands and intermediate landscape positions spanning an 1800 m regional elevation gradient (Fig. 3.2). Vegetation varies from flooding grasslands at low elevations to montane rainforest at higher elevations, with Miombo Woodlands occupying elevations up to 200 m (Ryan et al., 2012). The region experienced depopulation and high disturbance during the Mozambique civil war (1976-1992) and land use is currently undergoing reorganization, with re-establishment and regrowth of communities occurring alongside efforts to restore Gorongosa National Park. Shifting agriculture and grazing occur across the vegetation types and population densities are much lower inside than outside the park boundary.

2.2 Data

2.2.1 Field Data

Both case studies conducted or compiled tree inventories that recorded basal diameter, stem diameters at breast height (dbh) at georeferenced sites, and used Miombo-specific allometric equations to convert tree stem data to basal area biomass estimates. However, case studies had different research objectives, sampling and field site designs (Table 3.2). The Tabora study addressed how forest structure and land cover (canopy and ground cover materials) together changed with regrowth following cultivation over a 100-year regrowth chronosequence. It specifically considered site selection and sampling designs to scale tree inventories and field measurements of land cover to Landsat-scale satellite data. Sites were located in village clusters and national forest reserves that controlled for elevation, landscape position and distance from forest site edges (Fig. 3.2, Table 3.2). The Sofala dataset comes from a study that developed a regional calibration to map forest biomass and change between field and ALOS-PALSAR radar data (Ryan et al., 2012). It compiled field data from past studies with a variety of research objectives, including woodland regrowth responses to fire (Ryan & Williams, 2011) and the spatial variability of aboveground vegetation and belowground carbon stocks (Woollen, Ryan, & Williams, 2012). Tabora's dataset had a smaller number of sites (17) than Sofala (83) (Fig. 3.2, Table 3.2).

2.2.2 Satellite imagery pre-processing

We obtained Landsat data for each region from the USGS Earth Resources Observation and Science Center (EROS) Science Processing Architecture (ESPA) interface. We obtained Landsat 5 images pre-processed to surface reflectance using the LEDAPS procedure (Masek et al., 2006). Landsat 8 images were obtained pre-processed to surface reflectance using the L8SR algorithm (Vermote, Justice, Claverie, & Franch, 2016) (Table 3.3). We prioritized use of cloud and defect-free images collected during the same years as field data, which necessitated the use of Landsat 8 OLI data for Tabora and Landsat 5 TM data for Sofala regions. We chose early dry season images (June-July) to maximize spectral contrast between forest and non-forest land cover, and among forest sites of varying age and structural conditions (Halperin et al., 2016; Mayes et al., 2015). The Tabora study region occurred at boundaries of four Landsat tiles, which were radiometrically normalized to the path 170, row 063 scene using pseudoinvariant features of high, medium and low surface albedo. We found the geolocational uncertainty of Landsat data relative to field data was about a half-pixel for the Tabora landscape, using a third Worldview 2 image (September 2012) of 1.5 m pixel resolution to visually inspect the locations of field boundaries. No other geometric corrections were performed on the satellite imagery.

2.2.3 Land cover indicators: Landsat-derived greenness, wetness and albedo indices

We calculated three indices for land cover relating to surface greenness, moisture and albedo (Table 3.4). For greenness, we computed the Normalized Difference Vegetation Index (NDVI), an index of the steepness of the “red edge” slope caused by green vegetation’s characteristic reflection of near infrared (~0.85 um) and strong absorption of red light (~0.65 um), and a widely used proxy for green vegetation cover. For moisture, we calculated the Normalized Difference Moisture Index (NDMI), which tracks the slope of near infrared (~0.85 um) relative to shortwave infrared (~1.65 um) reflected light. NDMI shows a direct relationship with land cover surface moisture because water strongly absorbs energy at ~1.5 um, and often shows negative values in semi-arid environments where dry substrate often shows higher reflectance at 1.5 um than 0.85 um. For brightness, we summed reflectance across the six visible, infrared and shortwave infrared Landsat optical bands.

2.2.4 Environmental co-variates

Because our first goal was to investigate relationships among individual land cover indices and forest structure, we conducted a parsimonious analysis and limited the number of co-variables tested to only those available at sufficient spatial resolution that had clear mechanisms by which to affect land cover or forest structure conditions. We chose elevation, available at 15 m using the ASTER Global DEM version 2, because past research has found patterns of high basal area and biomass of forest vegetation occurring at low to intermediate-elevation landscape positions across the Miombo (Frost, 1996). These relationships are thought to relate to hydrologic conditions, soil moisture and nutrient status favoring tree over grass production (Frost, 1996). We also chose a surface soil texture variable (percent sand), available at 250 m pixel resolution via Africa Soil Information Service (AfSIS), which is hypothesized to relate positively to tree basal area and biomass at landscape scales through mediating freely draining conditions that favor tree over grass growth (Woollen et al., 2012).

2.3 Correlation analysis

As a first simple text of our hypotheses, we studied pair-wise Pearson correlations (*r*) among ground data on forest structure, satellite image-derived land cover indices and landscape covariates for each Miombo landscape separately. We conducted all correlation analyses using non-transformed data.

2.4 Analysis of variance and regression modeling to predict forest structure from land cover data and covariates

We used analysis of variance (ANOVA) to compare forest structure conditions of mature forest sites between Tanzania and Mozambique study regions. Mature forest sites were selected from the case study datasets using only sites labeled as mature forest with minimal recent disturbance in respective studies' metadata. Subsequently, building from results of correlation analyses, we conducted ordinary least squares (OLS) multiple-regression modeling to find the best-fitting parsimonious combinations of land cover indices and landscape covariates to predict forest structure for each region separately, using all available sites. For ANOVA and OLS we transformed variables with non-normal distributions to meet conditions of normal distribution required by OLS. We evaluated models quantitatively using the strength of correlation coefficients (r^2) and the Akaiki Information Criterion (AIC) (Johnson & Omland, 2004) . We conducted all analyses using standard regression modeling tools in R.

2.5 Derivation and assessment of regional biomass maps

We used regression models with the highest correlation coefficients and lowest AIC values to derive Landsat-based biomass maps at 30 m spatial resolution for each region, using the indices calculated from surface-reflected corrected satellite imagery and GIS data on covariates as inputs. Some additional pre-processing was necessary to exclude landscape areas in each region where land cover caused spectral confusion, and where field data did not adequately allow for calibration between land cover and satellite data. For Tabora, lowlands, wetlands and burned areas comprised the majority of excluded regions. Lowlands and wetlands, where land cover was dominated by dense grass that was both green and high albedo, confounded direct greenness- woody biomass and inverse albedo woody biomass relationships. Lowlands and wetlands were identified using masks from the Global Lakes and Wetlands (GLWD) database, and via thresholds of NIR (0.86 um) and summed shortwave infrared (1.5 + 2.21 um) reflectance. Burned areas were identified using thresholds of normalized burn ratio (NBR) images, where burned area NBR values were obtained using procedures in (Mayes et al., 2015). For Sofala, besides wetlands and burned areas, vegetation above 200 m elevation was masked out because few field sites were located above this elevation and forests began to transition in structure from Miombo to wetter montane forest. Finally, for all maps, pixels with modeled biomass < 0 Mg ha^{-1} and > 200 Mg ha^{-1} (Tabora) and >150 Mg ha^{-1} (Sofala) were assigned minimum and maximum values of 0 and 200/150 Mg ha^{-1} (Tabora/Sofala) based on the range of field-measured biomass values reported in regional and pan-Miombo studies (Chidumayo, 2013; Frost, 1996; Kalaba, Quinn, Dougill, & Vinya, 2013).

Finally, we assessed performance of this study's Landsat-based 30 m biomass maps and MODIS/ICESat-GLAS LiDAR –based 500m biomass maps (Baccini et al., 2012) between low biomass (<50 Mg ha^{-1}) and high biomass (>50 Mg ha^{-1}) forest sites. First, we compared satellite maps to field data by calculating and comparing the residuals between satellite and field measurements of biomass at field sites. This analysis was not an independent validation of the Landsat-derived maps because the same field sites were used to develop the relationships, but is illustrative of the scales of error between satellite estimates and ground data. Second, we compared the landscape-scale patterns and variability of the 30 m and 500 m biomass maps at forest management regions of interest in Tabora (Igombe, Ugalla) and Sofala (Gorongosa National Park) (Fig. 3.2).

3. Results

3.1 Field and landscape data: Forest structure, soil and terrain patterns between regions

Forest structure at mature, minimally disturbed sites showed significant differences across the study regions ($r^2 = 0.28$, $p < 0.01$) (Table 3.5). Biomass of Tabora mature forest sites (78.5 ±12.8 Mg ha^{-1}) was significantly higher than biomass at Sofala mature forests (43.2 ± 3.8 Mg ha^{-1}) (Table 5). Basal area of Tabora's mature forest sites (22 ± 3.2 m^2 ha^{-1})

was three times that of Sofala's mature forests (7.5 ± 0.5 $m^2\ ha^{-1}$) (Table 5). Stem densities were 50% higher at Tabora mature forest sites compared to Sofala. AfSIS-modeled soil textures at 250 m resolution were significantly sandier regionally at Sofala than Tabora forest sites.

From full inventories of forest sites, edaphic conditions and forest structure data also showed different values and distributions between the study regions (Fig. 3.3, Table 6). Compared to the Tabora region's forest sites, sites in the Sofala region were distributed across larger elevation ranges (150-200 m) and a wider variety of hillslope positions. Soil texture at Sofala was sandier than at Tabora (Table 3.6). Of Tabora sites, 8 occupied the lowest basal area (0-5 $m^2\ ha^{-1}$) and biomass (0-10 Mg ha^{-1}) categories, but otherwise biomass and basal areas were evenly distributed through the measured range with 1-3 sites per site category (Fig 3.3). At Sofala, site basal area and biomass showed right-skewed distributions (Fig 3.3). The range of site basal area data (17) was half that of Tabora sites (34), but the range of biomass data was similar to Tabora (Fig 3.3, Table 3.6).

3.2 Satellite data: patterns in land cover indicators among sensors and landscapes

The values and ranges of land cover indicators differed across regions and sensors (Fig 3.4, Table 3.7). At Tabora, NDVI (greenness) calculated with Landsat 8 data showed lower absolute values across sites than NDVI at Sofala sites, which was calculated from Landsat 5 data (Fig. 3.4, Table 3.7), but ranges were similar between regions. NDMI (surface moisture) trends were similar to NDVI (Table 3.7). The brightness indicator (reflectance band sum) calculated at Tabora with Landsat 8 showed larger absolute values and a larger range (0.46) compared to brightness ranges at Sofala (0.29) calculated from Landsat 5 data (Fig. 3.4, Table 3.7).

3.3 Pairwise correlations between forest structure, land cover indicators and covariates by site among landscapes

Correlations among forest structure and land cover indicators were strong and had similar patterns among Tabora and Sofala regions. NDVI (greenness) and NDMI (surface moisture) correlated positively to basal area and biomass, and brightness correlated negatively to basal area and biomass (Table 3.8). At Tabora, basal area correlated strongly to NDVI (0.86) and brightness (-0.83), but only moderately to NDMI (0.61), though both were high and outperformed basal area-NDMI (Table 3.8). Biomass-NDVI (0.79) and brightness (-0.79) had equal correlations (Table 3.8). At Sofala, correlations were highest between basal area and brightness (-0.65) and equal for basal area-NDVI and NDMI (0.62) (Table 3.8). For biomass, correlations to NDVI and NDMI were equal (0.61) and slightly higher than those to albedo (-0.59) (Table 3.8). For landscape co-variates, at Tabora soil texture (percent sand) had moderate inverse correlations to basal area and biomass, while elevation had weak or no correlations to other variables across sites (Table 3.8). At Sofala, elevation correlated positively to basal area and biomass while soil texture showed weak correlations.

3.4 Least-squares regression analyses to predict forest structure from land cover indicators and covariates

Basal area and biomass data were natural log-transformed to satisfy OLS conditions of normality before analysis for Tabora and square root-transformed for Sofala. At Tabora, NDVI was the strongest single predictor of basal area (r^2 = 0.68, AIC = 34) (Table 3.9). A single-factor model using brightness and a two-factor model using greenness and brightness performed similarly (Table 3.9). Inclusion of soil texture or elevation as a landscape covariate did not improve predictive relationships. For Tabora biomass, brightness and greenness performed equally as individual predictor variables ($r^2 = 0.67$, AIC = 46) (Table 3.9). A two-factor model using both variables to predict biomass performed similarly to the single-factor models (Table 3.9). NDMI was the weakest single-factor predictor variable for basal area and biomass at Tabora.

At Sofala, multiple-factor relationships significantly outperformed single-factor models for predicting basal area and biomass (Table 3.10). Brightness was the strongest single-factor predictor for basal area ($r^2 = 0.38$, AIC = 182) and biomass ($r^2 = 0.42$, AIC = 182) (Table 3.10). NDMI was the weakest single-factor predictor for both basal area and biomass. The same combination of predictor variables - NDVI, brightness and elevation – produced the strongest, most parsimonious models to predict basal area ($r^2 = 0.53$, AIC = 163) and biomass ($r^2 = 0.55$, AIC = 163).

3.5 Performance of new Landsat 30 m maps compared to MODIS/ICESat-GLAS 500 m maps (Baccini et al., 2012) for estimating forest biomass

Existing 500 m map (Baccini et al., 2012) estimates of forest biomass more closely matched field biomasses for high biomass sites (>50 Mg ha^{-1}) than low-biomass sites (<50 Mg ha^{-1}) in Tabora and Sofala regions (Fig. 3.5). In Sofala, the average absolute differences in 500 m map versus field site biomasses (residuals) was 34.1 (4.35) Mg ha^{-1} for high-biomass sites, and 60.0 (1.98) Mg ha^{-1} for low-biomass sites (Table 3.11). In Tabora, map-to-field residuals were more similar for high and low-biomass sites. The 500 m map had little sensitivity to low-biomass regions generally, with minimum estimates for biomass at field sites, about 40 Mg ha^{-1} for Tabora and 50 Mg ha^{-1} for Sofala, which were values 20-30% higher than the mean of all field site-measured biomass values for each region respectively (Fig. 3.5). The variability of 500 m biomass estimates are less noisy at the pixel level and provide simpler visualization of forest biomass conditions in larger, undisturbed forest regions such as the Ugalla reserve in Tabora than the 30 m maps.

For the new 30 m Landsat-based maps, biomass predictions more closely matched forest sites with low biomass (<50 Mg ha^{-1}) compared to high biomass values (Fig. 3.6-3.7, Table 3.11). At Tabora, three biomass maps were produced using the three strongest regressions: (1) NDVI as a single predictor, (2) brightness as a single predictor, and (3) a two-factor model using NDVI and brightness as predictors (Table 3.9). At Sofala, two biomass maps were produced using the two best regression models: (1) a three-factor model using NDVI, brightness and elevation as predictors (Model 1), and (2) a four-factor model using moisture as an additional predictor (Model 2) (Table 3.10). Map-field site biomass differences for the low-biomass sites were more than 50% lower for the Landsat maps than the existing 500 m map, with differences between 1-12 Mg ha^{-1} for sites under 50 Mg ha^{-1} at Tabora and about 10 Mg ha^{-1} for Sofala, (Table 3.11). For the Tabora region, map-to-field site residuals at high biomass sites were larger for 30 m maps than the 500 m map, but for the Sofala region, 30 m residuals were also smaller than 500 m map residuals. For low biomass field sites, the utility of individual land cover metrics for accurate estimations was clearer in Tabora than Sofala. In Tabora, the brightness only-based regression models yielded lower map-field site biomass differences at field sites than greenness and combined greenness-brightness land cover-based models (Fig 3.6, Table 3.11). For low-biomass sites at Sofala, the two top-performing regression models included multiple metrics and yielded similar map-field site biomass differences (Figure 3.7, Table 3.11).

In both Tabora and Sofala regions, the Landsat 30 m maps produced quantitative biomass estimates in the range of reported field values for over 90% of mapped areas (Tables 3.12-3.13). At Tabora, the NDVI-based map overestimated biomass (>200 Mg ha^{-1}) for larger percentages of the landscape (8.21%) than the other models, particularly in high-biomass regions (Table 3.12). In contrast, the brightness-based maps had the lowest percentage of pixels with biomass overestimates, but the highest percentage of underestimated pixels (10 to < 0 Mg ha^{-1}) (Table 3.12). The model combining NDVI and albedo had intermediate error rates for high and low biomass estimates. At Sofala, maps from both regression models modeled over 99% of pixels between 0-150 Mg ha^{-1} (>99%) (Table 3.13).

Landscape-wide, and at the specific regions of interest for forest monitoring, the Landsat 30 m maps capture variations in aboveground tree biomass on scales of 20-100 Mg ha^{-1} relating to known edaphic and land use-related factors that existing 500 m maps do not (Figure 3.8). The 30 m and 500 m maps report the most similar values in contiguous forest areas with >120 Mg ha^{-1} biomass, such as undisturbed sections of Igombe and Ugalla reserves in Tabora, and higher-elevation Miombo in Sofala (Figure 3.8). The largest difference between 500 m and 30 m maps in both Tabora and Sofala regions is that for low-biomass areas – including non-forest areas and locations of forest disturbance - the 30 m maps estimate values 0-20 Mg ha^{-1} while the 500 m maps report values of 35-50 Mg ha^{-1} (Figure 3.8). The 30 m map values more closely match field-estimated values at low-biomass sites than the 500 m map values. At Tabora, forest disturbances in Igombe Forest Reserve on the scales of 0.5-2 ha have 20-100 Mg ha^{-1} lower biomass than surrounding woodlands in the Landsat 30 m maps. At Sofala, denser woodland areas on hillslopes and following water courses have 25-75 Mg ha^{-1} higher biomass values than surrounding grasslands in the 30 m maps.

Some systematic biases occurred in the Landsat 30 m maps. For brightness-based maps, hillslope aspect was a source of confusion despite topographic correction in pre-processing. Pixels over mature or less disturbed forest on hillslopes with south-southwesterly aspects, facing away from the direction of illumination (north-northeast), that were modeled with biomass > 150 Mg ha^{-1}, may be overestimated. Conversely, pixels over such forest areas located on hillslopes with east or northeasterly aspects, with biomass estimates 15-30 Mg ha^{-1}, are likely underestimated. Additionally, biomass overestimates may also have occurred for forest regions with sub-canopy burns darkening land cover, but not to the extent that chosen NBR thresholds excluded them as burned. For greenness-based maps, biomass overestimates may have occurred in forests with grass cover not yet senesced, or in forests with canopies denser than those represented by field sites.

4. Discussion

Between Tabora and Sofala study regions, we found similar relationships among forest structure and land cover variables, despite significant differences in forest structure at mature sites, sampling designs, ranges of forest structures represented by field sites, and the use of different Landsat data across regions. Positive correlations of NDVI (greenness) and NDMI (moisture) to basal area and biomass, and negative correlations among brightness, basal and biomass, corroborated hypotheses about land cover relationships to forest biomass. NDVI and brightness correlations were strong compared to other optical satellite-forest structure relationships reported in other global tropical and Miombo studies (Foody et al., 2003; Ribeiro et al., 2008). NDMI (moisture)-forest structure relationships were weaker than the other metrics in Tabora. Possibly, canopy moisture as represented by NDMI at Landsat pixel scales may be confounded by the predominance and variability of senesced leaf and woody material relative to green leaf material in Miombo canopies in the early dry season (Mayes et al in prep, Chp 2). The consistent relationships we found among greenness and brightness metrics and forest structure across different Miombo landscapes are building blocks for developing transferrable approaches to use of optical imagery for mapping forest biomass in the broader Miombo region, and possibly other tropical dry forests.

The new Landsat-based 30 m maps greatly improve landscape-scale characterization of absolute values and variability of aboveground tree biomass in low-biomass regions, compared to existing 500 m maps. We found the 500 m maps significantly overestimated low-biomass sites across disturbed forest and non-forest regions, while the Landsat 30 m maps had biases due to landscape and land cover variability at finer spatial scales that made biomass estimates more variable in contiguous mature and undisturbed forest areas. The Landsat 30 m biomass maps resulting from this study's work, though preliminary, represent promising approaches for monitoring tree biomass variability within landscapes with less than 100-200 Mg ha^{-1} maximum forest biomass. These approaches will be increasingly relevant for the Miombo, where increasing proportions of standing forest are low-biomass and recent regrowth areas (Mayes et al., 2015). They may also be useful for other global tropical dry forest areas with low biomass, or facing widespread forest disturbance. Absolute values of 20-100 Mg ha^{-1} differences between intact and disturbed forest areas in Tabora, and 25-75 Mg ha^{-1} biomass gradients from low-to high tree cover areas across elevation and distance-to-stream gradients in Gorongosa Park are consistent with past field observations of biomass variability in Miombo woodlands (Frost, 1996; Mayes et al., 2015; Ryan et al., 2012; Williams et al., 2008).

This study highlights a number of considerations for improving study of forest structure in heterogeneous landscapes such as the Miombo with optical satellite data, including those for improved use of field and satellite data. Particularly in African tropical dry forests, more forest structure data are needed for calibration and validation of biomass maps that are collected in sampling frameworks designed for scaling to remotely sensed data, accounting for geolocation and spatial resolution of the satellite data (Bustamante et al., 2016). While the 30 m biomass maps this study produced show realistic patterns, back-comparison of map-predicted biomasses at field sites does not count as independent validation. Statistical methods such as leave-one-out cross-calibration and jackknifing methods could offer some means of validation, but these are difficult to use for the small datasets in these studies. However, besides needing biomass data at more sites, field surveys must cover sites encompassing broad ranges of land cover conditions and covariates, such as hillslope positions, soil types or disturbance status (including burning histories) that affect land cover-biomass relationships within landscapes (Halperin et al., 2016) . Strategic field sampling designs for biomass surveys should aim to account for sub-canopy burning and other factors whose data may not be available in regional-global geographic datasets, such as topography or soil characteristics. For improved use of optical image data, the sensitivity of land cover-forest structure relationships due to land cover variability, versus differences in sensor behavior among study regions, warrants further research. For example, in this study, it is unclear if the larger variability of the brightness land cover metric at Tabora than Sofala is due to use of 12-bit Landsat 8 data instead of 8-bit Landsat 5 data used at Sofala, or variability in land cover related to vegetation structure and land cover conditions. The increasing availability of diverse optical satellite data types in open archives (Landsat 5, 8) and new sources such as drones and UAVs, while a boon for repeat monitoring, also will make radiometric inter-calibration of optical data even more challenging. Improved optical data calibrations to forest structure can also make further use of concurrent radar, LiDAR and other active remote sensing data, as passive-active remote sensing data fusion products have shown promise for mapping of forest structure at continental to regional scales (Baccini et al., 2012; Matthew C. Hansen et al., 2016; Ribeiro et al., 2008).

5. Conclusions

This study performed one of the first cross-regional assessments of relationships between field data on forest structure and Landsat-scale land cover metrics in the expansive African Miombo Woodlands. Between two regions in Tanzania and Mozambique, using Landsat 8 (Tanzania) and Landsat 5 (Mozambique) data, we found consistent, strong positive correlations among NDVI (greenness), NDMI (moisture) and forest structure (basal area, biomass), and negative correlations between land cover brightness (sum of Landsat optical reflectance bands) and forest structure. Regressions between land cover indicators and field data at each region were used to produce 30 m resolution biomass maps from the Landsat data. Maps using land cover metrics besides NDVI (greenness), such as brightness metrics, or combinations of multiple Landsat-derived metrics and ancillary land cover data, improved estimates of biomass absolute values and variability at landscape scales. In both Tanzania and Mozambique landscapes, we found that an existing 500 m pan-tropical biomass map (Baccini et al., 2012) consistently and significantly over-estimated aboveground biomass in low-biomass areas (<50 Mg ha^{-1}) , such as disturbed forest and non-forest areas. The new 30 m maps reproduced known ranges of absolute values and spatial patterns of biomass in both Tabora and Sofala across landscape gradients due to land use and ecological factors, though need further validation and methodological refinements. The consistent forest structure-land cover metric relationships we found suggest the possibility of developing transferrable algorithms for aboveground biomass estimation at landscape scales using Landsat-style observations across the Miombo and other tropical dry forest regions. Hints to successful pursuit of such transferrable remote sensing relationships for landscapes include use multiple land cover metrics besides greenness, and appropriate representation of covariates affecting forest structure-land cover relationships in field datasets. The new 30 m biomass maps we developed provided new insight into landscape-scale biomass variability in Tanzania and Mozambique study regions, particularly at low-biomass areas, and offer ways forward for monitoring of forest condition beyond forest cover in these regions.

Acknowledgements

We thank collaborators at the Mbola-Millennium Villages Project and Agricultural Research Institute at Tumbi in Tabora, Tanzania for assistance with fieldwork and helping orient us to the western Tanzanian Miombo landscape. We thank University of Edinburgh collaborators and funding sources [fill in details] for the use of Sofala, Mozambique field data for this study. This study was funded by the NSF-PIRE program [details]. M. Mayes was also supported by a Dissertation Fellowship at Brown University during completion of the research.

References

Aber, J. A., & Mellilo, J. M. (1991). *Terrestrial ecosystems*. *Terrestrial Ecosystems*. http://doi.org/10.1016/S0378-777X(78)80104-8

Baccini, a., Goetz, S. J., Walker, W. S., Laporte, N. T., Sun, M., Sulla-Menashe, D., … Houghton, R. a. (2012). Estimated carbon dioxide emissions from tropical deforestation improved by carbon-density maps. *Nature Climate Change*, *2*(3), 182–185. http://doi.org/10.1038/nclimate1354

Banda, T., Schwartz, M. W., & Caro, T. (2006). Woody vegetation structure and composition along a protection gradient in a miombo ecosystem of western Tanzania. *Forest Ecology and Management*, *230*(1), 179–185. http://doi.org/10.1016/j.foreco.2006.04.032

Bustamante, M. M. C., Roitman, I., Aide, T. M., Alencar, A., Anderson, L. O., Aragão, L., … Vieira, I. C. G. (2016). Toward an integrated monitoring framework to assess the effects of tropical forest degradation and recovery on carbon stocks and biodiversity. *Global Change Biology*, *22*(1), 92–109. http://doi.org/10.1111/gcb.13087

Campbell, B. M. (1996). *The Miombo in Transition : Woodlands and Welfare in Africa*. *Forestry* (Vol. 72). Retrieved from http://books.google.com/books?hl=en&lr=&id=rpildJJVdU4C&oi=fnd&pg=PR9&dq=The+Miombo+in+Transition+:+Woodlands+and+Welfare+in+Africa&ots=FMsmiYa2th&sig=_hEtp4U1rk54Sn8tgXWfkMD-v-8

Chidumayo, E. N. (2013). Forest degradation and recovery in a miombo woodland landscape in Zambia: 22 years of observations on permanent sample plots. *Forest Ecology and Management*, *291*, 154–161. http://doi.org/10.1016/j.foreco.2012.11.031

Chidumayo, E. N., & Gumbo, D. J. (2013). The environmental impacts of charcoal production in tropical ecosystems of the world: A synthesis. *Energy for Sustainable Development*, *17*(2), 86–94. http://doi.org/10.1016/j.esd.2012.07.004

Foody, G. M., Boyd, D. S., & Cutler, M. E. J. (2003). Predictive relations of tropical forest biomass from Landsat TM data and their transferability between regions. *Remote Sensing of Environment*, *85*(4), 463–474. http://doi.org/10.1016/S0034-4257(03)00039-7

Frost, P. (1996). *The Ecology of Miombo Woodlands*. (B. M. Campbell, Ed.)*The Miombo in Transition: Woodlands and Welfare in Africa*. Bogor, Indonesia: Center for International Forestry Research. Retrieved from http://books.google.com/books?hl=nl&lr=&id=rpildJJVdU4C&pgis=1

Fuller, D. O., Prince, S. D., & Astle, W. L. (1997). The influence of canopy strata on remotely sensed observations of savanna-woodlands. *International Journal of Remote Sensing*, *18*(14), 2985–3009. http://doi.org/10.1080/014311697217161

Halperin, J., LeMay, V., Coops, N., Verchot, L., Marshall, P., & Lochhead, K. (2016). Canopy cover estimation in miombo woodlands of Zambia: Comparison of Landsat 8 OLI versus RapidEye imagery using parametric, nonparametric, and semiparametric methods. *Remote Sensing of Environment*, *179*, 170–182. http://doi.org/10.1016/j.rse.2016.03.028

Hansen, M. C., Potapov, P. V, Moore, R., Hancher, M., Turubanova, S. a, Tyukavina, a, … Townshend, J. R. G. (2013). High-resolution global maps of 21st-century forest cover change. *Science (New York, N.Y.)*, *342*(2013), 850–3. http://doi.org/10.1126/science.1244693

Hansen, M. C., Potapov, P., Goetz, S. J., Turubanova, S., Tyukavina, A., Krylov, A., … Egorov, A. (2016). Mapping tree height distributions in Sub-Saharan Africa using Landsat 7 and 8 data. *Remote Sensing of Environment*. http://doi.org/10.1016/j.rse.2016.02.023

Hosonuma, N., Herold, M., De Sy, V., De Fries, R. S., Brockhaus, M., Verchot, L., … Romijn, E. (2012). An assessment of deforestation and forest degradation drivers in developing countries. *Environmental Research Letters*, *7*(4), 044009. http://doi.org/10.1088/1748-9326/7/4/044009

Jin, S., & Sader, S. A. (2005). Comparison of time series tasseled cap wetness and the normalized difference moisture index in detecting forest disturbances. *Remote Sensing of Environment*, *94*(3), 364–372. http://doi.org/10.1016/j.rse.2004.10.012

Johnson, J. B., & Omland, K. S. (2004). Model selection in ecology and evolution. *Trends in Ecology & Evolution*, *19*(2), 101–108. http://doi.org/10.1016/j.tree.2003.10.013

Kalaba, F. K., Quinn, C. H., Dougill, A. J., & Vinya, R. (2013a). Floristic composition, species diversity and carbon storage in charcoal and agriculture fallows and management implications in Miombo woodlands of Zambia. *Forest Ecology and Management*, *304*, 99–109. http://doi.org/10.1016/j.foreco.2013.04.024

Kalaba, F. K., Quinn, C. H., Dougill, A. J., & Vinya, R. (2013b). Floristic composition, species diversity and carbon storage in charcoal and agriculture fallows and management implications in Miombo woodlands of Zambia. *Forest Ecology and Management*, *304*, 99–109. http://doi.org/10.1016/j.foreco.2013.04.024

Luoga, E. J., Witkowski, E. T. F., & Balkwill, K. (2002). Harvested and standing wood stocks in protected and communal miombo woodlands of eastern Tanzania. *Forest Ecology and Management*, *164*(1-3), 15–30. http://doi.org/10.1016/S0378-1127(01)00604-1

Masek, J. G., Vermote, E. F., Saleous, N. E., Wolfe, R., Hall, F. G., Huemmrich, K. F., … Lim, T. K. (2006). A landsat surface reflectance dataset for North America, 1990-2000. *IEEE Geoscience and Remote Sensing Letters*, *3*(1), 68–72.

http://doi.org/10.1109/LGRS.2005.857030

Mayes, M. T., Mustard, J. F., & Melillo, J. M. (2015). Forest cover change in Miombo Woodlands: modeling land cover of African dry tropical forests with linear spectral mixture analysis. *Remote Sensing of Environment*, *165*, 203–215. http://doi.org/10.1016/j.rse.2015.05.006

McNicol, I. M., Ryan, C. M., & Williams, M. (2015). How resilient are African woodlands to disturbance from shifting cultivation? *Ecological Applications*, 150407011925001. http://doi.org/10.1890/14-2165.1

Olson, D. M., & Dinerstein, E. (2002). The Global 200: Priority Ecoregions for Global Conservation. *Annals of the Missouri Botanical Garden*, *89*(2), 199. http://doi.org/10.2307/3298564

Ribeiro, N. S., Saatchi, S. S., Shugart, H. H., & Washington-Allen, R. A. (2008). Aboveground biomass and leaf area index (LAI) mapping for Niassa Reserve, northern Mozambique. *Journal of Geophysical Research*, *113*(G3), G02S02. http://doi.org/10.1029/2007JG000550

Rodríguez-Veiga, P., Saatchi, S., Tansey, K., & Balzter, H. (2016). Magnitude, spatial distribution and uncertainty of forest biomass stocks in Mexico. *Remote Sensing of Environment*, *183*, 265–281. http://doi.org/10.1016/j.rse.2016.06.004

Rudel, T. K., Rudel, T., DeFries, R., Rudel, T., Uriarte, M., Hansen, M., … Janzen, D. (2013). The national determinants of deforestation in sub-Saharan Africa. *Philosophical Transactions of the Royal Society of London. Series B, Biological Sciences*, *368*(1625), 20120405. http://doi.org/10.1098/rstb.2012.0405

Ryan, C. M., Hill, T., Woollen, E., Ghee, C., Mitchard, E., Cassells, G., … Williams, M. (2012). Quantifying small-scale deforestation and forest degradation in African woodlands using radar imagery. *Global Change Biology*, *18*(1), 243–257. http://doi.org/10.1111/j.1365-2486.2011.02551.x

Ryan, C. M., & Williams, M. (2011). How does fire intensity and frequency affect miombo woodland tree populations and biomass? *Ecological Applications*, *21*(1), 48–60. http://doi.org/10.1890/09-1489.1

Saatchi, S. S., Harris, N. L., Brown, S., Lefsky, M., Mitchard, E. T. A., Salas, W., … Morel, A. (2011). Benchmark map of forest carbon stocks in tropical regions across three continents. *Proceedings of the National Academy of Sciences*, *108*(24), 9899–9904. http://doi.org/10.1073/pnas.1019576108

Sankaran, M., Hanan, N. P., Scholes, R. J., Ratnam, J., Augustine, D. J., Cade, B. S., … Zambatis, N. (2005). Determinants of woody cover in African savannas. *Nature*, *438*(7069), 846–849. http://doi.org/10.1038/nature04070

Tang, L., & Shao, G. (2015). Drone remote sensing for forestry research and practices. *Journal of Forestry Research*, *26*(4), 791–797. http://doi.org/10.1007/s11676-015-0088-y

Tyukavina, A., Baccini, A., Hansen, M. C., Potapov, P. V, Stehman, S. V, Houghton, R. A., … Goetz, S. J. (2015). Aboveground carbon loss in natural and managed tropical forests from 2000 to 2012. *Environ. Res. Lett. Environ. Res. Lett*, *10*(10), 74002–74002. http://doi.org/10.1088/1748-9326/10/7/074002

United Nations, Department of Economic and Social Affairs, P. D. (2015). *World population prospects: key findings and advance tables.* (Vol. 1). Retrieved from http://esa.un.org/unpd/wpp/Publications/Files/Key_Findings_WPP_2015.pdf

Vermote, E., Justice, C., Claverie, M., & Franch, B. (2016). Preliminary analysis of the performance of the Landsat 8/OLI land surface reflectance product. *Remote Sensing of Environment*. http://doi.org/10.1016/j.rse.2016.04.008

Williams, M., Ryan, C. M., Rees, R. M., Sambane, E., Fernando, J., & Grace, J. (2008). Carbon sequestration and biodiversity of re-growing miombo woodlands in Mozambique. *Forest Ecology and Management*, *254*(2), 145–155. http://doi.org/10.1016/j.foreco.2007.07.033

Woollen, E., Ryan, C. M., & Williams, M. (2012). Carbon Stocks in an African Woodland Landscape: Spatial Distributions and Scales of Variation. *Ecosystems*, *15*(5), 804–818. http://doi.org/10.1007/s10021-012-9547-x

WRI. (2016). AFR100: Africa Restoring 100 Million Hectares of Deforested and Degraded Land by 2030. Retrieved from http://www.wri.org/our-work/project/AFR100/about-afr100

TABLES: CHAPTER THREE

Table 3.1 Locations and basic biogeographic data for two Miombo Woodland case study landscapes in Tanzania and Mozambique.

Landscape (Reference)	Location	Climate Mean annual precip^ (std. dev) - CHIRPS Temp ^{0}C*	Soil types	Population Density 2015 (GPWv4) Persons km^{-2}
Tabora, Tanzania (Mayes et al. 2015, Chp 1 & 2 in prep.)	4.6-5.1 ^{0}S, 32.5-32.7 ^{0}E	1060(190) mm	Aridisols, vertisols	40-80
Sofala, Mozambique Ryan et al. 2012)	18.9-19.1 ^{0}S, 34.1-34.3 ^{0}E	970 (220) mm	Aridisols, vertisols	20-40 near field sites 60-90 near towns

Table 3.2 Field data on forest structure collected across two Miombo Woodland locations in Tanzania and Mozambique. Values shown are means with standard errors in parentheses, and ranges in italics, for sites used in statistical analyses.

Location (Date)	Research objective	Geographic distribution of field sites	Number of sites (mature)	Site area and sampling design
Tabora, Tanzania 2014-15	Regrowth chronosequence (100 yr)	20 x 40 km^2 Inland plains	17 (5)	50 x 50 m square (0.25 ha) 4 x 10 m radius circular sub-plots (Williams et al. 2008)
Sofala, Mozambique 2006-09	Varied	25 x 25 km^2 Slope of Mt. Gorongosa	83 (35)	Varied 0.1 – 1.0 ha areas

Table 3.3 Landsat satellite data used for analyses.

Location	Sensor and image data	Date Path/Row
Tabora, Tanzania	Landsat 8 OLI 30 m 12 bit L8SR surface reflectance (Vermote et al., 2016)	14 July 2015 170/063
Sofala, Mozambique	Landsat 5 TM 30 m 8 bit LEDAPS surface reflectance (Masek et al, 2006)	13 June 2006 167/073

Table 3.4 Land cover indices calculated from Landsat data.

Land cover index	Description and ecological relevance	Formula	Citation
Normalized difference vegetation index (NDVI)	Green vegetation cover Leaf area, water and nutrient cycling	NIR (0.83 um) – RED (0.65 um)/ (NIR+RED)	Rouse et al. (1974)
Normalized difference moisture index (NDMI)	Surface moisture index Soil moisture, vegetation cover	NIR (0.83 um) – SWIR1 (1.65 um)/(NIR+SWIR1)	Jin and Sadler (2005)
Reflectance band sum ($\sum p$)	Surface brightness Proxy for albedo	$\sum$(All bands)	Fuller et al. (1997)

Table 3.5 Mature forest structure variables across mature Miombo Woodland sites in Tanzania and Mozambique. Values shown are means with standard errors in parentheses for sites used in statistical analyses. Soil texture is for 0-5 cm extracted from AfSIS 250 m continental soil grids. Elevation data was extracted from 15 m ASTER global elevation dataset (version 2). Forest structure variables in columns not sharing letters were significantly different in ANOVA and Tukey's HSD tests ($p < 0.05$ level).

Location	N sites	Soil texture (% sand)	Stem Density ha^{-1}	Basal area $m^2\ ha^{-1}$	Biomass $Mg\ ha^{-1}$
Tabora, Tanzania	5	63.6 (2.4)^a	638 (102)^a	22 (3.2)^a	78.5 (12.8)^a
Sofala, Mozambique	35	73.4 (0.5)^b	411 (31)^b	7.5 (0.5)^b	43.2 (3.8)^b

Table 3.6. Forest structure variables across all forest sites used for field-satellite data comparisons from two Miombo Woodland landscapes in Tanzania and Mozambique. Values shown are means with standard errors in parentheses, and ranges in italics.

Location	N sites (total)	Elevation^ m	Soil texture (% sand)	Stem Density ha^{-1}	Basal area $m^2\ ha^{-1}$	Biomass $Mg\ ha^{-1}$
Tabora, Tanzania	17	1177 (5) *1147-1207*	67.4 (1.5)	557 (77) *47 - 1090*	12.1 (2.5) *0.3-34.3*	33.4 (8.9) *0.3 – 119.4*
Sofala, Mozambique	83	93 (3) *42-162*	72.3 (0.5)	547 (93) *31-4893*	6.2 (0.5) *0.2-17.1*	35.2 (2.8) *0.5-119.2*

Table 3.7 Summary statistics for land cover indicators across forest sites from two Miombo Woodland landscapes in Tanzania and Mozambique. Values in parentheses are standard deviations, and the range across sites is shown in italics.

Location	N sites	Satellite data	NDVI (greenness)	NDMI (wetness)	Reflectance band sum (brightness)
Tabora, Tanzania	17	Landsat 8 14 July 2015	0.39 (0.08) *0.29-0.55*	-0.061 (0.045) *-0.129-0.041*	0.97 (0.16) *0.73-1.27*
Sofala, Mozambique	83	Landsat 5 13 June 2006	0.60 (0.07) *0.44-0.71*	0.078 (0.081) *-0.17-0.28*	0.64 (0.06) *0.51-0.80*

Table 3.8 Pearson correlations (*r)* between land cover and tree structure variables across two Miombo Woodland landscapes in Tanzania and Mozambique. Correlations shown are significant at $p < 0.01$; ns = not significant.

Location	Tree structure variable	Satellite greenness (NDVI)	Satellite moisture (NDMI)	Satellite brightness (Refl. sum)	Soil %Sand AfSIS 250m	Elevation ASTER 15m GDEM v2
Tabora, Tanzania 17 sites	Biomass Mg ha^{-1}	0.79	0.43	-0.79	-0.58	ns
	Basal area m^2 ha^{-1}	0.86	0.61	-0.83	-0.65	0.05
	Stem density ha^{-1}	0.68	0.73	-0.60	-0.40	0.17
	Height m	0.74	0.37	-0.71	-0.63	0.07
Sofala, Mozambique 83 sites	Biomass Mg ha^{-1}	0.61	0.61	-0.59	0.26	0.54
	Basal area m^2 ha^{-1}	0.62	0.62	-0.65	Ns	0.54
	Stem density ha^{-1}	ns	ns	ns	ns	-0.22

Table 3.9 Regression analysis results for land cover-based predictions of tree structure across Tabora, Tanzania Miombo Woodland sites.

Tree structure variable (y)	Land cover variable ($x_1 + x_{2...}x_n$)	r^2	p	AIC	Equation
Basal area $\ln(m^2\ ha^{-1})$	Greenness (NDVI)	0.68	<0.001	34	$y = -2.134 + 10.92*x_1$
	Moisture (NDMI)	0.29	<0.001	48	$y = 2.981 + 13.47*x_1$
	Brightness (Reflectance sum)	0.65	<0.001	36	$y = 7.378 – 5.340*x_1$
	Greenness + Bright. (NDVI+ Refl. sum)	0.67	<0.001	36	$y = 0.928 + 7.558*x_1 – 1.799*x_2$
Biomass $\ln\ (Mg\ ha^{1})$	Greenness (NDVI)	0.67	<0.001	46	$y = -3.179 + 15.10*x_1$
	Moisture (NDMI)	0.20	0.040	61	$y = 3.748 + 16.25*x_1$
	Brightness (Reflectance sum)	0.67	<0.001	46	$y = 10.11 – 7.61*x_1$
	Greenness + Bright. (NDVI+ Refl. sum)	0.67	<0.001	47	$y = 3.353 + 7.919*x_1 – 3.837*x_2$

Table 3.10 Regression analysis results for land cover-based predictors of tree structure across Sofala, Mozambique Miombo Woodland sites. Table continues for two pages.

Tree structure variable (y)	Land cover variable ($x_1 + x_{2 \ldots} x_n$)	r^2	p	AIC	Equation
Basal area $\sqrt{(m^2\ ha^{-1})}$	Greenness (NDVI)	0.36	<0.001	190	$y = -2.741 + 8.382*x_1$
	Moisture (NDMI)	0.33	<0.001	195	$y = 1.786 + 6.637*x_1$
	Brightness (Reflectance sum)	0.38	<0.001	182	$y = 8.729 - 10.06*x_1$
	Elevation	0.34	<0.01	193	$Y = 0.3359 + 0.0211*x_1$
	Greenness + Bright.	0.50	<0.001	165	$y= 4.441 - 3.18*x_1 - 6.934*x_2$
	Albedo + Elevation	0.42	<0.001	178	$y = 5.860 - 7.526*x_1 + 0.013*x_2$
	Greenness + Bright. + Elevation	0.53	<0.001	163	$y = 2.6712 + 2.975*x_1 - 5.223*x_2 + 0.0127*x_3$
	Greenness + Moisture + Bright. + Elevation	0.53	<0.001	164	$y = 3.644 + 0.3831*x_1 + 2.419*x_2 - 4.757*x_3 + 0.014*x_4$
Biomass $\sqrt{(Mg\ ha^{-1})}$	Greenness (NDVI)	0.37	<0.001	190	$y = -7.115 + 20.89*x_1$
	Moisture	0.33	<0.001	195	

(NDMI)				$y = 4.156 + 16.67*x_1$
Brightness (Reflectance sum)	0.42	<0.001	182	$y = 20.76 – 23.95*x_1$
Elevation	0.34	<0.01	193	$y = 0.530 + 0.0528*x_1$
Greenness + Bright.	0.54	<0.001	165	$y = 8.297 +11.08*x_1 -14.9*x_2$
Bright. + Elevation (NDVI+ Refl. sum)	0.45	<0.001	178	$y = 13.25 – 17.33*x_1 + 0.035*x_2$
Greenness + Bright. + Elevation	0.55	<0.001	163	$y = 3.704 + 8.909*x_1 – 10.46*x_2 + 0.0329*x_3$
Greenness + Moisture + Bright. + Elevation	0.55	<0.001	164	$y = 7.45 – 1.078*x_1 + 9.321*x_2 – 8.634*x_3 + 0.037*x_4$

Table 3.11 Average absolute differences between satellite predictions and field measurements of aboveground biomass at Tabora and Sofala regions at field sites, with focus on satellite model performances between low (<50 Mg ha^{-1}) and high (>50 Mg ha^{-1}) tree biomass sites.

Region	Model	Differences in Field-Map Biomass (Absolute value)	
		Sites < 50 Mg ha^{-1} Biomass	Sites > 50 Mg ha^{-1} Biomass
Tabora	Baccini et al. 2012 (500 m)	30.8 (3.33)	29.6 (13.6)
Sites < 50 Mg ha^{-1}: n = 12 Sites > 50 Mg ha^{-1}: n = 5	Landsat NDVI (30 m)	12.6 (5.17)	37.3 (7.40
	Landsat Bright. (30 m)	0.669 (2.90)	35.5 (8.38)
	Landsat NDVI + Albedo (30 m)	5.51 (3.53)	37.8 (6.96)
Sofala	Baccini et al. 2012 (500 m)	60.0 (1.98)	34.1 (4.35)
Sites < 50 Mg ha^{-1}: n = 63 Sites > 50 Mg ha^{-1}: n = 20	Landsat Model 1 (30 m)	9.62 (1.00)	22.2 (4.2)
	Landsat Mod 2 (30 m)	9.74 (1.01)	20.7 (4.10)

Table 3.12 Summary of Tabora region biomass map results derived from Landsat image metrics calibrated to local field sites.

Region	Model	Mapped area (x 10^3 km^2)	Percent area 0-200 Mg ha^{-1}	Percent area < 0 Mg ha^{-1}	Percent area > 200 Mg ha^{-1}
Tabora, Tanzania	Landsat NDVI	34.2	91.7	0.04	8.21
	Landsat Brightness	34.2	93.2	2.43	4.31
	Landsat NDVI + Brightness	34.2	92.6	0.54	6.85

Table 3.13 Summary of Sofala region biomass map results derived from Landsat image metrics calibrated to local field sites.

Region	Model	Mapped area (x 10^3 km^2)	Percent area 0-150 Mg ha^{-1}	Percent area < 0 Mg ha^{-1}	Percent area > 150 Mg ha^{-1}
Sofala, Mozambique	Landsat NDVI + Brightness + Elevation	5.1	99.9	0	0.09
	Landsat NDVI + NDMI + Brightness + Elevation	5.1	99.5	0	0.54

FIGURES: CHAPTER THREE

Figure 3.1 Locations of study regions at Tabora, Tanzania and Sofala, Mozambique in the Miombo Woodlands.

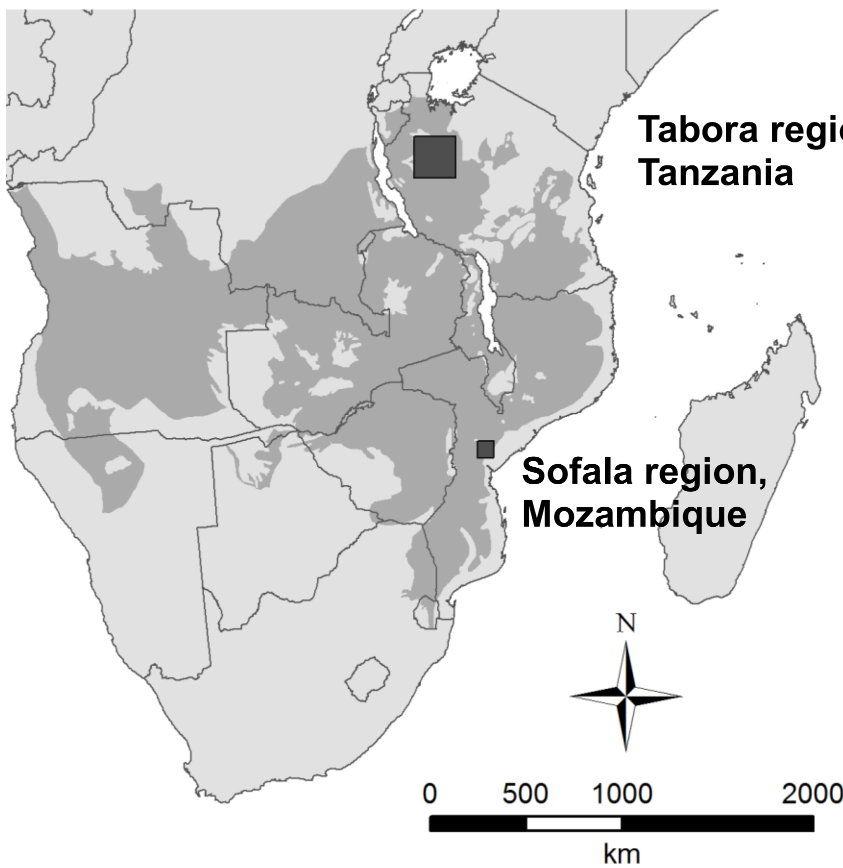

Figure 3.2 Land cover and terrain at Tabora, Tanzania and Sofala, Mozambique study regions. Left-side panels show false-color Landsat 8 imagery for Tabora, Tanzania (July 2015) and Landsat 5 imagery for Sofala, Mozambique (June 2006). Right-side panels show 15 m ASTER Global Digital Elevation Model (DEM) data (GDEMv2) with legend to the right. Yellow dots indicate locations of sites where field data from study regions was taken. Yellow boundaries indicate forest management areas that are regions of interest for monitoring.

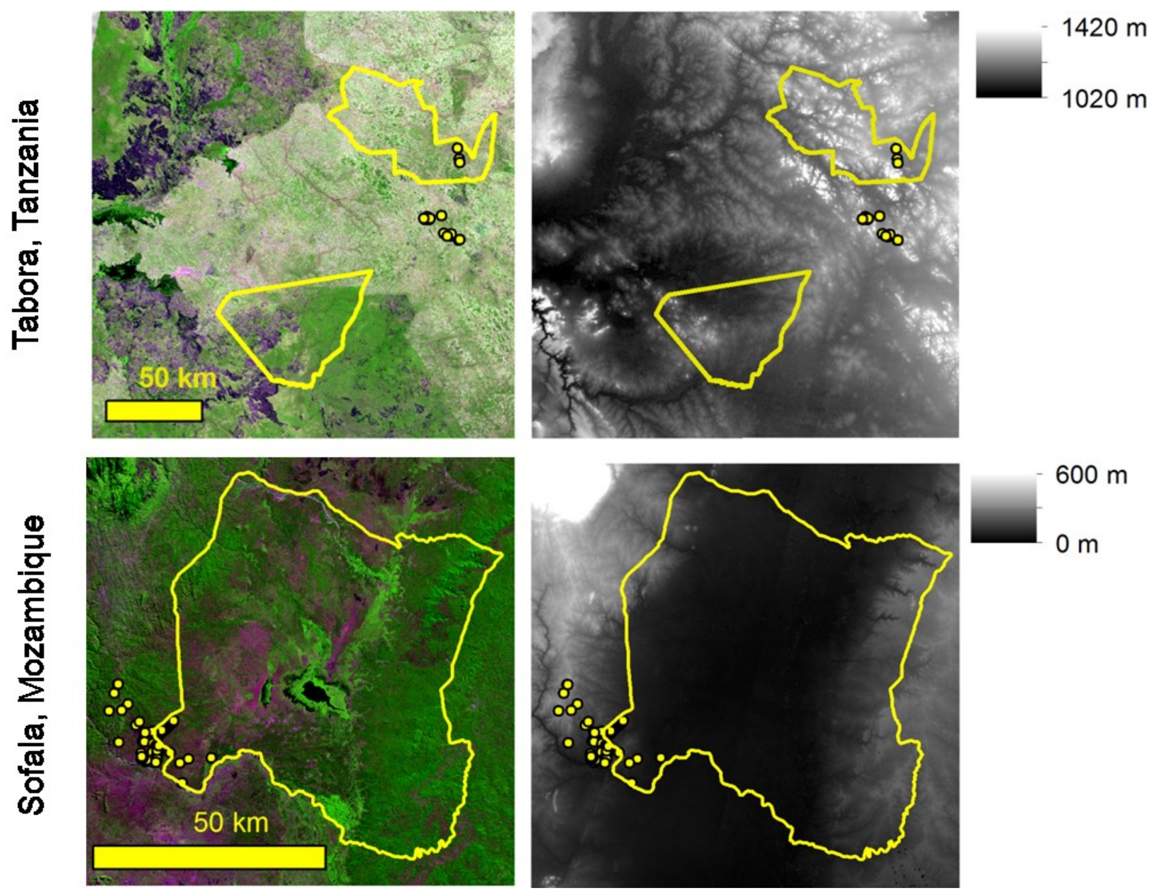

Figure 3.3 Distributions of ground-measured basal area and biomass values across Miombo Woodland sites in Tanzania and Mozambique.

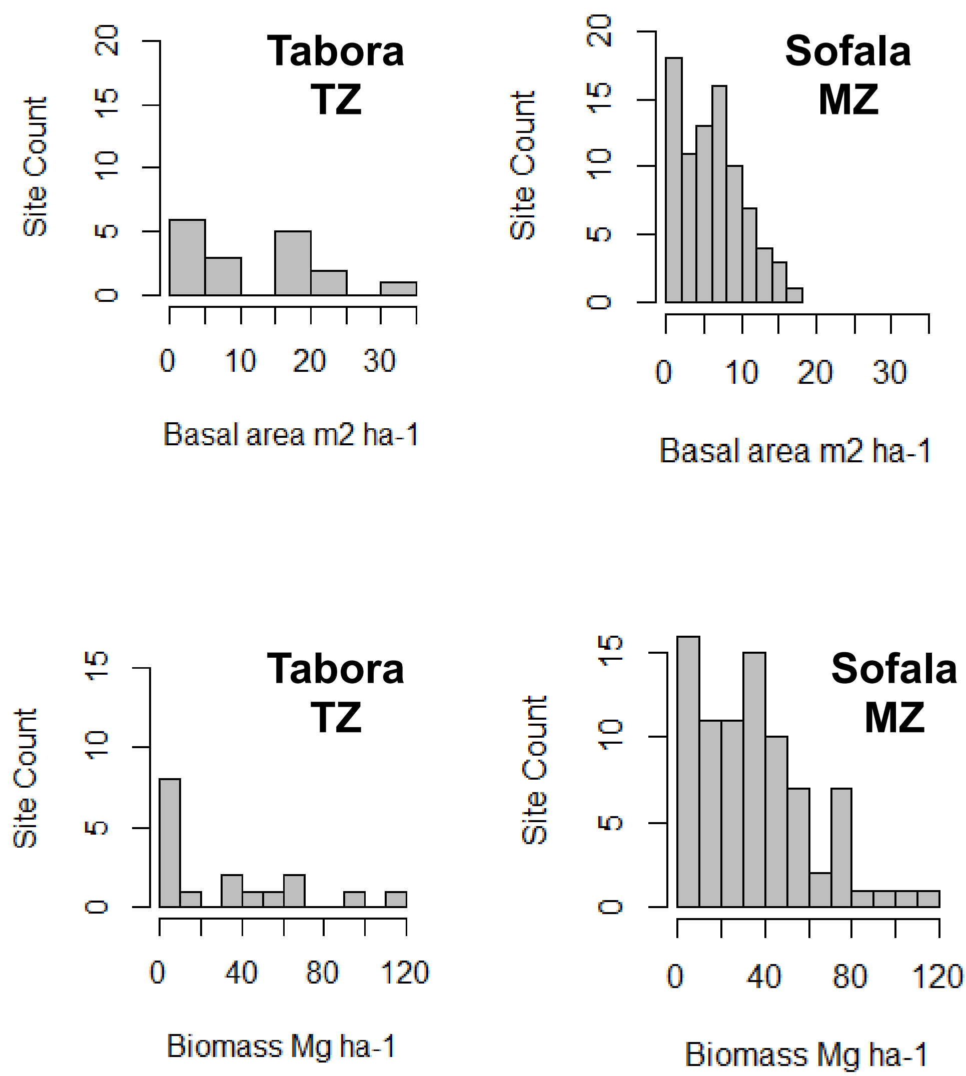

Figure 3.4 Distributions of Landsat satellite metrics across Miombo Woodland sites in Tanzania and Mozambique.

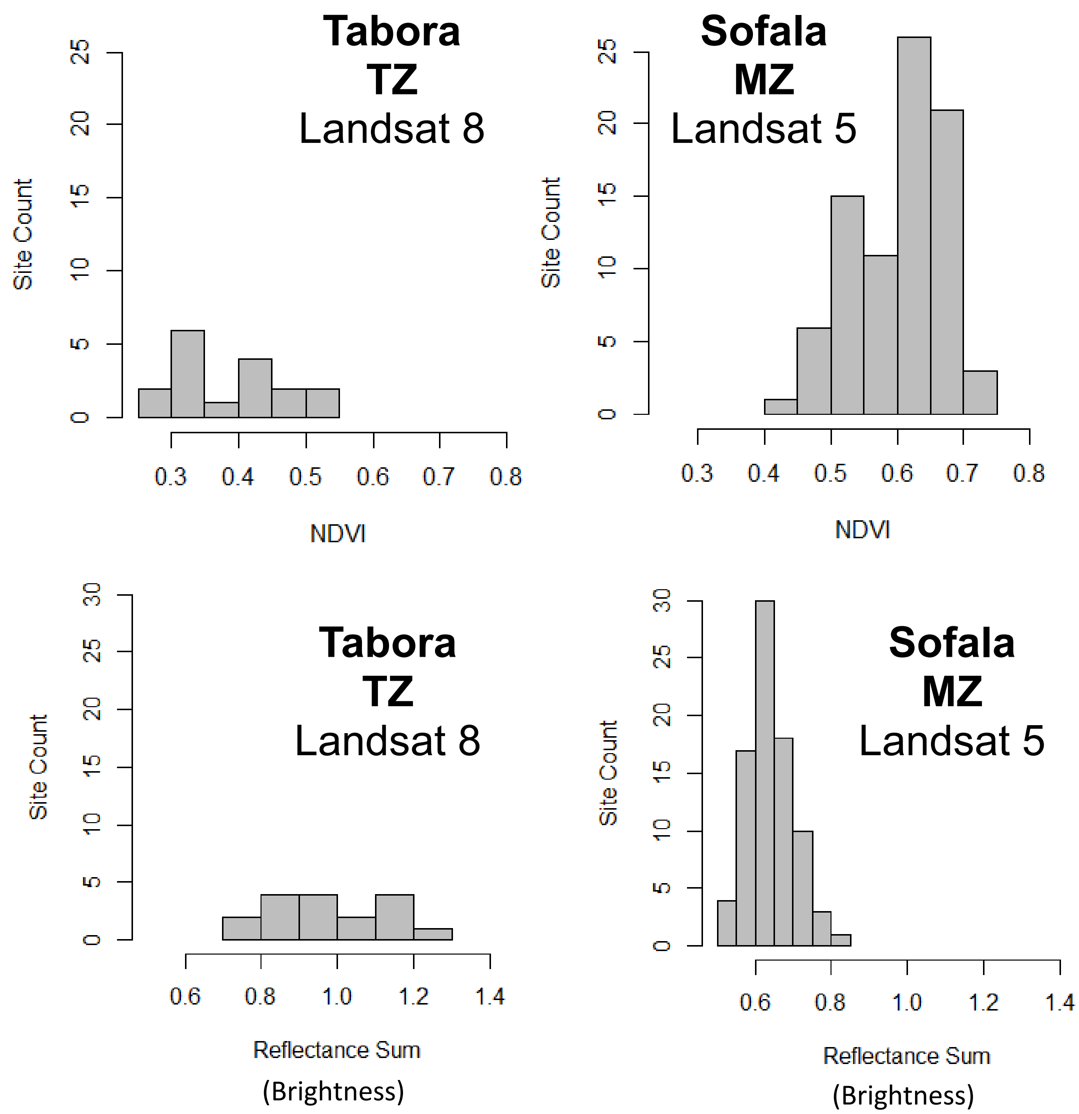

Figure 3.5 Existing 500 m pan-tropical biomass estimates (Baccini et al. 2012) compared to field-estimated aboveground tree biomass at Tabora, Tanzania and Sofala, Mozambique Miombo Woodlands. Horizontal vertical lines mark the average of forest biomass field estimates in past field studies for Tabora (Mayes et al, Chp 2 in prep) and Sofala regions (Williams et al. 2008, Ryan et al. 2012).

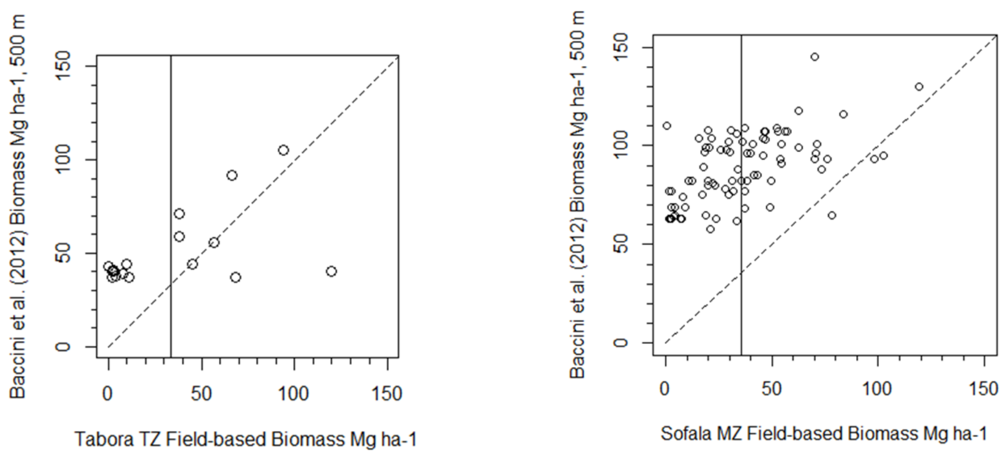

***Mean field-measured biomass: 33.4 Mg ha^{-1}**

***Mean field-measured biomass: 35.2 Mg ha^{-1}**

Figure 3.6 Landsat NDVI and brightness metric –based estimates of forest biomass compared to field data at Tabora, Tanzania. Left-panel figures show the full biomass ranges of field and satellite data. Right-side panels show data in the 0-50 Mg ha^{-1} low-biomass range (highlighted by heavy black boxed region in left-panel figures).

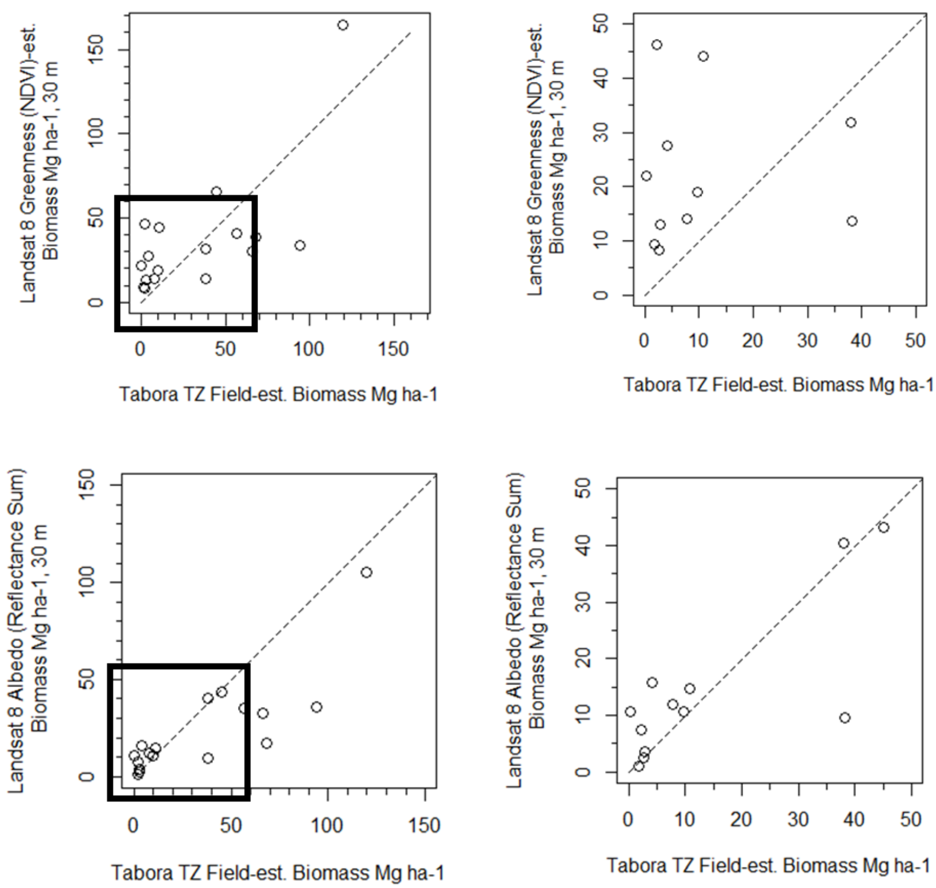

Figure 3.7 Landsat land cover metric–based estimates of forest biomass compared to field data at Sofala, Mozambique. Left-panel figures show the full biomass ranges of field and satellite data. Right-side panels show data in the 0-50 Mg ha^{-1} low-biomass range (heavy black boxed region in left-panel figures). Model 1 (top row) used Landsat greenness, brightness and elevation as predictors to model biomass. Model 2 (bottom row) used Landsat greenness, moisture, brightness and elevation as predictors to model biomass.

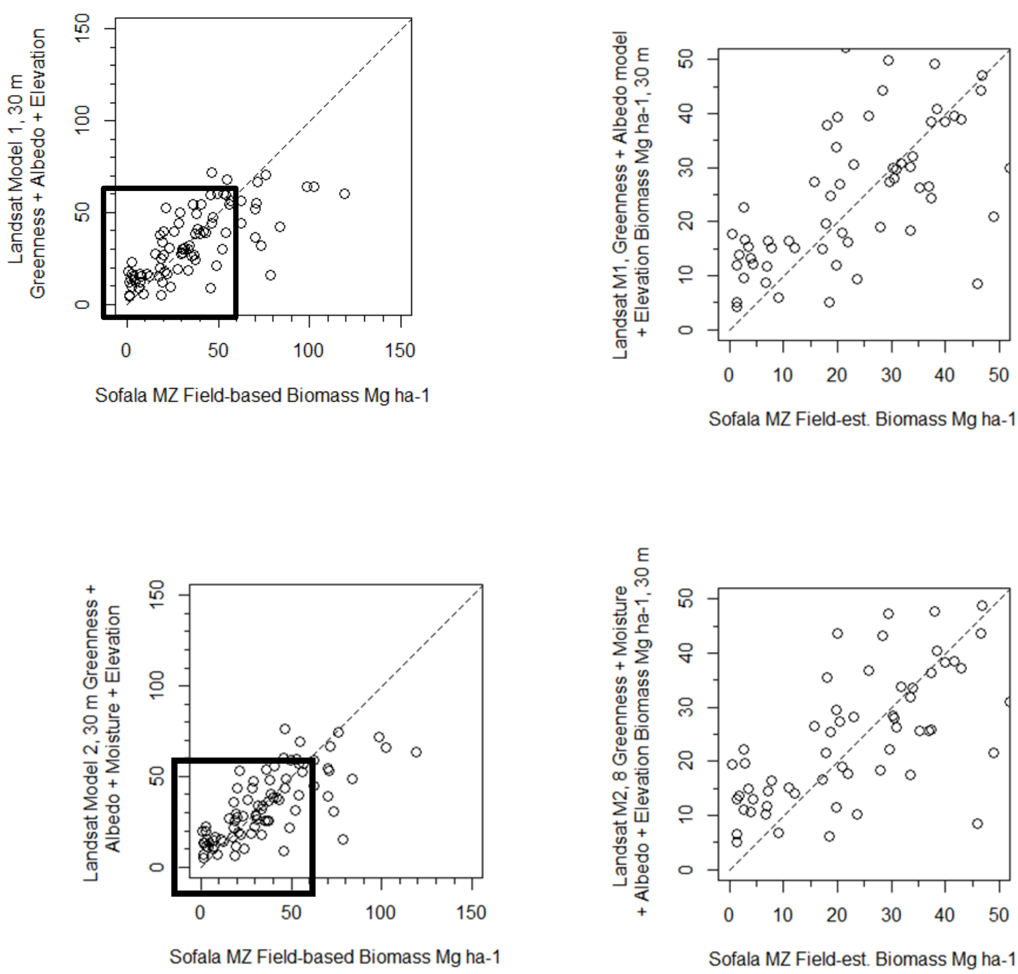

Figure 3.8 Comparison of aboveground biomass estimates at Tabora, Tanzania and Sofala, Mozambique from Baccini et al. (2012) 500 m pan-tropical maps, and this study's Landsat-scale 30 m regional maps. The Tabora map shown is produced from land cover brightness relationships to field-estimated aboveground tree biomass.

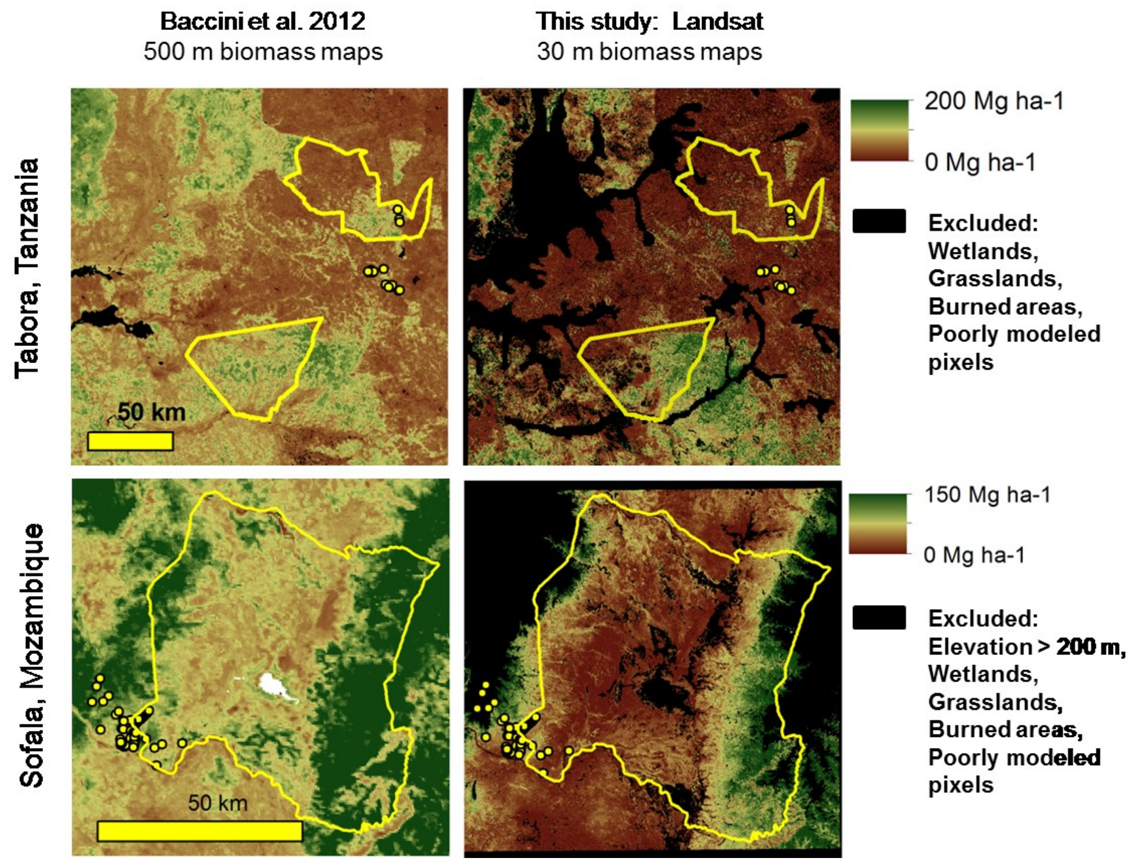

CONCLUSION

Overview

The goals of this thesis have been to address outstanding ecosystem science questions about forest nutrient cycling, and land cover-forest structure relationships to improve optical remote sensing of forest conditions in Miombo Woodlands. In addition to producing manuscripts for the peer-reviewed scientific literature, projects aimed to address information needs for inter- and multi-disciplinary professionals involved in forest and land resources conservation. This concluding chapter summarizes major scientific findings, uncertainties, and their implications for forest conservation by project. Subsequently, it discusses important future needs for ecosystem science research to support conservation in Miombo Woodlands and other tropical dry forests.

Chapter One: *Low nitrogen (N) availability across regrowth and mature Miombo forests indicates the importance of minimizing ecosystem N losses and maintaining N inputs to conserve forest productivity*

This project completed one of the first evaluations of N availability patterns across a forest regrowth chronosequence in the African dry tropics. Evidence from soil and vegetation N cycle indicators in a western Tanzania Miombo Woodland landscape suggested ecosystem N availability was low across sites, and that N cycle recovery was driven by N accumulation in tree biomass. Soil data primarily indicated low N availability conditions persisted across young and mature forests. Ammonium dominated plant-available mineral N (ammonium:nitrate) ratios, and total N pools 0-15 cm remained less than 1000 kg N ha^{-1} across sites, low compared to values across other global tropical dry forests (>2000 kg N ha^{-1}) with similar tree biomass (Waring *et al* 2015, Saynes *et al* 2005). The lack of significant recovery trends in either soil mineral N (ammonium and nitrate) concentrations, or wet-season mineralization rates with increasing site age, indicated plant-available mineral N supplies did not recover in the 40 yr regrowth timespan represented by field sites. In laboratory incubations, N mineralization potentials were 2-3 times higher in the wet season than dry season, suggesting that observed trends of shortening rainy seasons could result in lower mineral N availability to forest trees. Finally, we measured foliar $\delta^{15}N$ <0 across regrowth and mature forest sites in canopy-dominant N-fixing tree, *Pterocarpus angolensis*, for which past studies have found nitrogenase activity in root nodules in Tanzania (Högberg 1986). This is evidence that N fixation operates during regrowth and likely contributes, together with low levels of atmospheric N inputs, to the recovery of tree N pools. Altogether, our findings suggest that basic N cycling and low N-availability conditions in the Miombo are more similar to mixed tree-grass savannah systems such as the Brazilian cerrado, than humid or other Neotropical dry tropical forests (Bustamante *et al* 2004, Davidson *et al* 2007, Waring *et al* 2015, Saynes *et al* 2005).

The N cycling indicators studied provide striking first impressions of the Miombo as low-N ecosystems, but it was not possible to address all aspects of ecosystem N cycling in detail commensurate with other tropical systems that have been studied over many years (e.g. (Markewitz *et al* 2004). Limited infrastructure and challenging field logistics restricted the project to simple methods that have important limitations. For addressing ecosystem-scale N recovery with regrowth, the largest uncertainties involved the infeasibility of measuring N losses, quantifying N variability across broader sets of tree species, and further quantifying N inputs. With sandy soils low in organic matter, N leaching losses are likely more significant for ecosystem N budgets than gaseous losses mediated by processes such as denitrification, especially given ammonium-dominated mineral N pools indicating tight competition for mineral N among plants and microbes (Chikowo *et al* 2004, Schimel and Bennett 2004). Instead of denitrification, fire likely is the largest source of gaseous N losses, though understanding its effects on ecosystem N availability is a thorny problem. As fire volatilizes N-rich litter and topsoil organic matter, significant quantities of N are also deposited as ammonium (NH_4^+) in ash locally and redistributed regionally through atmospheric deposition processes (Stromgaard 1992, Lamarque 2013). For constraining the importance of N inputs via fixation, improved tree species inventories to estimate the basal area of N fixers, and testing for N-fixing activity are needed. Language barriers were the main challenge to understanding species distributions. A majority of tree species could be named and were recorded with stem inventories. However, precise identifies of many species were lost in translation between the local Nyamwezi and Sukuma languages, Swahili and scientific names. Addressing the questions of N leaching losses through lysimeter measurements in forests, and allocating time and money to linking local and scientific knowledge about tree species are low-hanging fruit for improving broad N cycle patterns in Miombo systems.

Feasible methods for quantifying N in trees and soil produced first-order estimates of tree and soil N pools, and to a limited extent, N supply rates from mineralization (laboratory incubation experiments over a 2-week period). They did not account for variability of wood or leaf chemistry across tree species and only represent canopy trees, not the understory. Leaf %N and wood chemistry of canopy and understory trees have been shown to vary among Miombo trees by species and niche in the canopy (Frost 1996, Chidumayo 1993). Total soil N stocks and mineral N were only measured 0-15 cm, and while the majority of ecosystem soil organic carbon and N is concentrated in the top 15 cm, Miombo trees have roots > 5 m and it is unclear how much soil N stocks at depth contribute to ecosystem N supplies (Frost 1996, Högberg 1986). Processes such as fate and transport of leaf biomass N between translocation and litterfall deposition, and timing of tree mineral N uptake, are important for interpreting the variability in total soil N stock data and understanding plant-soil N exchanges.

Several findings bear directly on Miombo forest conservation management with regard to maintenance of nutrient cycling for forest productivity. The most important are the combined findings of low N availability in soils, signs of >40 yr recovery in soil mineral N resources, and strong evidence that tree woody biomass accumulation drives the recuperation of combined (plant + soil) ecosystem N stocks during forest regrowth. These findings suggests that efforts to maintain N for forest productivity, encourage natural regeneration (unassisted regrowth of forest vegetation) or engage in reforestation or afforestation should minimize local ecosystem N losses by carefully managing fire, and discouraging the removal of tree biomass especially in regrowth forest sites, including cutting of live stems and removal of deadwood. These will be a challenging management problems, as wood biomass harvest (live stems and dead wood) for energy resources and building materials is widespread (Luoga *et al* 2000, Chidumayo and Gumbo 2013). Finally, *Pterocarpus angolensis*, the tree for which we found foliar $\delta^{15}N$ <0 indicating active fixation, is an endangered, highly-valued tree yielding rot and termite-resistant timber, and is used for load-bearing structures and high-value furniture (Schwartz *et al* 2002). Identification and protection of N-fixing trees could be an important part of strategies to maintain N in Miombo forest ecosystems.

Chapter Two: *Strong inverse correlations of non-green (senesced vegetation) land cover to tree structure indicates the utility of non-green landscape elements, in addition to green-vegetation features, for modeling Miombo tree structure with optical remotely sensed data*

This project completed one of the first land cover surveys linked to tree inventories in a Miombo Woodland landscape, and used forest structure relationships to optical Landsat satellite data to estimate forest basal area and biomass for a 2,470 km^2 region in western Tanzania. Its goals were to quantify land cover relationships to tree structure and test the utility of non-green land cover features for modeling tree structure at landscape scales. Patterns among field and Landsat-derived land cover metrics (green vegetation (GV) and non-photosynthetic vegetation (NPV) spectral mixture analysis (SMA) fractions, and NDVI) corroborated the hypothesis that exposure of bright, senesced vegetation correlated strongly to tree structure. In field data, tree canopy-mediated exposure of senesced vegetation on the ground had strong inverse correlations to tree basal area and biomass. The green leaf proportion of canopy cover had no correlation to tree structure on the ground. In field-to-satellite data relationships, we found that inverse correlations between Landsat SMA-NPV and tree structure were equivalent or stronger than correlations of green-leaf land cover measures (SMA-GL or NDVI). Three basal area and biomass maps for our study landscape, based on Landsat SMA-NPV, SMA-GV and NDVI respectively, modeled over 90% of per-pixel basal area and biomass values within ranges measured in the field. Maps derived from all metrics produced similar basal area and biomass estimates for high-biomass forest areas. Though class differences were not significant, village-managed forest areas had markedly higher basal area and biomass than national forest reserves. In non-forest areas, Landsat SMA-NPV based maps modeled basal area and biomass values that more closely matched measured values for young regrowth forests (3-4, 10-24 yr) and disturbed sites than metrics based on greenness measures. While more field data is needed to validate the landscape-scale tree structure estimates of these pilot maps, our results demonstrate that senesced vegetation metrics at Landsat scales are a promising means for improved quantification of tree structure conditions and change in African tropical dry forest landscapes.

This project's analyses with field and satellite data illustrated mechanisms for how Landsat SMA-NPV indicators relate to basal area and biomass in the early dry season, an optimum time for land cover differentiation in Miombo Woodlands (Mayes *et al* 2015) . These mechanisms are coherent with patterns of tree-grass structure and differences in grass-tree phenology found across the global dry tropics (Frost 1996, Eamus and Prior 2001). Biomass and forest structure maps were proof-of-concept exercises that NPV could be used to model forest structure with some advantages over greenness-based land cover metrics. A number of uncertainties are required to validate and develop these methods into more transferrable relationships. The main uncertainty is that the land cover signal measured by optical remotely sensed data does not directly measure vegetation structure, but rather integrated land cover (Goetz *et al* 2009). Many variables affect ground cover materials independently and can confound optical data relationships to tree structure. In the Miombo systems, fire is prevalent, and sub-canopy burns darken land cover to the point of altogether eliminating the ability to use land cover-optical image data relationships derived in non-burned areas (Frost 1996, Mayes *et al* 2015). Other environmental variations and land-use factors, such as flooding forest structures and cattle grazing pressure, can confound the land cover relationships to biomass developed in this study. Methods in this study depended on early dry season timing of optical imagery, which may not always be available. Combined use of optical and active remotely sensed data (radar, LiDAR) has been demonstrated as a leading way to deal with confounding variables affecting land cover (Ribeiro *et al* 2008, Baccini *et al* 2012). Further, for this study, only 17 sites and simple linear regressions were used to test relationships because of limited dataset size. While adequate to test novel hypotheses about land cover-forest structure relationships and develop pilot maps, ideally larger field datasets are necessary to improve calibrations to imagery, reserve sites for independent validation, or to use statistical validation approaches such as leave-one-out uncertainty estimates or jackknifing to quantify the uncertainty of per-pixel forest structure estimates.

For conservation management, this project has yielded insights for forest monitoring broadly, and landscape patterns in the Tabora, Tanzania case study landscape specifically. For forest monitoring practice, this study demonstrated the utility of planning land cover surveys alongside surveys of tree biomass to understand relationships to Landsat-scale and other optical satellite data. The land cover survey methods we used provided straightforward means of relating land cover to forest structure, and developing direct remote sensing approaches for local forest monitoring (Goetz *et al* 2009). Using inexpensive, simple spherical densitometer mirrors to quantify canopy features, and point-line transects for ground cover, they were easily communicable and repeatable. With sufficient resources, a larger number of sites can be measured to address small-sample size issues.

Two observations were striking about forest structure variability in Tabora, Tanzania related to current land management. First, at scales of hundreds of kilometers, sharp boundaries were apparent in forest cover at management area borders, indicating that large-scale land management, land use and forest policy has strongly affected present forest cover distributions. Second, although sample sizes were small, there was notably higher basal area and biomass in village-managed forest sites than nationally managed reserve forest sites in Tabora. These data speak to broader questions about what institutional structures and scales (local, regional, national) forest conservation is most effective in small-holder landscapes.

Chapter Three: *Brightness land cover metrics derived from Landsat satellite data (30 m pixels) improve predictions of aboveground tree biomass in low-biomass areas (<50 Mg ha^{-1}) across two distinct Miombo landscapes, indicating a promising approach for monitoring regrowth forests and other low tree biomass areas targeted for forest conservation projects.*

This study presented one of the first cross-regional assessments of relationships among field data on forest structure and Landsat-derived land cover metrics in the Miombo Woodlands. In parallel analyses based in western Tanzania and southern Mozambique regions, its goals were to identify if consistent land cover-forest structure relationships emerged that were useful for biomass monitoring within landscapes, focusing on low-biomass areas (<50 Mg ha^{-1}). The study also developed pilot forest biomass maps with Landsat 30 m data, and compared their performance to an existing pan-tropical forest biomass map combining optical and active remotely sensed data at 500 m resolution (Baccini *et al* 2012). Mature forests in Tanzania had significantly higher stem density, basal area and biomass than Mozambique, and the spatial variability of forest cover also strongly differed between regions. Nevertheless, in both regions green vegetation (NDVI) and surface moisture (NDMI) satellite metrics had positive correlations, and a brightness metric (sum of reflectance across optical bands) had negative correlations to forest basal area and biomass. In multiple regression analyses to predict forest structure, brightness metrics, and combinations of multiple land cover metrics and landscape co-variables (elevation, soil type), had relationships to forest structure that were as strong or stronger than those using greenness alone. In both regions, the 500 m pan-tropical biomass map (Baccini *et al* 2012) consistently and significantly over-estimated aboveground biomass in low-biomass areas (<50 Mg ha^{-1}). Regionally calibrated Landsat-scale 30 m maps produced absolute values and spatial patterns of biomass in both Tanzania and Mozambique that better matched field data ranges across known landscape gradients related to land use and ecological factors, though need further validation and methodological refinements. Our findings suggested successful pursuit of transferrable remote sensing relationships for Miombo landscapes should use multiple land cover metrics besides greenness measures, and appropriate representation of covariates affecting forest structure-land cover relationships in field datasets.

Chapter Three's analyses extended findings of Chapter Two and tested their transferability across different Miombo regions. Identifying transferrable strategies to relate optical remotely sensed data on land cover to forest structure in different regions, even within the same ecological zone, is an important problem for improving forest monitoring globally (Foody *et al* 2003). The chief limitations of Chapter Three's analyses were much the same those of Chapter Two. Chapter Three's brightness metric was a coarse proxy for the Landsat SMA-NPV senesced vegetation cover metric used in Chapter Two: low tree-cover areas dominated by senesced vegetation have brighter land cover surfaces than high tree-cover areas. The brightness metric, a simple sum of reflectance across Landsat optical bands, was easier to use for cross-regional analyses given the lack of land cover data in the Mozambique site, which precluded the kind of validation of land cover-forest structure relationships that was possible for the Tanzania site. The finding that strong inverse correlations between brightness, forest basal area and biomass held in the 83-site Mozambique dataset added confidence that both senesced and green vegetation land cover relationships in the smaller 17-site Tabora dataset were indeed transferrable. Further steps to refine Landsat optical data calibrations to forest structure in Tabora and

Mozambique could include analyses pooling data from both sites, and more sophisticated modeling methods than simple linear regression, such as decision tree approaches (Goetz *et al* 2009).

Chapter Three's work yielded two key advances forest conservation. The first were results that showed biases in an existing global-scale biomass map for low-biomass (<50 Mg ha^{-1}) tree structure regions in the Miombo. The second was evidence that use of Landsat 30 m optical remotely sensed data, non-green and green land cover indices for mapping biomass reduced errors for low-biomass tree structure regions compared to existing maps. The threshold of 50 Mg ha^{-1} biomass (roughly 25 Mg ha^{-1} carbon stocks) is important because it represents an average forest structure boundary between 30-40 year regrowth forests and mature forests found across the Miombo Woodland ecoregion (Williams *et al* 2008, Kalaba *et al* 2013, Chidumayo 2013, McNicol *et al* 2015). Across sub-Saharan Africa, and within landscapes, much of the Miombo Woodland forest areas are disturbed or recent regrowth, or through edaphic factors have biomass below 50 Mg ha^{-1}. The orientation of existing 500 m forest biomass maps is not on monitoring biomass variability within landscapes, but rather identifying high vegetation carbon-stock regions at larger scales for national or international-scale carbon assessments for programs such as REDD+ (Baccini *et al* 2012, Saatchi *et al* 2011). Improved, regionally tuned remote sensing methods for forest structure are needed to aid forest landscape restoration programs such as World Resource Institute's Afri100 Landscapes Initiative that focus largely on forest management in low-biomass areas of landscapes (Chazdon 2008, WRI 2016). Chapter Three's results, along with Chapter Two, show promising directions for remote sensing methods and understanding of optical satellite data-forest structure relationships that are needed to provide landscape-scale information on conditions and change in areas with low-biomass tree structure.

Future research directions and priorities

Land use and climate change pressures threaten the extent and productivity of tropical dry forests, their biodiversity and the resources they provide to millions of people in the Miombo Woodlands and across the global tropics. To address these challenges, there are needs for further research on ecosystem processes, forest monitoring, and conservation management that more equitably involve diverse stakeholders from local to international scales. Ecosystem science, in collaboration with other fields of expertise, can contribute toward meeting all of these needs.

Research in forestry, biogeochemistry, land cover/land use change and other fields has established basic understanding of a few important ecosystem processes in Miombo Woodlands. Namely, these include patterns in forest structure, carbon stocks and species variability across different Miombo regions and general 20-30 year timescales for forest carbon stock recovery from disturbance (Frost 1996, Williams *et al* 2008, Kalaba *et al* 2013, Banda *et al* 2006, McNicol *et al* 2015, Chidumayo 2013). Work in this thesis contributes knowledge of Miombo nitrogen cycling patterns with regrowth, and relationships between land cover, tree structure and optical remote sensing.

However, much of this past research has relied on data collected at only one or a few points in time (e.g. tree inventories), capturing relatively static snapshots of ecosystem conditions. There is relatively little understanding of how ecosystem processes function or mechanisms by which they respond to environmental change. Over the past 25 years, the select few studies on Miombo ecosystems involving repeat data collection have identified basic patterns in leaf nutrient resorption behavior (Chidumayo 1993) and inter-annual net ecosystem productivity variations (Kutsch *et al* 2011) that only begin to address process-oriented ecosystem biogeochemistry questions.

Climate change, particularly involving rainfall, stands to affect biogeochemistry and productivity of Miombo and other tropical dry forests worldwide (Wang *et al* 2015, Lyon and Dewitt 2012, Guan *et al* 2014). For forest conservation recommendations to be effective long-term, in some way, they will have to protect water and nutrient cycling processes necessary for forest growth in drier or more variable rainfall regimes. Thus, there is a great need for improved process-based understanding of forest productivity, nutrient cycling and phenology and how they respond to changes in water availability. Key questions include:

1. What are the basic patterns of Miombo forest carbon cycling, nutrient cycling (nitrogen, phosphorus, others), phenology and other processes surrounding major modes of water variability (wet-dry season) and points of change (before-after rainfall events)?

2. How do basic patterns in ecosystem processes and their responses to water availability change among Miombo forests of different ages, disturbance types and intensities, or with different species compositions?

3. How do changes in ecosystem processes (forest productivity, nutrient cycling, phenology) feed back among other important landscape-scale processes, such as fire?

Field-based studies that collect data at higher temporal resolutions, matching the scales of variability of hydrological conditions, will be necessary to address the questions above. At minimum, repeat data collection should cover wet and dry seasons. Studies could also focus on times before and after rainfall events. Ideally, data collection would occur over months or weeks for nutrient cycling data, or make use of continuous data collection for physical environmental conditions such as soil moisture or temperature. Use of automated data collection methods, from cameras to environmental sensors (e.g. Hobo loggers) are becoming common in the ecological literature (Richardson *et al* 2009). Structuring future field research to make use of well-characterized forest regrowth chronosequences can help address both questions 1 and 2 above. For question 3, use of emerging remotely sensed data for burned areas, which scale MODIS 500 m products to Landsat 30 m resolutions, can aid selection of field sites with different historical burn frequencies to study fire effects on ecosystem processes (Boschetti *et al* 2015).

Besides data collection at higher temporal resolutions, land cover and forest structure characterization at higher spatial resolutions can help improve characterization of forest ecosystems, and study processes like phenology at landscape scales. The use of small unmanned aerial vehicles/systems (drones, UAV/S) offers great promise as a tool to map 1-10 hectare-sized areas, or improve scaling between field and satellite observations. Researchers worldwide are beginning to use UAVs as part of ecosystem biogeochemistry and natural resource assessments (Rezayan and Erfanifard 2016, Paneque-Galvez *et al* 2014, Tang and Shao 2015). UAS data break the "spatial-spectral resolution" tradeoff inherent in optical satellite remotely sensed data, in that they offer both high-spatial and high temporal-frequency observation.

Involving local people and communities in scientific research, forest monitoring and management holds immense opportunities for improving ecosystem science and forest conservation in the Miombo Woodlands and other tropical dry forests. For research on land-use effects on forests in rural Miombo landscapes, involving local people is crucial to understanding what land-use activities are occurring and where, and how to frame research projects to be of most benefit to local management issues. Inter- and multi-disciplinary research is needed to identify what modifications to land-use practices are realistic for forest conservation, given local socioeconomic conditions and regionally tele-connected land use pressures (DeFries *et al* 2010) . A useful question thus is not "What are the effects of preventing wood-fuel harvesting in Miombo Woodlands?" because wood fuels are an irreplaceable resource for many people. Rather, questions surrounding what are the impacts of varying harvest pressures, or harvest rotations for wood fuels are more productive. Coupled with field studies involving local land users, ecosystem modelling approaches to these questions will also be useful for estimating sustainable resource use rates (Rastetter *et al* 2013). Development of strong working relationships with regional government officials, local scientists and diverse groups of people living within study landscapes is critical to create productive, secure circumstances to attempt use of new technologies, such as high temporal-resolution monitoring sensors and UAVs, to achieve scientific advances and project goals of ecosystem scientists and forest conservation interests.

Forest resource conservation needs create ecosystem science opportunities. This thesis has addressed questions about forest nutrient cycling and land cover-forest structure relationships for the ecosystem science community and highlighted findings that are practical for forest conservation management in Miombo landscapes. A network of scientists, professionals, teachers and friends across continents and cultures inspired its work. It is my hope that work in this thesis serves as a helpful example for approaching ecosystem science at landscape scales to other broad thinkers, driven to do work that helps people.

References

Baccini a., Goetz S J, Walker W S, Laporte N T, Sun M, Sulla-Menashe D, Hackler J, Beck P S a., Dubayah R, Friedl M a., Samanta S and Houghton R a. 2012 Estimated carbon dioxide emissions from tropical deforestation improved by carbon-density maps *Nat. Clim. Chang.* **2** 182–5 Online: http://dx.doi.org/10.1038/nclimate1354

Banda T, Schwartz M W and Caro T 2006 Woody vegetation structure and composition along a protection gradient in a miombo ecosystem of western Tanzania *For. Ecol. Manage.* **230** 179–85

Boschetti L, Roy D P, Justice C O and Humber M L 2015 MODIS–Landsat fusion for large area 30m burned area mapping *Remote Sens. Environ.* **161** 27–42

Bustamante M M C, Martinelli L a., Silva D a., Camargo P B, Klink C a., Domingues T F and Santos R V. 2004 15 N Natural Abundance in Woody Plants and Soils of Central Brazilian Savannas (Cerrado) *Ecol. Appl.* **14** 200–13 Online: http://www.esajournals.org/doi/abs/10.1890/01-6013

Chazdon R L 2008 Beyond Deforestation : Restoring Degraded Lands *Communities* **1458** 1458–60 Online: http://www.ncbi.nlm.nih.gov/pubmed/18556551

Chidumayo E N 2013 Forest degradation and recovery in a miombo woodland landscape in Zambia: 22 years of observations on permanent sample plots *For. Ecol. Manage.* **291** 154–61 Online: http://dx.doi.org/10.1016/j.foreco.2012.11.031

Chidumayo E N 1993 Phenology and nutrition of miombo woodland trees in Zambia *Trees* **9** 67–72

Chidumayo E N and Gumbo D J 2013 The environmental impacts of charcoal production in tropical ecosystems of the world: A synthesis *Energy Sustain. Dev.* **17** 86–94 Online: http://dx.doi.org/10.1016/j.esd.2012.07.004

Chikowo R, Mapfumo P, Nyamugafata P and Giller K E 2004 Mineral N dynamics, leaching and nitrous oxide losses under maize following two-year improved fallows on a sandy loam soil in Zimbabwe *Plant Soil* **259** 315–30

Davidson E a, de Carvalho C J R, Figueira A M, Ishida F Y, Ometto J P H B, Nardoto G B, Sabá R T, Hayashi S N, Leal E C, Vieira I C G and Martinelli L a 2007 Recuperation of nitrogen cycling in Amazonian forests following agricultural abandonment. *Nature* **447** 995–8

DeFries R S, Rudel T, Uriarte M and Hansen M 2010 Deforestation driven by urban population growth and agricultural trade in the twenty-first century *Nat. Geosci.* **3** 178–81 Online: http://www.nature.com/doifinder/10.1038/ngeo756

Eamus D and Prior L 2001 *Ecophysiology of trees of seasonally dry tropics: Comparisons among phenologies* vol 32 Online: http://cat.inist.fr/?aModele=afficheN&cpsidt=14091981

Foody G M, Boyd D S and Cutler M E J 2003 Predictive relations of tropical forest biomass from Landsat TM data and their transferability between regions *Remote Sens. Environ.* **85** 463–74

Frost P 1996 *The Ecology of Miombo Woodlands* ed B M Campbell (Bogor, Indonesia: Center for International Forestry Research) Online: http://books.google.com/books?hl=nl&lr=&id=rpildJJVdU4C&pgis=1

Goetz S J, Baccini A, Laporte N T, Johns T, Walker W, Kellndorfer J, Houghton R A, Sun M, DeFries R, Houghton R, Hansen M, Field C, Skole D, Townshend J, Achard F, DeFries R, Eva H, Hansen M, Mayaux P, Stibig H, Herold M, Johns T, Laporte N, Stabach J, Grosch R, Lin T, Goetz S, Asner G, Knapp D, Broadbent E, Oliveira P, Keller M, Silva J, Houghton R, Brown S, Houghton R, Lawrence K, Hackler J, Brown S, Houghton R, Goetz S, Kasischke E, Melack J, Dobson M, Tatem A, Goetz S, Hay S, Walker W, Kellndorfer J, Pierce L, Dubayah R, Drake J, Lefsky M, Harding D, Keller M, Cohen W, Carabajal C, Espirito-Santo F D B, Hunter M, Oliveira R de, Hurtt G, Dubayah R, Drake J, Moorcroft P, Pacala S, Blair J, Fearon M, Drake B, Dubayah R, Knox R, Clark D, Blair J, Sun G, Ranson K, Kimes D, Blair J, Kovacs K, Hansen M, Stehman S, Potapov P, Loveland T, Townshend J, DeFries R, Pittman K, Arunarwati B, Stolle F, Steininger M, Carroll M, DiMiceli C, Goetz S, Brown S, Gillespie A, Lugo A, Chave J, Andalo C, Brown S, Cairns M, Chambers J, et al 2009 Mapping and monitoring carbon stocks with satellite observations: a comparison of methods *Carbon Balance Manag.* **4** 2 Online: http://cbmjournal.springeropen.com/articles/10.1186/1750-0680-4-2

Guan K, Good S P, Caylor K K, Sato H, Wood E F and Li H 2014 Continental-scale impacts of intra-seasonal rainfall variability on simulated ecosystem responses in Africa *Biogeosciences* **11** 6939–54 Online: http://www.biogeosciences.net/11/6939/2014/

Högberg P 1986 Nitrogen-fixation and nutrient relations in savanna woodland trees (Tanzania) *J. Appl. Ecol.* **23** 675–88 Online: http://www.jstor.org/stable/2404045\nhttp://www.jstor.org/stable/pdfplus/2404045.pdf?acceptTC=true

Kalaba F K, Quinn C H, Dougill A J and Vinya R 2013 Floristic composition, species diversity and carbon storage in charcoal and agriculture fallows and management implications in Miombo woodlands of Zambia *For. Ecol. Manage.* **304** 99–109

Kutsch W L, Merbold L, Ziegler W, Mukelabai M M, Muchinda M, Kolle O and Scholes R J

2011 The charcoal trap: Miombo forests and the energy needs of people. *Carbon Balance Manag.* **6** 5 Online: http://www.pubmedcentral.nih.gov/articlerender.fcgi?artid=3189094&tool=pmcentrez&rendertype=abstract\nhttp://www.cbmjournal.com/content/6/1/5

Lamarque J-F 2013 Multi-model mean nitrogen and sulfur deposition *Atmos. Chem. Phys. Discuss* **13** 6247–94

Luoga E J, Witkowski E T F and Balkwill K 2000 Subsistence use of wood products and shifting cultivation within a miombo woodland of eastern Tanzania, with some notes on commercial uses *South African J. Bot.* **66** 72–85

Lyon B and Dewitt D G 2012 A recent and abrupt decline in the East African long rains *Geophys. Res. Lett.* **39** 1–5

Markewitz D A M, Davidson E R I C D and Outinho P A M 2004 Nutrient Loss and Redistribution After Forest Clearing on a Highly Weathered Soil in Amazonia **14** 177–99

Mayes M T, Mustard J F and Melillo J M 2015 Forest cover change in Miombo Woodlands: modeling land cover of African dry tropical forests with linear spectral mixture analysis *Remote Sens. Environ.* **165** 203–15

McNicol I M, Ryan C M and Williams M 2015 How resilient are African woodlands to disturbance from shifting cultivation? *Ecol. Appl.* **25** 2330–6

Paneque-Galvez J, McCall M K, Napoletano B M, Wich S A and Koh L P 2014 Small drones for community-based forest monitoring: An assessment of their feasibility and potential in tropical areas *Forests* **5** 1481–507

Rastetter E B, Yanai R D, Thomas R Q, Vadeboncoeur M A, Fahey T J, Fisk M C, Kwiatkowski B L and Hamburg S P 2013 Recovery from disturbance requires resynchronization of ecosystem nutrient cycles *Ecol. Appl.* **23** 621–42 Online: http://doi.wiley.com/10.1890/12-0751.1

Rezayan F and Erfanifard Y 2016 Estimating biophysical parameters of Persian oak coppice trees using UltraCam-D airborne imagery in Zagros semi-arid woodlands *J. Arid Environ.* **133** 10–8

Ribeiro N S, Saatchi S S, Shugart H H and Washington-Allen R A 2008 Aboveground biomass and leaf area index (LAI) mapping for Niassa Reserve, northern Mozambique *J. Geophys. Res.* **113** G02S02 Online: http://doi.wiley.com/10.1029/2007JG000550

Richardson A D, Braswell B H, Hollinger D Y, Jenkins J P and Ollinger S V. 2009 Near-surface remote sensing of spatial and temporal variation in canopy phenology *Ecol. Appl.* **19** 1417–28 Online: http://doi.wiley.com/10.1890/08-2022.1

Saatchi S S, Harris N L, Brown S, Lefsky M, Mitchard E T A, Salas W, Zutta B R, Buermann W, Lewis S L, Hagen S, Petrova S, White L, Silman M and Morel A 2011 Benchmark map of forest carbon stocks in tropical regions across three continents *Proc. Natl. Acad. Sci.* **108** 9899–904

Saynes V, Hidalgo C, Etchevers J D and Campo J E 2005 Soil C and N dynamics in primary and secondary seasonally dry tropical forests in Mexico *Appl. Soil Ecol.* **29** 282–9

Schimel J and Bennett J 2004 Nitrogen mineralization: challenges of a changing paradigm *Ecology* **85** 591–602 Online: http://onlinelibrary.wiley.com/doi/10.1890/03-8002/epdf

Schwartz M W, Caro T M and Banda-Sakala T 2002 Assessing the sustainability of harvest of Pterocarpus angolensis in Rukwa Region, Tanzania *For. Ecol. Manage.* **170** 259–69

Stromgaard P 1992 Immediate and long-term effects of fire and ash- fertilization on a Zambian miombo woodland soil **41** 19–37

Tang L and Shao G 2015 Drone remote sensing for forestry research and practices *J. For. Res.* **26** 791–7 Online: http://link.springer.com/10.1007/s11676-015-0088-y

Wang L, Manzoni S, Ravi S, Riveros-Iregui D and Caylor K 2015 Dynamic interactions of ecohydrological and biogeochemical processes in water-limited systems *Ecosphere* **6** art133 Online: http://doi.wiley.com/10.1890/ES15-00122.1

Waring B G, Becknell J M and Powers J S 2015 Nitrogen, phosphorus, and cation use efficiency in stands of regenerating tropical dry forest *Oecologia* 887–97 Online: http://dx.doi.org/10.1007/s00442-015-3283-9

Williams M, Ryan C M, Rees R M, Sambane E, Fernando J and Grace J 2008 Carbon sequestration and biodiversity of re-growing miombo woodlands in Mozambique *For. Ecol. Manage.* **254** 145–55

WRI 2016 AFR100: Africa Restoring 100 Million Hectares of Deforested and Degraded Land by 2030 Online: http://www.wri.org/our-work/project/AFR100/about-afr100